



5-2014

Hardware-In-Loop Evaluation of Microgrid Protection Schemes

Kevin Michael Dowling

University of Tennessee - Knoxville, kdowlin2@utk.edu

Follow this and additional works at: https://trace.tennessee.edu/utk_gradthes



Part of the [Power and Energy Commons](#)

Recommended Citation

Dowling, Kevin Michael, "Hardware-In-Loop Evaluation of Microgrid Protection Schemes. " Master's Thesis, University of Tennessee, 2014.

https://trace.tennessee.edu/utk_gradthes/2708

This Thesis is brought to you for free and open access by the Graduate School at TRACE: Tennessee Research and Creative Exchange. It has been accepted for inclusion in Masters Theses by an authorized administrator of TRACE: Tennessee Research and Creative Exchange. For more information, please contact trace@utk.edu.

To the Graduate Council:

I am submitting herewith a thesis written by Kevin Michael Dowling entitled "Hardware-In-Loop Evaluation of Microgrid Protection Schemes." I have examined the final electronic copy of this thesis for form and content and recommend that it be accepted in partial fulfillment of the requirements for the degree of Master of Science, with a major in Electrical Engineering.

Leon Tolbert, Major Professor

We have read this thesis and recommend its acceptance:

Fred Wang, Fangxing Li

Accepted for the Council:

Carolyn R. Hodges

Vice Provost and Dean of the Graduate School

(Original signatures are on file with official student records.)

Hardware-In-Loop Evaluation of Microgrid Protection Schemes

A Thesis Presented for the
Master of Science
Degree

The University of Tennessee, Knoxville

Kevin Michael Dowling

May 2014

Copyright © 2014 by Kevin Michael Dowling

All rights reserved.

DEDICATION

This thesis is dedicated to my fiancé Ashton who has been my source of love, comfort, motivation, and inspiration through many trials and triumphs. I thank God for you and eagerly await a lifetime of joy and adventures together.

This thesis is also dedicated to my parents, Darryl and Sherrie, for their guidance, love, unwavering belief, patience, and open refrigerator. I am truly blessed beyond measure on your account.

ACKNOWLEDGEMENTS

Thank you to Dr. Leon Tolbert, Dr. Yan Xu, Travis Smith, Phillip Irminger, and Kumaraguru Prabakar, for all your guidance, assistance, and encouragement.

Thank you to DOE, ORNL, and CURENT for supporting this research.

ABSTRACT

Distributed energy resources are becoming more common in distribution systems. Higher energy prices and increased interest in alternative energy sources are two of the driving forces behind this trend. Local utilities, however, anticipate very serious distribution system protection problems resulting from high penetration of these resources.

The microgrid concept has been proposed as a possible solution to integrating distributed energy resources without adversely impacting the distribution system. Protection schemes have been proposed to work within this microgrid structure, but very little testing with real hardware is available. Without a practical solution for microgrid protection, backed by extensive studies, microgrids are unlikely to receive wide acceptance.

This thesis outlines modeling of microgrids for protection testing using a real time digital simulator. In addition, the construction of a low voltage, low power, hardware-in-loop test bed using relays and an automation controller is detailed. The results of testing possible microgrid protection schemes using this apparatus are presented along with conclusions and suggestions for future work.

TABLE OF CONTENTS

Chapter 1, Introduction and General Information	1
Microgrids.....	2
Microgrid Structure	3
Introduction to System Protection.....	4
Protection Reliability	5
Protection Selectivity	5
Protection Speed	6
Protection Simplicity	7
Protection Economics	8
Electromechanical Relays	8
Digital Relays	14
Real Time Automation Controller	15
Real Time Digital Simulator	16
Thesis Outline	17
Chapter 2, Literature Review	20
Real and Reactive Power Control	20
Frequency and Voltage Droop Control	23
Application of Existing Generation Controls to Microgrids	25
Modeling A Microgrid System.....	28
Modeling Utility Connections.....	28
Modeling Distributed Energy Resources.....	29
Microgrid Protection Challenges.....	31
Fault Isolation	31
Decreased Fault Current	32
False Tripping	34
Protection Blinding.....	36
Protection Schemes	36
Overcurrent Protection.....	37
Directional Overcurrent Protection.....	40
Differential Protection	42
Pilot Protection.....	44
Genetic Algorithms	46
Summary	47
Chapter 3, Materials and Methods	49
Microgrid Model.....	49
Microgrid Structure	49
Distributed Energy Resources	52
Control Tuning with Genetic Algorithm	58
Hardware-In-Loop	64
SEL 351S.....	64
RTAC and HMI	69
Summary	76
Chapter 4, Results and Discussion	77

Time Overcurrent Protection	77
Variable Setting Overcurrent	83
Variable Setting Overcurrent With Directional Control.....	86
Variable Setting Overcurrent With Bus Differential.....	88
Differential Overcurrent Protection	91
Summary.....	98
Chapter 5, Conclusions and Future Work	100
Conclusions.....	100
Future Work.....	102
Summary.....	103
REFERENCES	104
APPENDIX.....	107
Vita.....	116

LIST OF TABLES

TABLE 1.1 INVERSE TIME OVERCURRENT RELAY CHARACTERISTIC COEFFICIENTS.	12
TABLE 2.1 CALCULATED FAULT CURRENTS IN MICROGRID USING CAPE.	34
TABLE 3.1 RESULTANT SCALE FACTORS FOR 351S INPUT MODULE FROM RELAY MANUAL.	67
TABLE 4.1 OVERCURRENT RELAY SETTINGS.	78
TABLE 4.2 OVERCURRENT PROTECTION OPERATING TIMES.	78
TABLE 4.3 VARIABLE SETTING OVERCURRENT RELAY SETTINGS.....	83
TABLE 4.4 VARIABLE SETTING OVERCURRENT PROTECTION OPERATING TIMES.....	84
TABLE 4.5 VARIABLE SETTING OVERCURRENT PROTECTION WITH BUS DIFFERENTIAL RELAY OPERATING TIMES.	89
TABLE 4.6 DIFFERENTIAL OVERCURRENT PROTECTION OPERATING TIMES FOR THREE- PHASE FAULTS USING VERY INVERSE (U3) CURVE.....	94
TABLE 4.7 DIFFERENTIAL OVERCURRENT PROTECTION OPERATING TIMES FOR SINGLE- PHASE FAULTS USING VERY INVERSE (U3) CURVE.....	95
TABLE 4.8 DIFFERENTIAL OVERCURRENT PROTECTION OPERATING TIMES FOR THREE- PHASE FAULTS USING EXTREMELY INVERSE (U4) CURVE.	95
TABLE 4.9 DIFFERENTIAL OVERCURRENT PROTECTION OPERATING TIMES FOR SINGLE- PHASE FAULTS USING EXTREMELY INVERSE (U4) CURVE.	95
TABLE 4.10 DIFFERENTIAL OVERCURRENT PROTECTION OPERATING TIMES FOR THREE- PHASE FAULTS USING SHORT-TIME (U5) CURVE.....	96
TABLE 4.11 DIFFERENTIAL OVERCURRENT PROTECTION OPERATING TIMES FOR SINGLE- PHASE FAULTS USING SHORT-TIME (U5) CURVE.....	96
TABLE 4.12 DIFFERENTIAL OVERCURRENT PROTECTION OPERATING TIMES FOR THREE- PHASE FAULTS USING INSTANTANEOUS OVERCURRENT CHARACTERISTIC.....	96
TABLE 4.13 DIFFERENTIAL OVERCURRENT PROTECTION OPERATING TIMES FOR SINGLE- PHASE FAULTS USING INSTANTANEOUS OVERCURRENT CHARACTERISTIC.....	97

LIST OF FIGURES

FIGURE 1.1 BUS CONFIGURATIONS FOR LOOP AND MESHED NETWORK STRUCTURES.	4
FIGURE 1.2. US TIME OVERCURRENT CHARACTERISTIC CURVES (TD = 2.0 SECONDS.)	13
FIGURE 1.3. IEC TIME OVERCURRENT CHARACTERISTIC CURVES (TD = 2.0 SECONDS.)	13
.....	13
FIGURE 2.1 FAULT ISOLATION IN SYSTEM WITH DERs.....	32
FIGURE 2.2 FALSE TRIPPING FOR FAULT ON PARALLEL LINE.....	35
FIGURE 2.3 A) CURRENT TRANSFORMER CONNECTION. B) VOLTAGE TRANSFORMER CONNECTION.....	38
FIGURE 2.4 COORDINATION OF OVERCURRENT RELAYS IN A RADIAL SYSTEM.....	39
FIGURE 2.5 RULES OF THUMB FOR SETTING OVERCURRENT RELAYS.	40
FIGURE 2.6 A) PHASOR REPRESENTATION OF 60 DEGREE DIRECTIONAL ELEMENT. B) DIRECTIONAL ELEMENT SUPERVISION OF OVERCURRENT OPERATION.	41
FIGURE 2.7 DIRECTIONAL OVERCURRENT RELAY CONNECTION.	42
FIGURE 2.8 DIFFERENTIAL RELAY CONNECTION.....	43
FIGURE 2.9 DIFFERENTIAL OPERATING REGIONS WITH DUAL SLOPE CHARACTERISTIC. .	44
FIGURE 2.10 PILOT PROTECTION OPERATING LOGIC.	45
FIGURE 3.1 DECC LAB MICROGRID MODEL.....	51
FIGURE 3.2 RSCAD MODELS USED FOR MODELING A) INVERTERS AND B) LOAD BANKS.	52
FIGURE 3.3 REAL AND REACTIVE POWER CONTROL.	54
FIGURE 3.4 ADAPTATION ON PQ CONTROL FOR FREQUENCY AND VOLTAGE.....	55
FIGURE 3.5 ADAPTATION OF PQ CONTROL FOR CURRENT LIMITING.....	55
FIGURE 3.7 RESULTS OF GENETIC ALGORITHM OPTIMIZATION PROCESS FOR THREE ITERATIONS WITH DIRECT CARRYOVER OF TOP TWO RESULTS FROM EACH GENERATION.	62
FIGURE 3.8 FLOWCHART OF TUNING ALGORITHM.....	63
FIGURE 3.9 RTDS ANALOG OUTPUT MODELS ACCOUNTING FOR ANALOG TO DIGITAL CONVERSION INSIDE RELAY.	66
FIGURE 3.10 SEL 351S INPUT PIN OUT CONNECTIONS.	67
FIGURE 3.11 INPUTS FOR CIRCUIT BREAKER CONTROLS FROM SEL 351S RELAYS.	68
FIGURE 3.12 SIGNALS BETWEEN RTDS AND 351S RELAYS.	69
FIGURE 3.13 SEL RTAC 3530.	70
FIGURE 3.14 CIRCUIT BREAKER AND INVERTER STATUS OUTPUT SIGNALS TO RTAC. ..	71
FIGURE 3.15 EXAMPLE EVENT COLLECTION FILES.....	72
FIGURE 3.16 A) RELAY COMMUNICATION SETTINGS. B) RTAC CONNECTED DEVICES AND ACCESS POINTS.....	73
FIGURE 3.17 CUSTOM LOGIC FOR BREAKER STATUSES AND SETTING GROUP CHANGES USING RELAY REMOTE BITS.....	74
FIGURE 3.18 A) REMOTE BITS CONTROLLING RELAY SETTING GROUP CHANGES. B) REMOTE BIT CONTROLLING THE CIRCUIT BREAKER STATUS SIGNAL IN THE RELAY. .	74
FIGURE 3.19 RTAC HMI ONE LINE DIAGRAM.	75
FIGURE 3.20 RTAC HMI RELAY CHILD DIAGRAM.....	76

FIGURE 4.1 A) FAULT IN BUILDING #3114 WHILE ON GRID. B) FAULT IN BUILDING #3114 WHILE OFF GRID.	79
FIGURE 4.2 A) BUILDING #3114 BUS VOLTAGES DURING FAULT IN BUILDING #3114 WHILE ON GRID. B) BUILDING #3114 INVERTER RMS CURRENT OUTPUT DURING FAULT. C) INVERTER CURRENT PASSING THROUGH CIRCUIT BREAKER 2 DURING FAULT.....	79
FIGURE 4.3 A) FAULT IN BUILDING #3129 WHILE ON GRID. B) FAULT IN BUILDING #3129 WHILE OFF GRID.	80
FIGURE 4.4 A) BUILDING #3114 BUS VOLTAGES DURING FAULT IN BUILDING #3129 WHILE ON GRID. B) BUILDING #3114 INVERTER RMS CURRENT OUTPUT DURING FAULT. C) BUILDING #3114 INVERTER CURRENT PASSING THROUGH CIRCUIT BREAKER 2.	80
FIGURE 4.5 A) FAULT IN BUILDING #3114 WHILE ON GRID. B) FAULT IN BUILDING #3114 WHILE OFF GRID.	84
FIGURE 4.6 A) BUILDING #3114 BUS VOLTAGES DURING FAULT ON THAT BUS WHILE OFF GRID. B) BUILDING #3114 INVERTER RMS CURRENT OUTPUT DURING FAULT. C) BUILDING #3114 INVERTER CURRENT PASSING THROUGH CIRCUIT BREAKER #2...	85
FIGURE 4.7 ALL VOLTAGE MEASUREMENTS INSIDE MICROGRID ARE REDUCED TO ZERO DURING FAULTS.	88
FIGURE 4.8 A) FAULT IN BUILDING #3114 WHILE ON GRID. B) FAULT IN BUILDING #3114 WHILE OFF GRID.	90
FIGURE 4.9 A) FAULT ON THE MICROGRID CABLE WHILE ON GRID. B) FAULT IN THE MICROGRID CABLE WHILE OFF GRID.	90
FIGURE 4.10 THREE-PHASE DIFFERENTIAL CURRENT OBSERVED BY THE RELAY FOR A THREE-PHASE FAULT WHILE GRID CONNECTED.	93
FIGURE 4.11 THREE-PHASE DIFFERENTIAL CURRENT OBSERVED BY THE RELAY FOR A THREE-PHASE FAULT WHILE OFF GRID.	93
FIGURE 4.12 A) FAULT ON MICROGRID CABLE WHILE ON GRID. B) FAULT ON MICROGRID CABLE WHILE OFF GRID.	97

List Of Acronyms

CT	Current transformer
DER	Distributed energy resource
DG	Distributed generation
F	Frequency
GTAI	Gigabit transceiver analog input
GTAO	Gigabit transceiver analog output
GTDI	Gigabit transceiver digital input
GTDO	Gigabit transceiver digital output
HIL	Hardware-in-the-loop
HMI	Human-machine interface
P	Real power
PCC	Point of common coupling
PI	Proportional-integral
PLL	Phase lock loop
PV	Photovoltaic
Q	Reactive power
R	Resistance
RTAC	Real Time Automation Controller
RTDS	Real Time Digital Simulator
S	Complex power
V	Voltage
VT	Voltage transformer
X	Reactive impedance
Z	Complex impedance

CHAPTER 1, INTRODUCTION AND GENERAL INFORMATION

The developed world is built around ready access to energy, particularly electrical energy. Electrical infrastructure is on equal terms with water and transportation in terms of the importance of its growth for developing areas, and in the importance of its maintenance in developed countries. Not only are these resources on equal terms of importance, they are interdependent to an extent that each would struggle to operate without the others.

Electrical power and its mastery have enabled the standard of living and industrialization society enjoys and expects. Devices are growing smarter, machines becoming more efficient, and consumers are more ecologically conscious than ever before. In response, electrical infrastructure must grow more reliable, more adaptable, more ecologically responsible, and occupy a smaller footprint in order to keep pace with these changing demands.

Distributed generation (DG) is one possible solution to satisfy these new demands. This philosophy of generating electricity favors generating comparatively small amounts of power, on the order of tens of kilowatts to tens of megawatts. This power is also generated in close proximity to where it is being consumed. This is a radical departure from traditional grid operation where hundreds of megawatts, even gigawatts, are produced in large power plants and transmitted over long distances to serve loads.

The distributed approach has many benefits. It favors many technologies considered either renewable or more environmentally friendly. It also reduces demand on centralized power plants, allowing less favorable technologies to be

upgraded or phased out altogether. DG also promises to reduce transmission line congestion and the need to invest in new transmission infrastructure.

The distributed energy resources (DERs) used in the DG philosophy can be microturbines, photovoltaics (PV), diesel generators, fuel cells, batteries, industrial cogeneration, or any other energy resource that can be installed in close proximity to loads. Dramatically increasing the number of generation sources in the power system will require an equally dramatic increase in the system's communication, coordination, and protection abilities. Organizing sections of the power system containing concentrations of DERs into microgrids has been suggested as a possible solution to these new challenges.

Microgrids

A microgrid, as defined by the U.S. Microgrid Exchange Group, 2010, is a group of interconnected loads and distributed energy resources within clearly defined electrical boundaries that acts as a single controllable entity with respect to the grid. A microgrid can connect and disconnect from the grid to enable it to operate in both grid-connected or island-mode [1]. Microgrids can be conceptualized as electrical islands with the ability to connect and disconnect from the rest of the power system at will.

Microgrids are not a new notion. An early microgrid was created to power the INMARSAT satellite control station in Antarctica in the 1970's [2]. Later, they were proposed as a solution for providing power to remote areas in developing countries unable to construct traditional electrical infrastructure. More recently,

they have received growing interest for use on military bases [3] where the potential benefits of a self-contained electrical system can warrant the added expenditure on microgrid technologies. Military bases are also a convenient proving ground for future microgrid technologies like renewable DERs and electric vehicles that actively participate in system operation. The U.S. Department of Defense and Department of Energy are both pursuing research into the benefits and enabling technologies associated with microgrid deployment. Microgrids are also becoming a viable option for providing a resilient power supply for critical loads like hospitals and shelters during disasters.

Microgrid Structure

Most electrical distribution systems are largely composed of feeder lines radiating from sub transmission substations. Although there is some backfeed ability built in, the system is generally operated in a radial configuration with power flow in a single direction during normal operation. Microgrids, however, are intended to reconfigure connections and redistribute power to maintain service to loads. A loop, or mesh, connected system is thus a more advantageous structure for microgrids, as shown in figure 1.1. Power flows in this system will change constantly based upon balances between local generation and load with power coming from the utility to make up the difference.

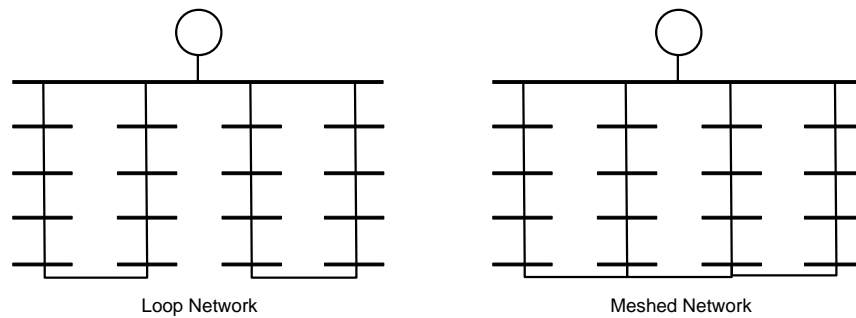


Figure 1.1 Bus configurations for loop and meshed network structures.

Microgrids, unlike most distribution systems, require some level of communication in order to operate, though the amount required remains a subject for debate. The answer will likely be determined by other discussions related to microgrids. For instance, will DERs be owned and operated by utilities or private customers? Also, what will the role of microgrids be within the larger context of the power grid? Answers to these and other questions will likely require microgrids to employ much more communication, control, and automation than typically required for distribution systems.

Introduction to System Protection

The overall objective of system protection is to isolate areas containing disturbances quickly, while preserving the rest of the system. Thus, unacceptable operating conditions are detected and removed, though not prevented. A protection system must meet five criteria in order to perform successfully. These are (1) reliability, (2) selectivity, (3) speed, (4) simplicity, and (5) economy [4]. It is not reasonable to expect all five factors to be maximized in a protection system; therefore a skilled protection engineer is required to manage the tradeoffs.

Protection Reliability

Reliability is generally a measure of the likeliness that system protection will operate as intended. Reliability is the combination of two other metrics, dependability and security. Dependability is the expectation that protection will operate when it is needed. Security is the expectation that protection will not operate when it is not needed. These two requirements are commonly in conflict due to the ambiguous difference between tolerable and intolerable system events. This ambiguity means that the best knowledge source for designing protection systems is usually prior experience, though simulations and staged tests can provide some insight.

Protection Selectivity

Selectivity, or relay coordination, involves the ability of a protective system to operate as quickly as possible for events in its zone of protection while providing time delayed backup to relays in other zones of protection. These zones of protection would commonly enclose a single bus, line, or piece of equipment [5]. Time delay on relays is necessary to allow relays near faults a chance to isolate the problem. This can be accomplished in overcurrent relays by using more than one definite time setting with longer time delays for lower pickup currents. For an inverse time overcurrent characteristic, the time delay can be set appropriately in order to coordinate with other relays in the system. This is covered in more detail in chapter two.

The goal of protection selectivity is to ensure that the portion of the system taken out of service is minimized while still completely isolating the problem. Therefore, operation of relays outside the immediate vicinity of the fault is only desirable when relays near the fault have failed to operate. The benefit of high selectivity in a protection system is to provide maximum continuity of service to customers while minimizing lost revenues, fines paid, and equipment damage.

Protection Speed

Speed is simply the minimum fault duration allowed by the protection system. Fast isolation of faults helps to minimize equipment damage and system instability resulting from disturbances. The desire for protection speed can be at odds with the desire for protection selectivity. This is especially true where relay coordination comes into play, where increasing operation speed can increase the number of unwanted operations.

Using high-speed relays and circuit breakers can increase the speed of protection. A high-speed relay, by definition, operates in less than three cycles, while instantaneous relays have no intentional operational delay [6]. Though their definitions differ, the two categories operate almost identically, and the terminology is used interchangeably. High-speed circuit breakers will typically operate in one to three cycles.

Implementing high-speed protection on transmission lines is more difficult than with buses or other equipment. This is largely due to the large distances spanned by most transmission lines [7]. Communications assisted protection

schemes must communicate over long distances, which can be complicated and expensive. Protection schemes without communication may be slower because they are dependent exclusively on local information that may not reveal a complete picture of the overall system state.

Speed is not always as important in low voltage parts of the system, though it is certainly not trivial. These tend to be distribution systems where relay coordination is simpler and a brief fault is unlikely to significantly impact system stability. Speed can also be reduced when high impedance faults occur. The high impedance of the fault will limit the available fault current, making the fault more difficult to detect. The presence of DERs on a line can also blind the protection by feeding the fault, resulting in reduced fault current through the relays. This will be discussed further in chapter two.

Protection Simplicity

Simplicity is important to protection systems because of the role it plays in protection reliability. Each component in a protection system is likely individually reliable. However, by increasing the number of components dependent on one another, the overall reliability is decreased and the likelihood of problems increased. The potential benefit of each additional component must be weighed against the increased potential for failures, required maintenance, and the cost incurred as a result of a protection failure.

Protection Economics

Costs in power systems cannot be ignored, and protection equipment can be expensive. However, lower priced protection equipment may have higher maintenance, installation, and operating costs. The cost of the equipment being protected can be many magnitudes higher than the cost of quality protection. Likewise, the cost associated with lost revenues due to service outages is very high. Utilities can also be held responsible for equipment damage resulting from problems on the distribution system. The expense to appropriately protect the system is almost always justifiable in light of the consequences for a protection failure. That being said, there is always a price at which return on investment begins diminishing.

Electromechanical Relays

Electromechanical relays have been the primary technology used for power system protection for several decades. Multiple designs exist but one of the oldest and most instructive models is the induction disk relay. This design is useful for demonstrating the principles of electromechanical relay operation, which, initially, was very similar to the operation of induction disk watt-hour meters.

Current on the secondary side of a current transformer (CT) creates flux in the core of a driving electromagnet. The air gap of this driving magnet is designed to provide two slightly separated flux paths through a metal disk. The amount of flux traveling through the second path is altered with the addition of

either shading coils or rings resulting in the fluxes shown in equations (1.1) and (1.2).

$$\phi_1 = \Phi_{1M} \sin(\omega t) \quad (1.1)$$

$$\phi_2 = \Phi_{2M} \sin(\omega t + \theta) \quad (1.2)$$

These fluxes create a potential difference between them and corresponding current flow in the disk. The current from path one reacts with the flux in path two, and vice versa, producing two opposing forces, equations (1.3) and (1.4), that act on the disk. The resulting net mechanical force is shown as the sum of the two forces in equation (1.5).

$$i_{\phi_1} \propto \frac{d\phi_1}{dt} \propto \Phi_{1M} \cos(\omega t) \quad (1.3)$$

$$i_{\phi_2} \propto \frac{d\phi_2}{dt} \propto \Phi_{2M} \cos(\omega t + \theta) \quad (1.4)$$

$$F = F_2 - F_1 \propto (\phi_2 i_{\phi_1} - \phi_1 i_{\phi_2}) \quad (1.5)$$

Because this force is acting tangentially to the edge of the disk, the resulting torque attempts to rotate the disk, shown in equation (1.6), where α is the phase difference between the currents resulting from the effect of the shading

coil. However, a restraining magnet is situated opposite the driving magnet to resist the applied torque on the disk. A spring is also included to augment the restraining magnet and reset the relay after the fault is cleared. By carefully calibrating the amount of restraining torque, the relay can be set to operate only when input currents rise above a predetermined threshold. This parameter is referred to as the pickup current, denoted I_p .

$$\tau = kI_1I_2 \sin \alpha \quad (1.6)$$

When the disk rotates sufficiently, contacts mounted to the disk complete the electrical circuit controlling the circuit breaker. One contact is fixed to the rotating disk and the other is stationary beside the disk. Because the disk will rotate at a rate proportional to the magnitude of the input current, setting the distance between the two contacts, denoted TD , will set the relay operational time delay. This gives protection and coordination engineers the ability to customize protection schemes for each application. Additionally, different designs and configurations will have different operating characteristics for the same settings. Equation (1.7) is the general equation for inverse time overcurrent relay tripping [8]. Equation (1.8) is used for resetting overcurrent relays after tripping. Table 1.1 lists the coefficients of A , B , and P used to define some of the more commonly used operating characteristics.

$$t_{op} = TD \left(B + \frac{A}{\left(\frac{I}{I_p}\right)^P - 1} \right) \quad (1.7)$$

$$t_{reset} = TD \left(\frac{T_R}{1 - \left(\frac{I}{I_p}\right)^2} \right) \quad (1.8)$$

The differences in the different characteristic curves are shown in figures 1.2 and 1.3. This also shows that the same type of curve has different definitions in US and IEC standards.

Table 1.1 Inverse Time Overcurrent Relay Characteristic Coefficients.

<i>Characteristic</i>	<i>A</i>	<i>B</i>	<i>P</i>	<i>T_R</i>
US Moderately Inverse (U1)	0.0104	0.0226	0.02	1.08
US Inverse (U2)	5.95	0.1800	2.0	5.95
US Very Inverse (U3)	3.88	0.0963	2.0	3.88
US Extremely Inverse (U4)	5.67	0.0352	2.0	5.67
US Short Time Inverse (U5)	0.00342	0.00262	0.02	0.323
IEC Standard Inverse (C1)	5.64	0.0	0.02	13.5
IEC Very Inverse (C2)	13.5	0.0	1.0	47.3
IEC Extremely Inverse (C3)	80.0	0.0	2.0	80.0
IEC Long Time Inverse (C4)	120.0	0.0	1.0	120.0
IEC Short Time Inverse (C5)	0.05	0.0	0.04	4.85

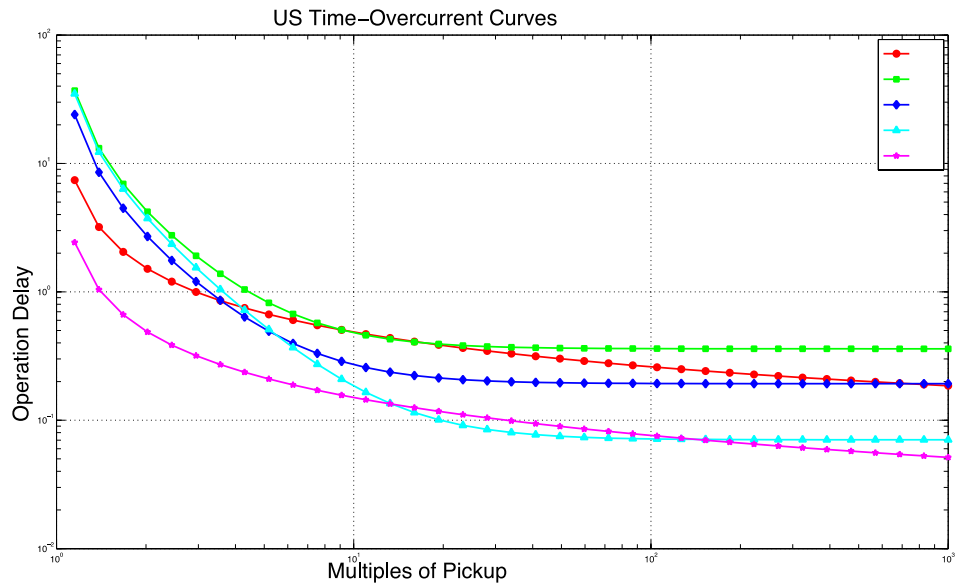


Figure 1.2. US time overcurrent characteristic curves (TD = 2.0 seconds.)

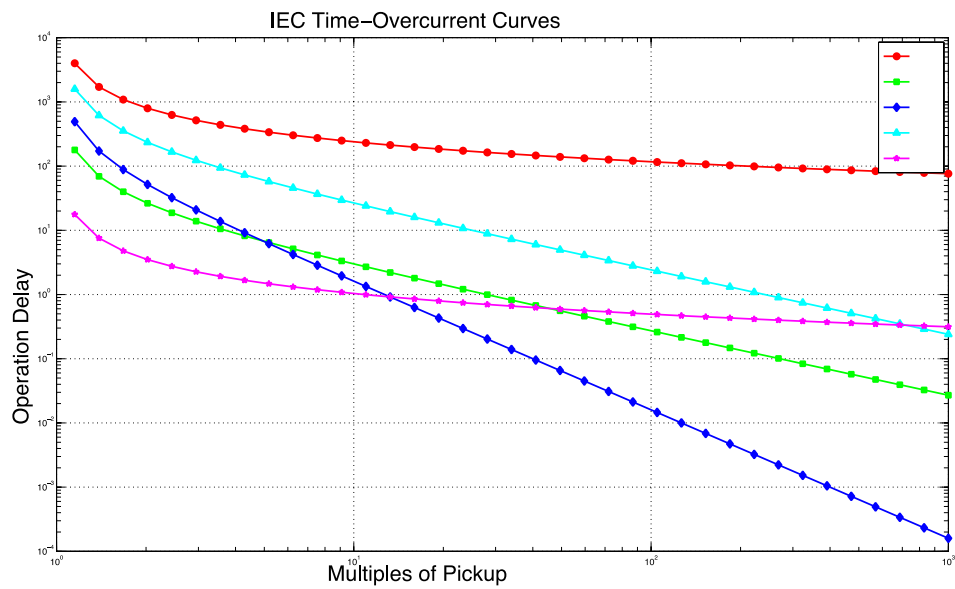


Figure 1.3. IEC time overcurrent characteristic curves (TD = 2.0 seconds.)

Digital Relays

As with most other technologies, microprocessors are changing how protection equipment is designed. Digital relays are replacing the old electromechanical relays, particularly in new installations. Yet, the work required to retrofit an existing installation with digital relays is slowing their adoption into existing systems.

Circuit breakers only require a DC voltage from either a battery or station auxiliary power system in order to operate. The role of the relay is to act as an intelligent switch in this DC circuit, opening and closing contacts, which, in turn, control the circuit breakers. Even though the relay may be digital, the contacts inside it are still mechanical. The various contacts are likely to be driven by a cam inside the relay.

These new relays have many advantages over their predecessors. Because digital relays are microprocessor based, they are able to accommodate multiple setting groups. Control logic can also be customized because the operating characteristics are implemented computationally rather than as a function of the relay design. Because digital relays do not rely on their design to produce an operating characteristic, they are capable of implementing several protection elements and metering functions in a single device. The analog to digital conversion used in digital relays also has a lower burden than the electromagnetic systems. A full complement of communication ports allows for

communication assisted tripping as well as coordination between relays using an automation controller or other supervisory system.

The result of all these capabilities is that protection systems, which used to occupy entire buildings and require manual setting, now occupy a single cabinet and can be managed remotely. It is worth noting that despite the numerous advantages of digital relays, electromechanical relays still make up the majority of systems in service. Concerns over the digital relay's ability to operate when the system is down, and the effort required to set them cause many protection engineers to stick with the older models. This again demonstrates the paramount importance of reliability and experience in designing protection systems.

Real Time Automation Controller

The real time automation controller (RTAC) is an imbedded controller designed for substation controls and industrial applications [9]. This microprocessor-based system has a variety of communication ports and a real time operating system with customizable functionality, making it ideal for protection system coordination. Additionally, the RTAC can host a human-machine interface (HMI) to enable protection engineers to easily monitor and control the system remotely via a web interface.

The RTAC is also a convenient platform for gathering and concentrating data about the current state of the system. Information can be retrieved via the web interface, removing the need for protection engineers to travel to the

substation in order to change settings and monitor operation. This is especially useful for examining event reports after the fact to determine exactly what the relay was measuring when it decided to operate, and the values of specified system tags.

Real Time Digital Simulator

The Real Time Digital Simulator (RTDS) is a high resolution, real time simulation tool used for power system studies and research. RTDS is distinguished from other simulation technologies by its real time simulation ability, which is aimed at performing hardware-in-the-loop (HIL) testing.

RTDS power system simulations operate with a $50\mu\text{s}$ time step. This is equivalent to 333 samples per electrical cycle, plenty of resolution for most power system studies. This resolution can be increased slightly if needed. Controls and power electronics simulations typically require higher resolution simulation than power systems, however. This higher resolution is needed to accurately simulate high switching frequencies and for the calculations used in the power electronic controls. For this, RTDS uses a $5\mu\text{s}$ time step, equivalent to 3333 samples per cycle. Simulating power electronics in this smaller time step requires special models designed for small time step simulation, all of which must be placed in specially defined small time step subsystems. A large to small time step transformer is used in the simulation to link the two parts of the model.

RTDS is able to interface with external equipment using four different types of I/O cards. Gigabit transceiver analog input (GTAI) and output (GTAO)

cards are used to handle analog signals. The ports on the GTAO and GTAI cards can handle signals between ± 10 volts. Signals output with the GTAO card refresh every $1\mu s$ but are only voltage signals [10]. Signals requiring current must make use of an external power amplifier. GTAI ports refresh every $6\mu s$. Because these ports are not capable of handling large magnitude signals directly, scaling is usually required in order to move signals through these ports. It is assumed that most signals will require scaling so this function is built into the GTAO connection control block in the simulation model. The scaling must also be taken into account by externally connected equipment.

Forced real time simulation is a strength and weakness of RTDS. It is very useful for conducting hardware-in-the-loop testing. However, the number of available processors limits the size and detail of a simulation. RTDS is designed only for real time simulations, so there is no provision for simulating slower in order to increase the simulation size. Upgrading the RTDS capabilities is straightforward as it is designed to be scalable and multiple cubicles can be tied together with an Ethernet connection. RTDS hardware is expensive. Connection cards typically cost a few thousand dollars each, processor cards tens of thousands of dollars, and whole cubicles hundreds of thousands of dollars. The RSCAD software is also very expensive.

Thesis Outline

This section outlines the structure of the thesis and provides a brief summary of topics covered in each chapter.

Chapter 1 – A definition of a microgrid, its structure, and historical use is covered. Key concepts used to evaluate protection systems are discussed. The operation of electromechanical relays is used to explain the physical basis for relay operating characteristics. The advantages of digital relays and the RTAC are also briefly discussed. RTDS is also introduced.

Chapter 2 – Control methodologies used for transmission systems are introduced. These include real and reactive power (P&Q) control, and frequency and voltage (F&V) control. Then applications of these methodologies are formed for microgrid systems and the required changes detailed. The challenges associated with protecting a microgrid system are discussed. Methods used to create an RTDS model of a microgrid for protection studies are shown. Applicable protection schemes are outlined. The background for the genetic algorithm used to tune model controls is also discussed.

Chapter 3 – A detailed discussion of the microgrid model is given. The genetic algorithm used to tune the controls is also described in detail. The construction of the testing apparatus is discussed along with the communications settings and user defined logic used.

Chapter 4 – Testing is conducted on a time overcurrent scheme, and a time overcurrent scheme with two setting groups. Testing is attempted on a time overcurrent scheme with the addition of directional control and the difficulties are discussed. A differential scheme making use of overcurrent relays to implement differential protection is also evaluated.

Chapter 5 – Results of testing are discussed and conclusions are drawn.
Recommendations for future work are also made.

Appendix – Connection diagrams and code created for the project are
included in this section.

CHAPTER 2, LITERATURE REVIEW

This chapter introduces general generator control methodologies, including real and reactive power control, frequency and voltage droop control, and fault current limiting control. Specific control topologies used to accomplish these objectives are also presented. Methods of modeling microgrids and utility interconnections are explained along with considerations for adapting transmission control strategies for use in microgrids. Relevant relay protection strategies are also explained. Finally, the theoretical background for the genetic algorithm used for control tuning is presented.

Real and Reactive Power Control

Controlling real and reactive power injected into the electrical system is a common objective for grid-connected generators of all sizes. Power flow in a transmission line is described in equation (2.3) where P is real power, Q reactive power, S complex power, V_1 the voltage at the sending end of the line, V_2 the receiving end voltage, I the current flowing in the line, and Z the complex impedance of the line.

$$P + jQ = S = V_1 I^* = V_1 \left(\frac{V_1 - V_2}{Z} \right)^* \quad (2.1)$$

$$P + jQ = V_1 \left(\frac{V_1 - V_2 e^{j\delta}}{Z e^{-j\theta}} \right) \quad (2.2)$$

$$P + jQ = \frac{V_1^2}{Z} e^{j\theta} - \frac{V_1 V_2}{Z} e^{j(\theta + \delta)} \quad (2.3)$$

Separating this equation into its real and imaginary parts yields the specific equations for real and reactive power flow in a transmission line, shown in equations (2.4) and (2.5).

$$P = \frac{V_1^2}{Z} \cos \theta - \frac{V_1 V_2}{Z} \cos(\theta + \delta) \quad (2.4)$$

$$Q = \frac{V_1^2}{Z} \sin \theta - \frac{V_1 V_2}{Z} \sin(\theta + \delta) \quad (2.5)$$

Substituting $R + jX$ for $Z e^{j\theta}$ allows equations (2.4) and (2.5) to be rewritten in terms of resistive (R) and reactive (X) impedances, equations (2.6) and (2.7).

$$P = \frac{V_1}{R^2 + X^2} [R(V_1 - V_2 \cos \delta) + X V_2 \sin \delta] \quad (2.6)$$

$$Q = \frac{V_1}{R^2 + X^2} [-R V_2 \sin \delta + X(V_1 - V_2 \cos \delta)] \quad (2.7)$$

Generally speaking, R can be assumed to be considerably smaller than X for overhead transmission lines [11]. Because $X \gg R$, R can be neglected for these lines. Also, the power angle δ is assumed to be small, meaning that the

approximation $\sin\delta = \delta$ and $\cos\delta = 1$ is valid. These assumptions allow equations (2.6) and (2.7) to be simplified for cases involving overhead transmission lines to equations (2.8) and (2.9).

$$P = \frac{V_1 V_2}{X} \delta \quad (2.8)$$

$$Q = \frac{V_1(V_1 - V_2)}{X} \quad (2.9)$$

Equation (2.8) reveals that real power flow from one end of a transmission line to the other is assumed to be directly proportional to the phase difference δ between the two ends of the line. Likewise, equation (2.9) shows that reactive power flows from high to low voltage ends of the line and is proportional to the difference between the two voltages. Therefore, controlling the power angle δ between a generator and the point of interconnection with a system will allow the real power injection to be controlled. Controlling the voltage of the generator relative to the system voltage will allow for control of reactive power injection or consumption. It should be restated, however, that these relationships are based on the assumption that $X \gg R$. In a lower voltage system, this assumption is not always valid.

Frequency and Voltage Droop Control

Frequency and voltage are the two most important parameters for maintaining system operation. Synchronous generators in the U.S. will attempt to operate at a constant 60 Hz frequency. The electrical system frequency, however, is subject to deviations caused by mismatched generation and load. Insufficient generation to service connected loads will cause the system frequency to drop, whereas the opposite will cause the frequency to increase. This makes sense when the power grid is imagined to be a large rotating machine. Injecting more power than is being taken out will cause this conceptual machine to spin faster as the spare energy is converted into rotational momentum. Significant frequency deviations will cause generators and loads to start disconnecting from the system to prevent equipment damage. This increases the potential for system instability, as other generators will try to pick up additional load to balance the generation and load; potentially exceeding their own limits and being removed from service themselves.

System voltage deviations can occur for a variety of reasons, including system faults, lack of reactive power to support voltage, and extreme load behavior. Like frequency deviations, system voltage deviations will cause machine damage, and system instability. High voltage will cause insulation problems throughout the system and connected machinery and can potentially burn out lighting and electronic systems. Low voltage is also a major problem because motors will start to increase the amount of current they draw in order to

satisfy their power demand, eventually exceeding their current rating. Motors will also eventually stall in low voltage conditions, prolonging the voltage recovery period after a disturbance.

When the assumptions from equations (2.8) and (2.9) are valid, frequency deviations are proportionally related to real power injection into the system, so long as load remains constant over the period the frequency is measured. This proportionality allows a constant gain to be used to equate the two parameters, shown in equation (2.10) [12].

$$f - f_0 = -k_p(P - P_0) \quad (2.10)$$

This equation is implemented in a variety of control systems aimed at regulating system frequency. The main systems are generator governors, automatic generation controls, and manual transmission system controls. These all differ in the scope of their influence and how rapidly they respond, but they are all using this principle in order to regulate the system frequency.

Voltage control operates on a similar principle. The voltage at the point of connection relative to the voltage of the generator is proportionally related to the amount of reactive power being injected into the system. Therefore, an equation similar to (2.10) can be formulated to control the system voltage at the point of system connection, equation (2.11).

$$V_1 - V_2 = -k_q(Q - Q_0) \quad (2.11)$$

Synchronous machines, generators, and condensers, are the most effective devices for controlling system voltage with reactive power support, but they are not the only devices with this capability. Shunt reactors, series and shunt capacitors, and other grid-connected technologies are also capable of injecting reactive power. In fact, many of these other technologies are preferable in most cases because large rotating machines are very expensive and have a large footprint, making them an unlikely choice in a distribution system. Control of voltage in this manner must also be somewhat restrained so that the voltage at the generator terminals does not exceed the machine ratings.

Application of Existing Generation Controls to Microgrids

Several control schemes can be applied to DERs in microgrids to accomplish either frequency and voltage regulation or direct real and reactive power control. These schemes all require voltage and current measurements at the point of interconnection in order to synchronize with the grid and to estimate how much real and reactive power is being injected into the system.

If the microgrid is a low voltage system, the frequency and voltage controls will be unlikely to work properly if they are based on the same assumptions as high and medium voltage frequency and voltage regulation. Typically $X \gg R$ in high and medium voltage systems, but low voltage systems tend to be more resistive than inductive. This means that the relationships between P, F, Q , and V are no longer approximately linear. Because these relationships are no longer approximately linear, a simple droop setting will no

longer be sufficient. Instead a separate, non-linear, control system is required to control F and V in place of P and Q .

Set points and modes of operation can either be set by the owner of the DER or obtained from a microgrid controller via a communication channel. Each has its merits and demerits. For instance, centralized DER control in a microgrid is desirable because problems with load sharing are avoided and the microgrid is able to work together as a whole in order to preserve frequency by matching load and generation. However, costs associated with centralized control are higher due to communication and control hardware that must be installed, serviced, and powered. This may be especially true when microgrids cover large areas or where many DERs are installed. If the DERs are not owned directly by the utility, the equipment owners may also be reluctant to relinquish control of their private equipment to the utility company. This scenario avoids the capital expenditure on the part of the utility but would make organized microgrid control problematic.

Allowing DERs to be controlled independently of a central control hierarchy is advantageous because it avoids the need for communications between a central controller and every generator in the microgrid. Yet, in this scenario it is difficult to ensure that enough generating assets will be available to match load should the microgrid be suddenly islanded. Also, an adequate number of DERs would need to be operating on frequency and voltage droop control in order to regulate the system operation, a difficult problem if operation modes are left to private owner's choice.

It is also worth mentioning again that the assumptions made in developing equations (2.10) and (2.11) are not necessarily valid in a low voltage microgrid because the system is no longer overwhelmingly inductive, meaning that the F and V controls become more complex and more sensitive to system changes. Also, the average DER may not have enough capacity to regulate frequency and voltage without the help of other DERs providing some real and reactive power. There would be no way of guaranteeing this aid if set points and modes of operation are left entirely at the discretion of private DER owners.

Furthermore, the most economic sharing of load is unlikely to be achieved. A high concentration of DERs on a single line could even completely bar other DERs on the same line from generating because doing so would create an overvoltage on the line. This scenario undermines the economic benefit associated with installing DERs to sell power back to utilities.

The ideal scenario for a privately owned DER would be a plug and play system. This sort of system would only require installation and connection to the microgrid. Any sort of communication would be forgone and the DER would only be concerned with either injecting maximum power into the microgrid, subject to voltage constraints, or regulating frequency and voltage at the point where it is connected to the microgrid without having to custom tune and update the DER controls for each new installation. When such a plug and play DER control solution is developed, decentralized microgrids will be able to take advantage of the cost savings from forgoing the communications infrastructure and making participating in microgrid generation more accessible to the private sector.

Modeling A Microgrid System

Models commonly used for distribution system protection studies resemble models used for dynamic simulation studies in transmission systems. Utility connections are assumed to be ideal sources capable of providing fault currents five or six times higher than the load current. Systems are also generally connected radially with power flowing in one direction. This system topology is considered to be static, never changing how the various lines are connected. This sort of configuration lends itself to easily identifying fault currents and producing relay settings to effectively protect the system.

However, these assumptions do not necessarily apply to microgrids. The presence of DERs and increasingly interconnected systems can create bidirectional power flow. The effect of an ever-changing topology within the microgrid is that a single set of overcurrent relay settings will struggle to adequately protect the microgrid in all situations without misoperation. Therefore, in order to set microgrid overcurrent protection, multiple scenarios must be analyzed. To conduct HIL tests, a complete model, including controls, sources, loads, and cables must be created. A hardware test bed must be created as well if physical relays are to be integrated into the simulation.

Modeling Utility Connections

The connection of the microgrid to the utility need not be exhaustively modeled in order to accurately model microgrid operation. This is because the utility can usually be assumed to be much more robust than the microgrid itself

and any internal microgrid change or disturbance will have a negligible effect on the utility. Given that the power grid is composed of synchronous generators working in unison to manage frequency and voltage, it is reasonable to model the connected utility as a single synchronous generator with a generation capacity much larger than what the microgrid can provide. If the utility capacity is sufficiently larger than the microgrid, the utility can be further simplified to an ideal voltage source [13].

Modeling Distributed Energy Resources

Distributed energy resources can be rotating machine or inverter based. Modeling the machines and inverters themselves is straightforward, given that the machine or inverter parameters are available. Neatly packaged models for these sources are generally included in simulation packages. The controllers for these resources, however, may not be premade and require some amount of effort to model. Because the microgrid system, described in chapter three, to be modeled only contains inverter-based resources, the controls examined in this thesis will be specific to grid-connected inverters.

The first requirement for controlling a grid-connected inverter is accurate measurement of the system phase and frequency at the point of common coupling (PCC) of the inverter. This is accomplished with a phase lock loop (PLL). Measuring the voltage phase angle at the PCC is necessary for synchronization of the inverter control signals with the system. Controlling the phase difference between the inverter and system will be an important part of the

control method. PLLs are almost always included with simulation packages meant for simulating power electronics.

The most common control mode used by grid-connected inverters is control of the real and reactive power delivered to the grid by the DER. This introduces the need to calculate the power being delivered by the inverter. This can be done in the normal time domain or by transforming the voltage and current measurements into either the stationary $\alpha\beta$ or rotating dq reference frame using the conversion matrices in equation (2.12) and (2.13). Controlling inverters in either the $\alpha\beta$ or dq reference frame offers the advantage of time invariant controls. Time variant controls are difficult to implement because of their dependency on the time domain to perform calculations. Consequently, time invariant controls are usually preferable to time variant controls.

$$\vec{V}_{\alpha\beta\gamma} = \sqrt{\frac{2}{3}} \begin{bmatrix} 1 & -\frac{1}{2} & -\frac{1}{2} \\ 0 & \frac{\sqrt{3}}{2} & -\frac{\sqrt{3}}{2} \\ \frac{1}{\sqrt{2}} & \frac{1}{\sqrt{2}} & \frac{1}{\sqrt{2}} \end{bmatrix} * \vec{V}_{abc} \quad (2.12)$$

$$\vec{V}_{dq0} = \sqrt{\frac{2}{3}} \begin{bmatrix} \cos \theta & \cos(\theta - \frac{2\pi}{3}) & \cos(\theta + \frac{2\pi}{3}) \\ -\sin \theta & -\sin(\theta - \frac{2\pi}{3}) & -\sin(\theta + \frac{2\pi}{3}) \\ \frac{1}{\sqrt{2}} & \frac{1}{\sqrt{2}} & \frac{1}{\sqrt{2}} \end{bmatrix} * \vec{V}_{abc} \quad (2.13)$$

The direct power control method uses the $\alpha\beta$ reference frame to control real and reactive power directly. This method is similar to the direct torque control

technique and uses no internal current loops or pulse width modulation component, working on the error between power set points and estimated power output obtained through power calculations. The advantage to this control strategy is its simplicity, although it does require a high sampling frequency [12]. The specifics of this control strategy and variations of it are discussed in detail in chapter three.

Microgrid Protection Challenges

The unique structure of microgrids makes their protection challenging. DERs, non-radial systems, and changing utility connections create several problems, not present in traditional distribution systems, which must be overcome before microgrids can see wide acceptance.

Fault Isolation

In a radially connected system, fault isolation means opening the circuit breaker closest to the fault between the fault and the substation the feeder is connected to. This means that all loads beyond the fault will lose power, though in a radial system without DERs this is unavoidable. Therefore, opening more than one breaker is unnecessary, as the end result is the same. This makes coordinating overcurrent relays simple. All that is required is to simulate a fault at the far end of the line and set pick up currents and time delays such that the relays operate with the desired coordination time interval, usually 12-15 cycles.

A microgrid system, with its potentially non-radial structure and DERs, is a more difficult system for fault isolation. Now it is essential to open breakers at both ends of a line in order to prevent DERs from feeding a fault on the line, as shown in figure 2.1. Likewise, all the breakers on a faulted bus must be opened instead of just the one on the line feeding the bus. This is difficult because fault currents coming from different directions could be very different depending on the way the system is connected.

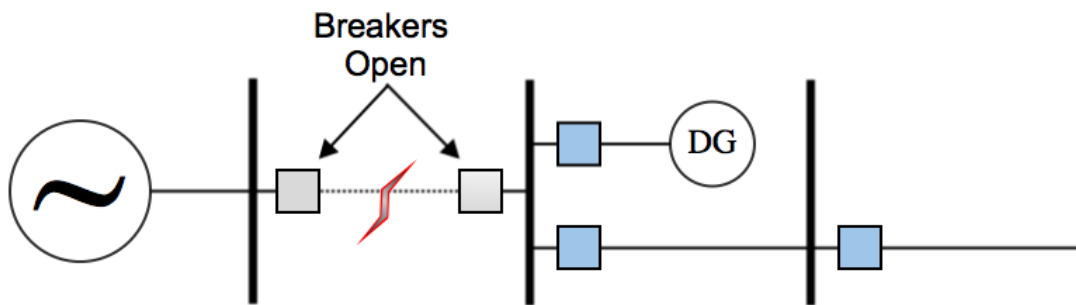


Figure 2.1 Fault isolation in system with DERs.

Fault isolation can also be a problem when auto-reclosing schemes are used and DERs feed faults, preventing the ionized path inside the circuit breaker from dissipating. Some additional loss of mains protection would be needed to detect this condition and shut the DER off so the ionized path could dissipate and the fault clear. This is likely only a concern for medium and high voltage microgrid systems with powerful generation sources.

Decreased Fault Current

The difference in available fault current is the most severe challenge for using overcurrent protection in microgrids. Fault current from the utility is usually

easy to distinguish from load current within the microgrid. This is because the utility connection tends to behave like a large synchronous machine during faults, outputting several times the rated current.

With so much fault current is available from the utility, the limiting factor in the system is the current ratings on the lines. Therefore, the protection is set above the current rating for the lines, knowing that current at this level is almost certainly due to a fault. This includes the choice of CT ratios and relay settings. The protection is set above the continuous current rating of the lines so that the system can be loaded to its maximum without the protection operating.

When the microgrid disconnects from the utility, the limiting factor in the system is no longer the line ratings. Most often, the generation in the microgrid will be much less than the power the utility can provide. Therefore the limiting factor is now the maximum output of the DERs. Rotating machines used as DERs are capable of providing fault currents much higher than the maximum rated current, but this increase is limited by the size of the machine. The result is nothing like the fault current provided from the utility. In addition, inverter based DERs will provide even less fault current. Individual inverter output varies based on the model and control scheme used but typical values can range from 110 to 200% rated current during faults. An example of this difference is shown in the fault current calculations for line 2-3 of a real system is shown in table 2.1. This system is detailed in chapter three.

Table 2.1 Calculated fault currents in microgrid using CAPE.

<i>Fault On Bus 3</i>	<i>Line 1-2 (A)</i>	<i>Line 1-3 (A)</i>	<i>Line 2-3 (A)</i>
On Grid	4819.5	0.0	4819.5
Off Grid	0.2	0.0	359.8

False Tripping

When a fault occurs on a looped or meshed system, currents will tend to alter their flow direction to feed into the fault. In a microgrid distribution system this can occur where multiple feeders attached to the same bus or substation have DERs installed on them. Normally, the current provided by the DERs will flow to the loads on that line, with some excess flowing to other lines connected to the same substation bus. However, a fault on one of these lines will cause almost all of the current from DERs connected to lines from the substation to travel through the substation or bus and down the faulted line, as shown in figure 2.2.

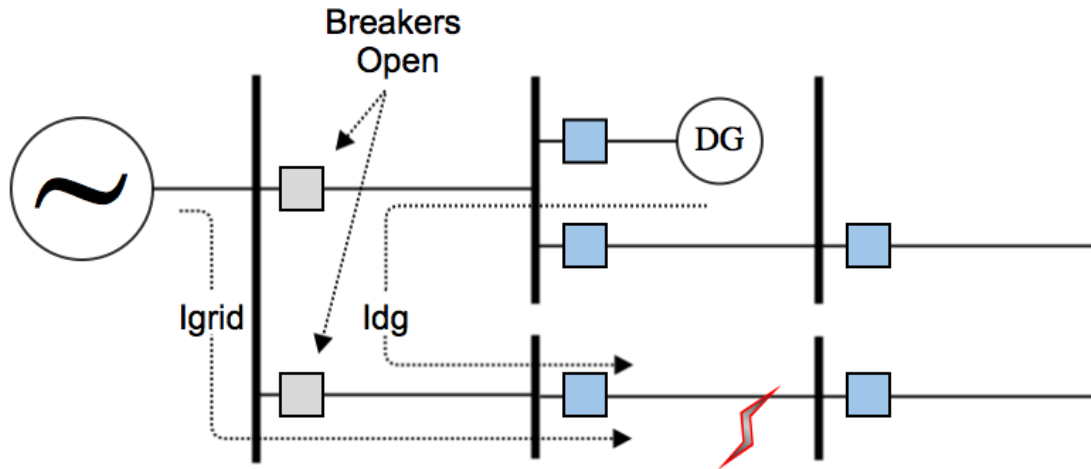


Figure 2.2 False tripping for fault on parallel line.

This fault current provided by DER units will have to pass through the healthy part of the system in order to reach the fault. Depending on the type of DER and the sensitivity of the line relay settings, this can cause the relay on the healthy line to operate on overcurrent [13]. This problem could be very prevalent on a short line with DG units because the relay near the substation would likely have a much lower time delay setting than a relay on a long line where multiple coordination intervals have to be accounted for.

Increasing the time delay for the affected relay on the healthy line could potentially solve this problem. Increasing the time delay, however, may not be practical, as faults on that line would then take longer to clear. Adding directional elements to relays protecting line terminals connected in parallel to other lines could be another possible solution.

Protection Blinding

Adding a DER unit to a line can have the unintended effect of blinding protective relays at the sending end of the feeder to faults occurring beyond the DER unit. In a radial system without DG units the protection would be set up for a two-phase fault at the remote end of the line. Faults at the remote end would cause the predicted large surge of current feeding into the fault. A DER in between the fault and feeder substation would add to the overall fault current at the fault location. However, the two sources are now in parallel with respect to the fault, so they split the fault current contribution. As a result, the current increase from the substation when the fault is applied is less dramatic. This phenomenon, if pronounced enough, can delay protection operation, even preventing it from operating until the DER is taken out of service [14].

A case study for this protection problem is given in [13], and [15]. In this example the protection-blinding problem is studied in the context of a medium voltage microgrid system. It is likely that this problem would apply mostly to such medium and high voltage microgrid systems where DERs can have much larger generation capacities than those found in a low voltage microgrid.

Protection Schemes

Many protection schemes exist and each one has advantages and disadvantages in each application. The following is a discussion of a few schemes to be tested for application to microgrids.

Overcurrent Protection

Protecting electrical systems using overcurrent detection is the simplest and most widespread form of distribution system protection. This can be accomplished using either fuses or overcurrent relays and circuit breakers. This protection detects the increased phase or ground current, depending on how it is connected, which results from the sudden decrease in impedance caused by faults. While fuses are a type of overcurrent protection, they are not used for coordinated system protection. Because they are not resettable, fuses are more often used as a last resort for isolating equipment threatened with damage due to an uncleared fault.

A combination of relays and circuit breakers are most often the choice for primary system protection. Circuit breakers are different from fuses in that they isolate faults by mechanically opening contacts instead of melting at a prescribed current level like a fuse. Relays control circuit breaker operation based on a defined operation characteristic, discussed in chapter one. These well defined characteristics, coordination ability, and ability to reset, make relays and breakers far more preferable to fuses for primary system protection.

Overcurrent protection is in widespread use because of its low cost relative to other techniques. This protection strategy tends to be the least expensive option because it only requires CTs to operate. Other schemes may require voltage transformers (VTs) in order to operate. CTs are usually less expensive than VTs because they are not physically attached to the power line, whereas a VT must be rated for the full phase to ground voltage of the line.

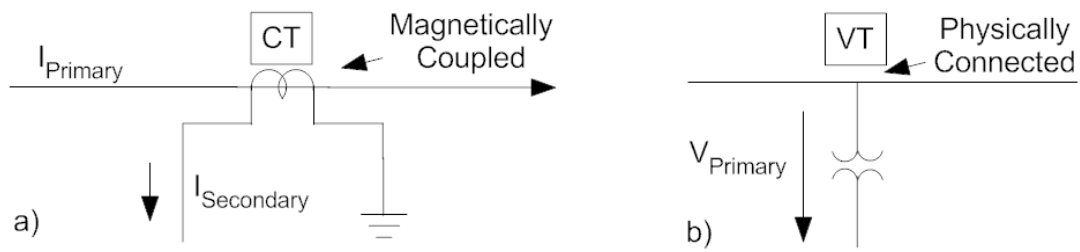


Figure 2.3 a) Current transformer connection. b) Voltage transformer connection.

In this case the less expensive solution is not a trade-off in reliability. Overcurrent protection has proven adequate for radially connected distribution systems, where the goal is to remove faulted lines and prevent damage to the distribution system and connected machines. Inverse time overcurrent relays are able to take advantage of the unidirectional power flow in this configuration to make protection coordination relatively simple [7].

In figure 2.4 CTI refers to the coordination time interval between relay settings. This CTI is typically 12-15 cycles.

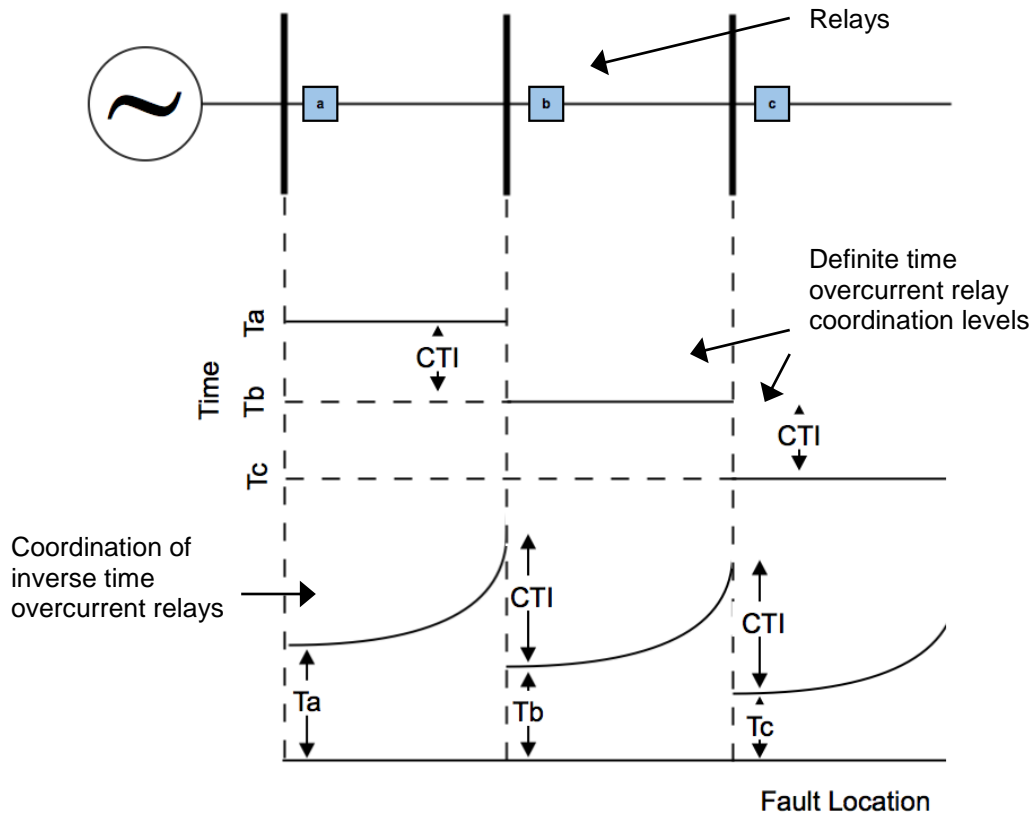


Figure 2.4 Coordination of overcurrent relays in a radial system.

In addition to time overcurrent operation, overcurrent relays can be set to operate instantaneously when measured current exceeds a set limit. This sort of operation is useful when no coordination is required and large inrush currents are not expected. This instantaneous operation can also have a set time delay incorporated, known as a definite time element. Digital relays are typically able to operate in all these modes simultaneously with instantaneous and definite time settings above the expected inrush currents to guarantee that large fault currents will be detected and cleared as quickly as possible.

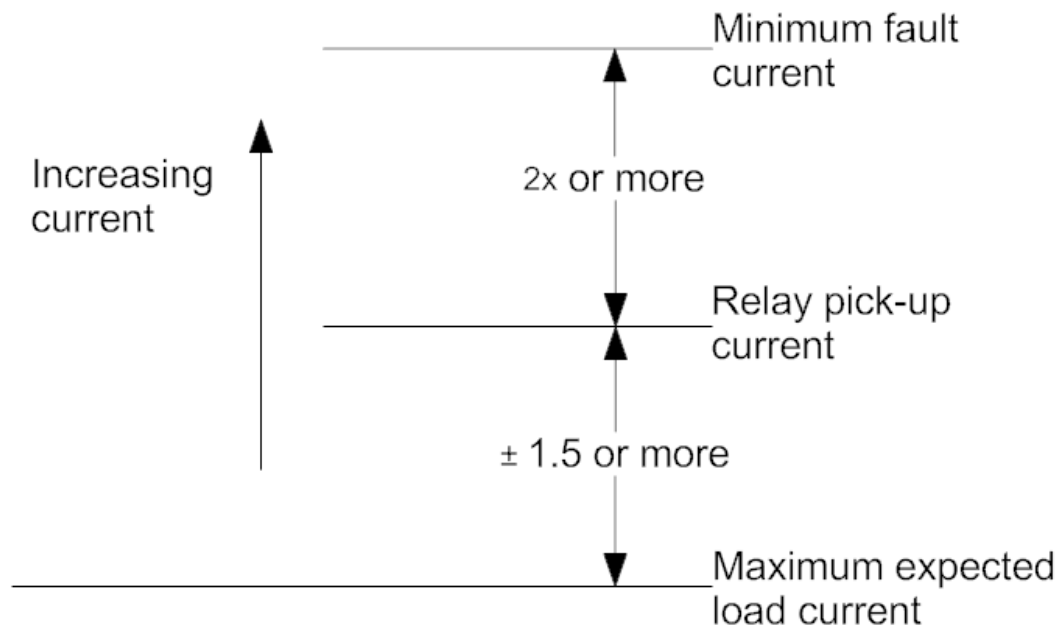


Figure 2.5 Rules of thumb for setting overcurrent relays.

Directional Overcurrent Protection

Directional overcurrent elements are used to supervise relay operation, making it sensitive only to faults in the desired direction. This is accomplished by comparing the measured operating current from the system to a polarizing quantity. Many directional relay designs exist, and each one is polarized differently and has different maximum torque, operation, and restraint characteristics.

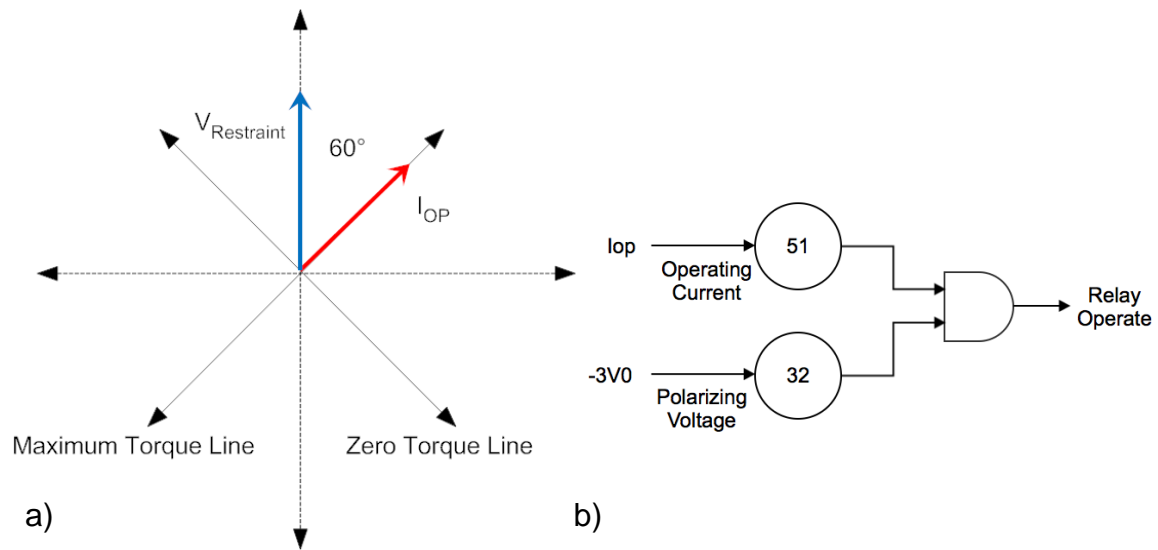


Figure 2.6 a) Phasor representation of 60 degree directional element. b) Directional element supervision of overcurrent operation.

Typical polarizing inputs are the negative sum of phase voltages, $-3V_0$, for phase-to-phase fault protection, or the neutral current on the wye connected side of a close by transformer, I_0 , for ground fault protection. These are good polarizing signals because phase voltages keep approximately the same phase relationship during phase-to-phase faults and transformer neutral currents will be in phase with the fault current for ground faults.

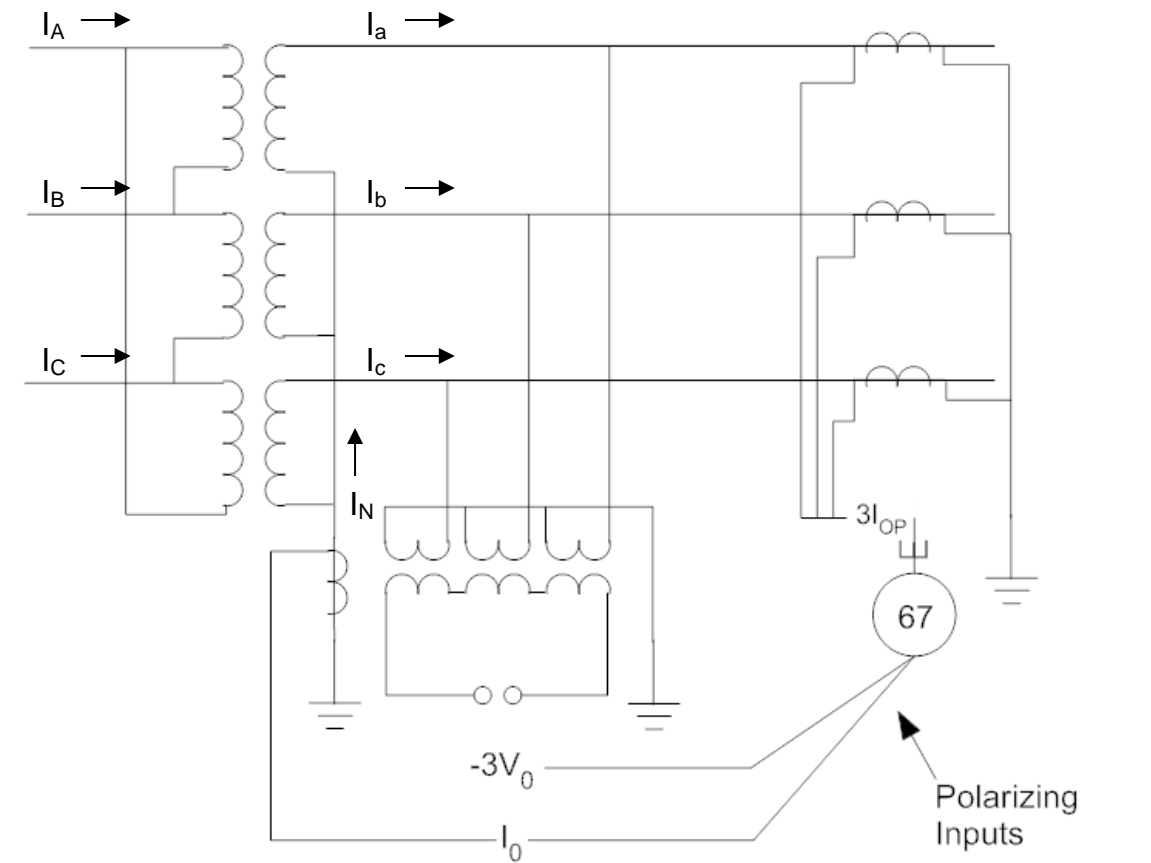


Figure 2.7 Directional overcurrent relay connection.

In practice, the directional element would likely be used to supervise the operation of an overcurrent relay, blocking operation for reverse faults.

Differential Protection

Differential protection is one of the most effective protection techniques in use for detecting faults. It works on the same principle as the ground fault circuit interrupters found in homes and commercial systems. Currents entering and exiting the zone of protection are measured with current transformers and compared. If the difference between these currents is not within the range expected as a result of CT mismatches, internal power dissipation, and small

phase differences between the two measurements, then a fault is assumed to exist inside the zone and the differential relay will operate circuit breakers on both sides of the zone. Each zone would commonly be a single line or bus, but can include transformers and more complex arrangements.

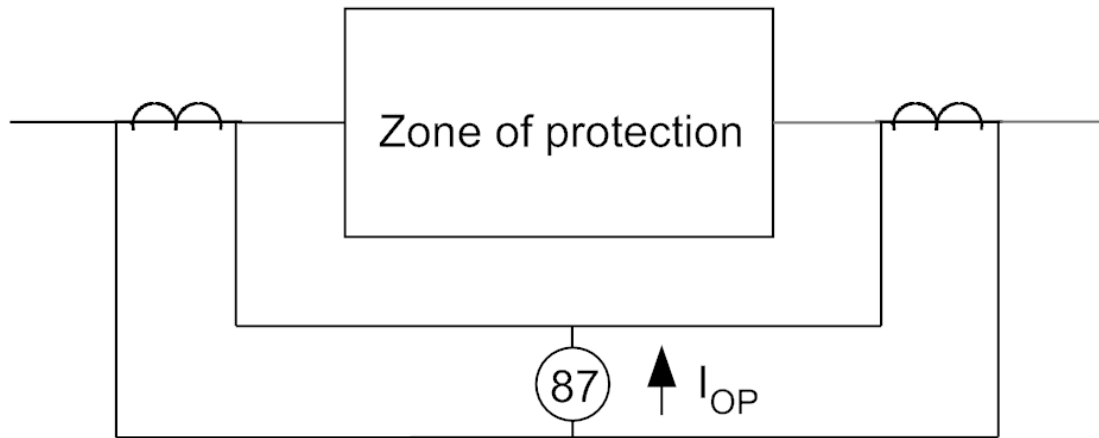


Figure 2.8 Differential relay connection.

This protection scheme is very effective in most applications, and is insensitive to external faults. Overlapping differential schemes ensure that no piece of the system is left unprotected. In order to improve security, many differential relays use restraint windings in order to set a minimum differential current required to operate the relay. Further, slope characteristics are also used to account for CT tap mismatches and other factors that prevent measured currents from perfectly cancelling. For all of its benefits, the need to have CTs at both ends of the protection zone physically wired into a comparison circuit creates a practical limitation for the size of the zone to be protected. It is also

more expensive than an overcurrent approach due to the added hardware needed to implement the differential scheme.

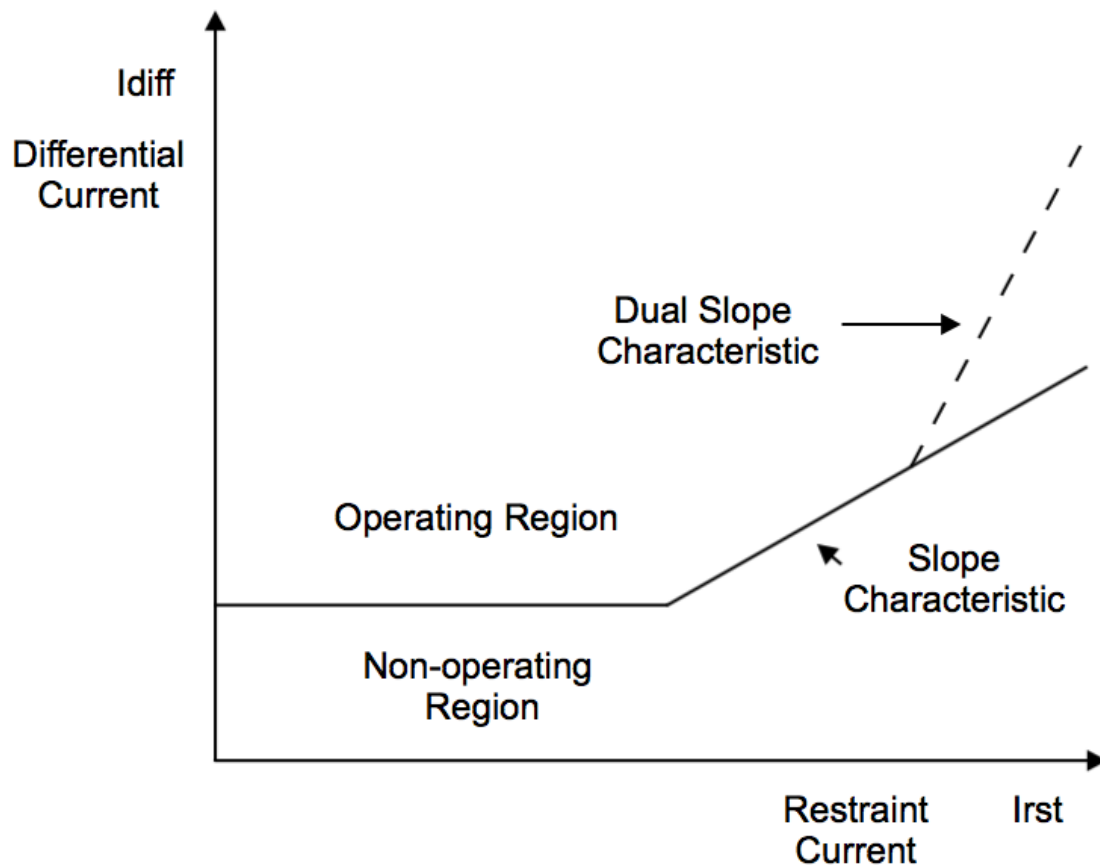


Figure 2.9 Differential operating regions with dual slope characteristic.

Pilot Protection

Protection using communication channels, pilot relaying, behaves very much like differential protection. The difference is that each relay makes its own measurements and decisions but also coordinates with the relay at the other end of the line via communications, rather than comparing currents in a control circuit. Before the relays will actually operate, they will look for permission from the relay

at the other end of the line. They may operate together or individually based on the specific pilot protection scheme in use.

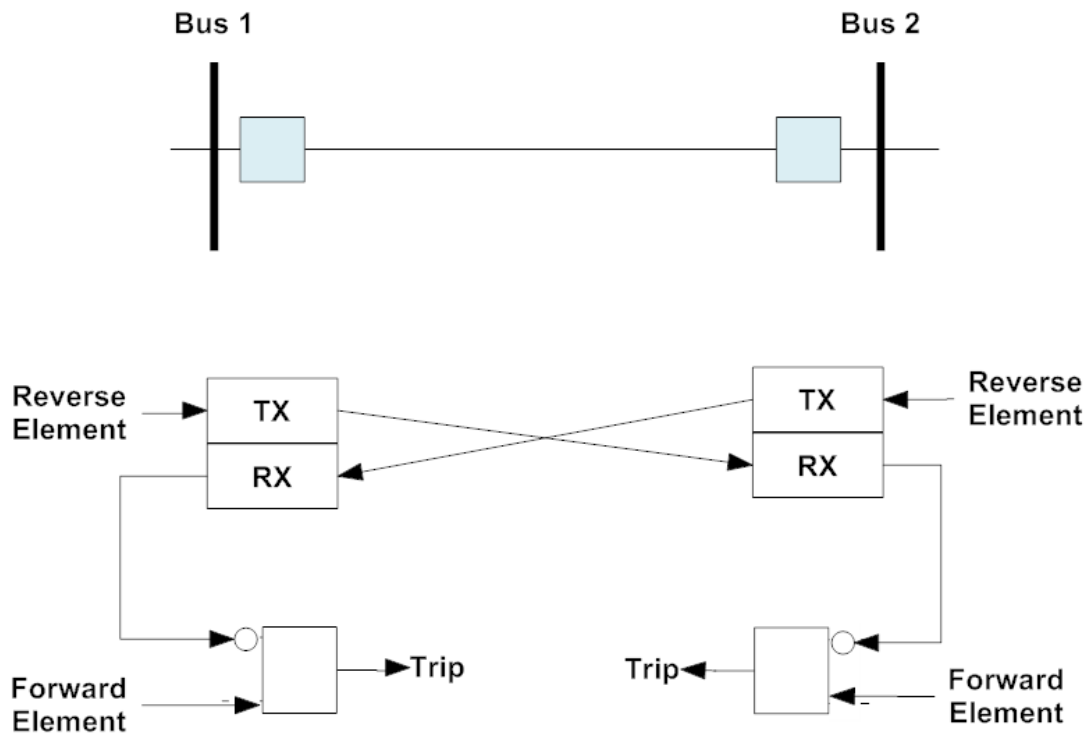


Figure 2.10 Pilot protection operating logic.

Several pilot protection schemes are used for specific protection applications. Each has its own operating logic determining how the operation of one relay affects the operation of the other. Using a communication channel rather than a comparison circuit allows this differential-like scheme to cover protection zones over much longer distances. However, communication channels can fail and create an added expense.

Genetic Algorithms

The genetic algorithm is an optimization process modeled on biological evolution. Genetic algorithms are not likely to produce an analytically perfect solution; in fact it is extremely unlikely that the perfect solution will be reached. However, a progressively better solution will be reached after each generation until an acceptable solution is reached which, though imperfect, is adequate.

In a simple genetic algorithm, the classifier being optimized would be a binary string referred to as the chromosome. This chromosome is mapped to the features of the problem being optimized. Because the individual elements in the chromosome are being mapped, the order of the elements within the chromosome is unimportant, so long as the order remains consistent. Genetic algorithms use three genetic operators to control the replication process. These are replication, crossover, and mutation.

The replication operator simply reproduces a parent chromosome without any changes. Crossover mixes elements of two chromosomes into a new chromosome. The intent is to account for effect of mating in the optimization process. In crossover, elements of a chromosome will be swapped with the corresponding elements in another chromosome with a probability P_{co} . The hope of the crossover operator is that the best elements of two chromosomes would be combined to form a chromosome better than either of its parents. The mutation operator gives each element in the new chromosome a probability P_{mut} of changing from a zero to a one [17].

In practice, the set of chromosomes are randomly initialized to form a starting generation and each one is tested. During testing, each chromosome is evaluated by an objective function related to the behavior being optimized. This objective function, along with any additional evaluation metrics, is used to create a fitness function for each chromosome. All chromosomes in the generation are sorted based on the fitness functions and the best are replicated to create the next generation. Mutation and crossover modify the chromosomes before they are all reevaluated. This continues until the finishing criteria are met.

Summary

This chapter has presented much of the relevant subject matter for the modeling and testing that are conducted in the following chapters. The principles used for controlling real and reactive power injection along with frequency and voltage regulation have been discussed. Some considerations for applying these control strategies to microgrids have also been examined.

The methods of modeling microgrid systems have also been discussed along with ways to reduce the complexity of the model without affecting the results. Microgrids present many unique protection challenges, which were presented in this chapter. General protection strategies with possible application to microgrids were also examined. Finally, the generic structure of the genetic algorithm was detailed for use in tuning of controls.

Most of the topics presented in this chapter have been examined before either individually or with a few of the other topics. However, this thesis will be

bringing them all together in order to conduct protection strategy and hardware testing. Hardware testing related to protection is seldom conducted, making microgrid protection testing with real hardware a largely unexplored topic.

CHAPTER 3, MATERIALS AND METHODS

This chapter will explain how the microgrid model is designed and the accompanying hardware test bed is constructed.

Microgrid Model

The microgrid modeled for this thesis is a simplified model of the Oak Ridge National Laboratory Distributed Energy Communications and Controls (DECC) lab microgrid. It is simplified in the sense that unbalanced sources and loads have been omitted. Simplified inverter models have also been substituted.

Microgrid Structure

The ORNL DECC lab microgrid is a radial two-bus system spread over two buildings fed by 2.4 kV lines. The microgrid circuit in both buildings operates at 480 V. Each building contains an inverter with 144 kW DC power supply powered from an independent circuit, along with resistive and inductive load banks more than capable of handling the maximum output from the inverters.

The cables in the two buildings are sized for the maximum expected load current supplied by the utility. This is between 300 and 350 A, so most of the cables are either 2/0 or 4/0 AWG. This is an adequate rating for microgrid operation as well. A 480 V cable also exists between the two buildings in addition to the 2.4 kV cable coming from the substation. This connection allows both buildings to operate together in microgrid mode while disconnected from the 2.4 kV system. The cable is actually a combination of two parallel runs of 336 kcmil

three-conductor cable with a third two-conductor run acting as the neutral. This cable is rated for a combined 600 amps.

The DECC microgrid also has many single-phase devices which are being neglected in this model. These devices include battery storage, a photovoltaic installation, and several heat pump testing stations. These devices are being neglected in order to simplify the modeling and because they will introduce imbalances which are not yet within the scope of the protection testing. Several three-phase motors and a synchronous condenser are also being ignored in the model due to their infrequent use. The microgrid also employs a unified power flow controller to change the impedance of the 480 V line between the two buildings. In the future, it will be used to redistribute power flow in a looped system. This device has been neglected because modeling it in RSCAD would be very difficult, and the impedance of the lines is assumed to be constant during the small time frame the protection study is interested in.

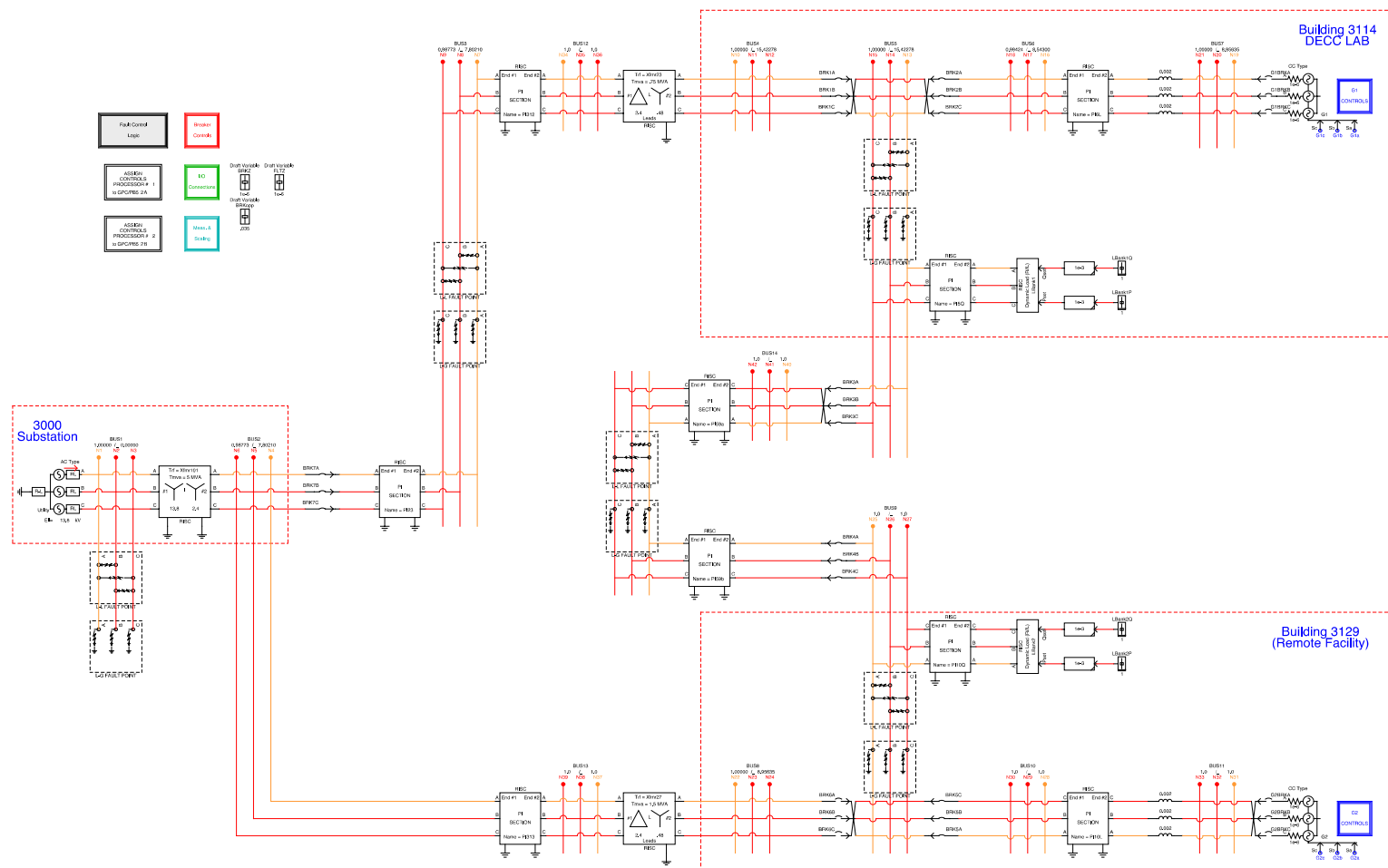


Figure 3.1 DECC lab microgrid model.

Distributed Energy Resources

Modeling the individual power sources is not necessary for protection purposes. It is assumed that their power output and DC bus voltage will be essentially constant during the period of the fault. Therefore, it is sufficient to model grid-connected inverters independent of the battery bank or photovoltaic installation they are connected to. A solely inverter based microgrid has been chosen for two reasons. First, it best matches what is actually in the DECC lab microgrid. Second, the choice of an all inverter-based microgrid creates a worst-case scenario for detecting off grid fault currents. Reduced fault current during islanding is the primary difficulty for microgrid protection. A rotating machine will always produce more fault current than an equally sized inverter, likely several times more. The choice of an all inverter model is also likely to be the most forward thinking scenario because it favors very heavy penetration of battery storage, photovoltaics, and fuel cells.

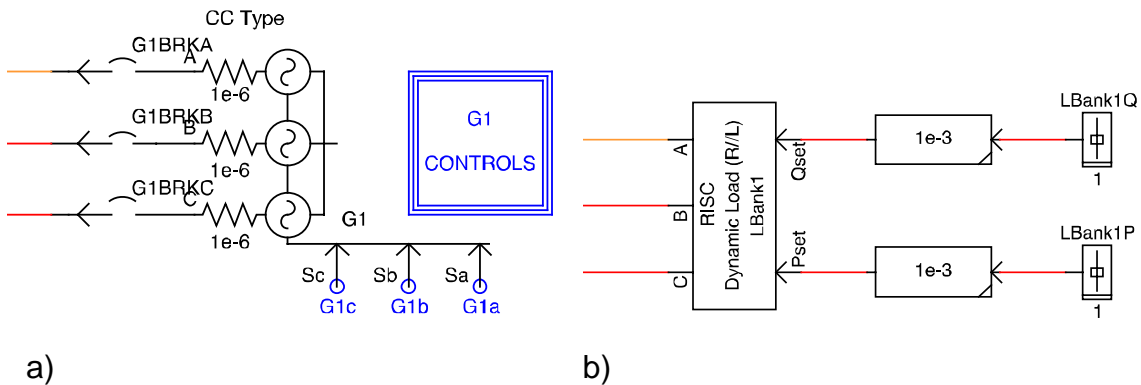


Figure 3.2 RSCAD models used for modeling a) inverters and b) load banks.

In lieu of creating a switching model of the inverters in RSCAD, a controlled voltage source is being used to model the DER inverters. This choice allows the amount of processing power needed to run the model on RTDS to be reduced. Also, switching harmonics and the model of the energy source attached to the inverter DC bus are not necessary for studying protection.

The controlled voltage source accepts the modulation signal that would normally be compared to a saw tooth waveform to generate firing pulses in a switching model. In essence, this controlled voltage source is an ideal inverter of sorts with an extremely high switching frequency, and an infinite power source on the DC bus. The series impedance for the voltage source is just a $2\ \mu H$ inductor and the connected cables.

Inverter switching may be ignored in this model, but the majority of the inverter controls used to create the modulation waveforms are still being modeled. The control scheme chosen is the direct power control discussed earlier. This control scheme is based on active and reactive power calculations in $\alpha\beta$ coordinates shown in equations (3.1) and (3.2).

$$P = V_{\alpha}I_{\alpha} + V_{\beta}I_{\beta} \quad (3.1)$$

$$Q = -V_{\beta}I_{\alpha} + V_{\alpha}I_{\beta} \quad (3.2)$$

The error between each measurement and its associated set point is minimized using proportional-integral (PI) controllers. The outputs of these

controllers are voltage signals in the rotating dq reference frame. Using phase of the grid voltage measured by a PLL, these dq signals are converted into polar form resulting in signals in $\alpha\beta$ coordinates. These signals are then converted into three-phase voltages in the time domain. These voltage signals will be of different magnitude and out of phase with the grid voltage such that the desired amount of active and reactive power will be injected.

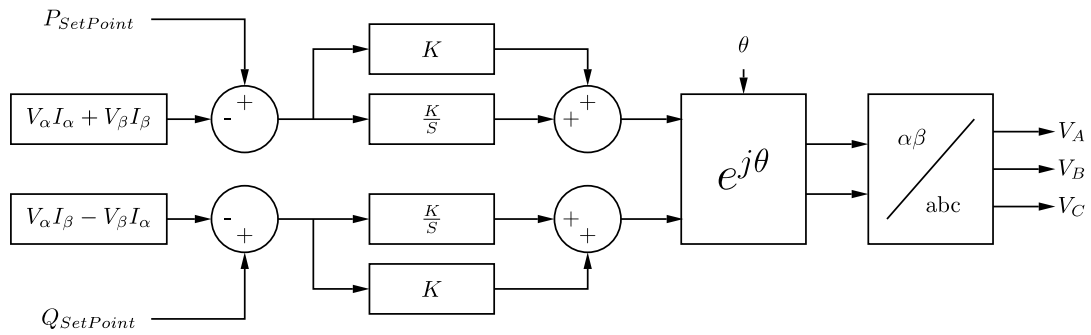


Figure 3.3 Real and reactive power control.

Frequency and voltage regulation using direct power control is just an extension of real and reactive power control. From the previous chapter it is known that carefully balancing the amount of real and reactive power injected will result in regulation of frequency and voltage. However, in this model the cable reactance is not several magnitudes larger than the resistance. Therefore, the relationships between P , F , Q , and V are no longer approximately proportional. This necessitates using separate PI controllers for frequency and voltage, instead of just a proportional gain input to the real and reactive power control.

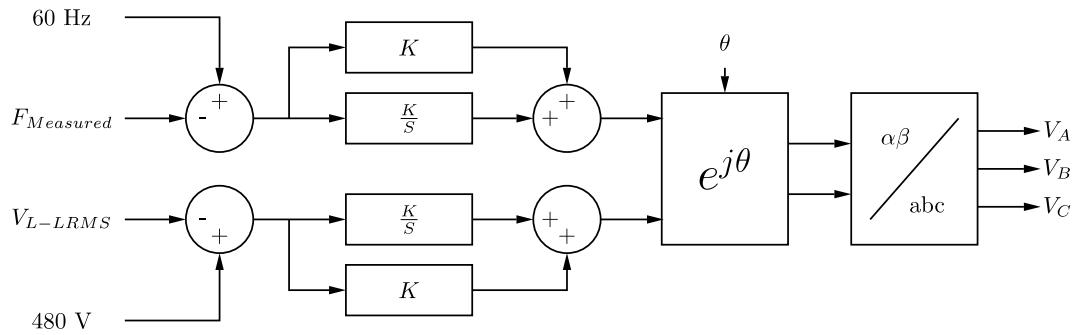


Figure 3.4 Adaptation on PQ control for frequency and voltage.

The DERs being modeled are inverter systems, and can only be expected to provide 120% of rated current during faults. To accomplish this, an additional current limiting controller is needed. Either the real and reactive power control or the frequency and voltage regulation control would try to ramp current output very high during faults so this current limiting control must be completely separate from the existing controllers. This control will only be used for the instant that the fault is present.

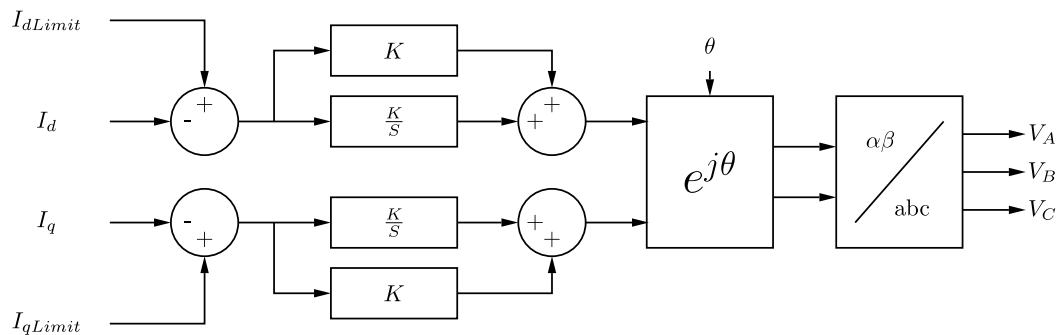


Figure 3.5 Adaptation of PQ control for current limiting.

The frequency and voltage controllers are switched in or out depending on the status of the microgrid switch, so long as the frequency and voltage control are enabled. Current limiting control is switched in when measured output current exceeds 105% of the inverter current rating and a fault is present on the system. Should current limiting control fail to limit fault currents, the inverter will shutdown when the measured current reaches 200% of rating. For this thesis, 120% of normal rated load current is assumed to be the fault current magnitude.

A black start may also be required in some cases. For this, ideal three-phase waveforms are fed directly to the controlled voltage source for one second. This simply acts as a reference signal for the frequency and voltage control to synchronize to until they begin regulating the system on their own.

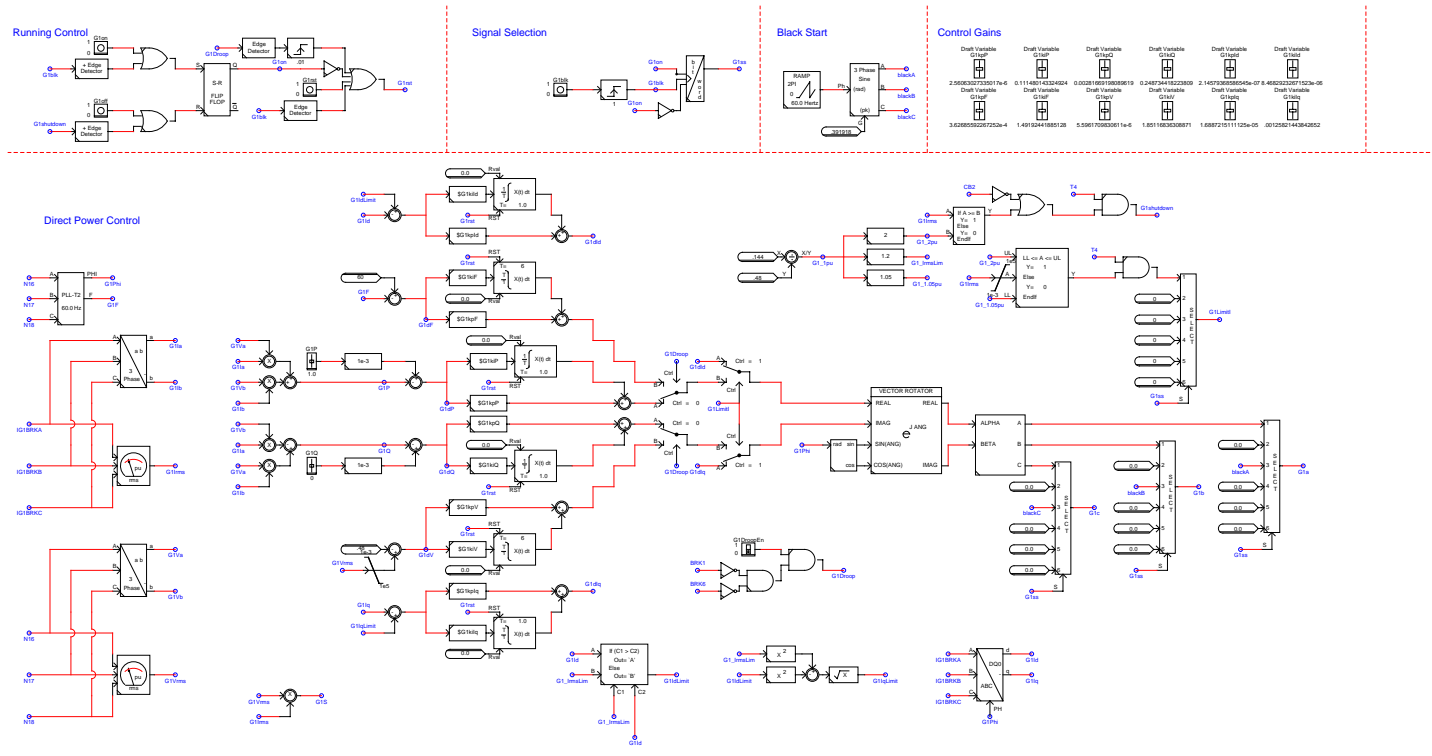


Figure 3.6 RSCAD inverter control model.

Control Tuning with Genetic Algorithm

Gains used in the PI controllers for the DER controls are tuned using a variation of the basic genetic algorithm structure described in chapter two. This method was chosen for several reasons. The first was the speed with which an answer was provided. This method is able to provide a solution quickly relative to tuning the controls by hand or with an average model. Working gain parameters were found for pairs of PI controllers in times ranging from one to six hours depending on the accuracy of the initial guesses, and the number of chromosomes, or sets of gains, tested in each generation. This is much faster than other optimization techniques. Simulated annealing, for example, could take almost a day to optimize the same set of controls. Increasing the number of chromosomes per generation in a genetic algorithm increases the chances of guessing a working combination, increasing the accuracy of the final result. This also increases the chances of making a lucky guess, finding an acceptable solution in the first generation of parameter sets.

The second reason the genetic algorithm is chosen for tuning is to take advantage of automating the tuning process. This is advantageous because it allows gains to be retuned quickly every time either the controls or the microgrid model are significantly changed. This ability is key to the overall development of the control scheme, as the ideal control method is not always immediately clear at the beginning of the project. Automating the tuning process allows multiple schemes to be tested quickly and their performances compared. Automation also

benefits the overall process by allowing other tasks to be pursued while the gain tuning is taking place, allowing for progress on multiple fronts simultaneously.

The third reason for using a genetic algorithm to automate the tuning process is that an analytically perfect solution is not necessarily needed for microgrid controls because the system topology is constantly changing. It is true that each possible topology has a perfect solution, which can be calculated in advance and applied to the controls depending on the current system topology, but this requires a level of effort beyond the scope of this thesis. Rather, a parameter set which works well over the range of expected conditions is found, and the system is assumed to always be operating in a configuration other than what the controls were optimized for.

The genetic algorithm used to tune the controls differs from the simple algorithm presented in chapter two in many important areas. The chief difference is that the elements in each chromosome are real numbers rather than binary values. Because of this, the range of values used to generate the initial generation of chromosomes becomes very important, as initial values more than one or two orders of magnitude away from working values will likely not result in any working parameter sets. Therefore, using a range of values spanning many orders of magnitude is recommended. However, some experiential knowledge may provide some insight into the range encompassing the acceptable gain values, allowing better initial guesses to shorten the tuning process.

Using real numbers instead of binary strings also changes the way the crossover and mutation operators function within the algorithm. The crossover

operator spliced whole sections of binary strings chromosomes into other chromosomes in the simple algorithm. The use of real numbers for the chromosome elements prompts the decision to treat each element independently with respect to crossover. This decision is based on the observation that proportional and integral gains likely differ by several orders of magnitude. Therefore, allowing a value evaluated in a position corresponding to a proportional gain to be inserted into a position corresponding to an integral gain will very likely produce an inferior result.

The intent of the mutation operator is to introduce a helpful degree of randomness into the algorithm. For a binary string, this is accomplished by swapping binary values, ones for zeros. When using real numbers this involves scaling with a random number. Without this scaling, the possible values for each gain would be limited to the set of initial values used to initialize the algorithm. This scaling is based on a random value taken from a normal distribution centered at one with a standard deviation of one as well. The absolute value of this random value is used to ensure that the gains remain positive. The result of this is an algorithm that favors small changes in values being tested, but that leaves room for the occasional large change on the off chance that it will be beneficial.

An additional operator included in the algorithm, which was not a part of the simple example given in chapter two, is tracking the overall best two chromosomes from all generations and reinserting them into each new generation unchanged. This addition was envisioned when the observation was

made in practice that a generation many times produced a single chromosome which performed significantly better than all the other chromosomes. Sometimes, when the top chromosomes were used to create the next generation, none of the new chromosomes performed as well as the outstanding chromosome from the previous generation. This operator is added to prevent well performing chromosomes from being diluted by inferior parameter sets through subsequent generations.

Most of the gains used in the microgrid model controls fell in the range of $1E^{-7} - 1E^{-3}$, making this a reliable range over which to initialize the first generation of chromosomes. These initial values are combined in a random process where each number is just as likely to be used as any other. When a full set of initial chromosomes is complete each number is multiplied by a different value taken from the normal distribution described earlier. This forms the set of initial parameter sets to be evaluated.

Generation 1	Generation 2	Generation 3
Obj. Parameters	Obj. Parameters	Obj. Parameters
10 -----	10 -----	5 -----
30 -----	15 -----	7 -----
50 -----	30 -----	10 -----
60 -----	40 -----	12 -----
75 -----	45 -----	15 -----
100 -----	50 -----	20 -----
.
.
.
.

Figure 3.7 Results of genetic algorithm optimization process for three iterations with direct carryover of top two results from each generation.

Each chromosome, meaning parameter set, is inserted into an RTDS simulation designed to highlight the behavior being optimized and an objective function quantifying the chromosome's performance is measured after a set time passes. For this thesis, the objective function is simply the sum of the absolute values of the error between set points and measured values being controlled by the PI controllers being tuned. This is known as single objective function optimization; multiple function objective functions are possible if a very specific behavior is sought after. Because just a single objective function is used, the fitness function is simply the inverse of the measured objective function. This is where the overall best two performing chromosomes would be added. Since this is the first iteration of the algorithm, these two chromosomes are initialized to

zero and have a very low fitness function so that they will not affect the algorithm this first time through.

All of the chromosomes are then sorted based on their fitness functions, and the top six are used to create the next generation of chromosomes. The chromosomes with higher fitness functions are more likely to have their elements used in creating this new generation. The set of new chromosomes are multiplied by random values from a normal distribution, as before, and the process repeats.

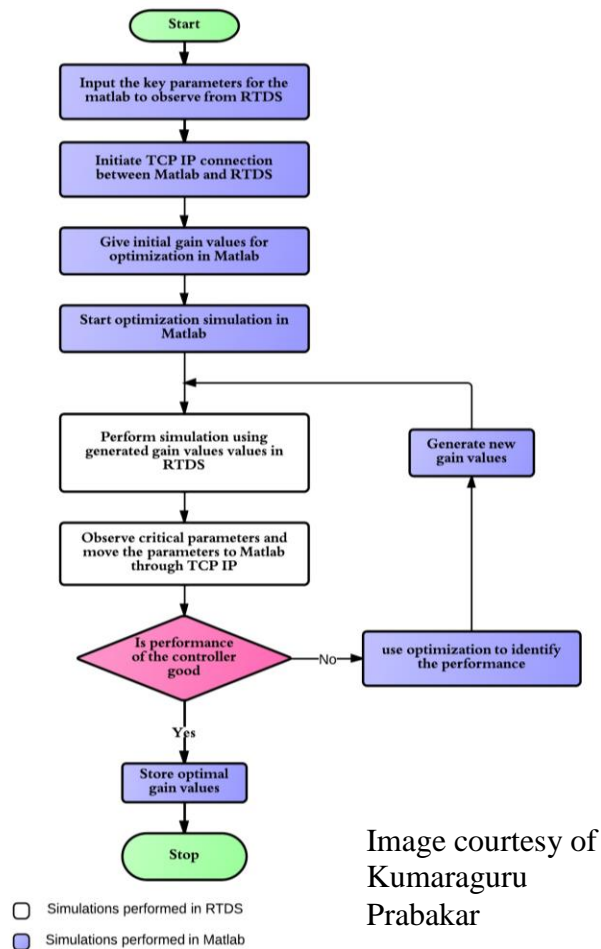


Figure 3.8 Flowchart of tuning algorithm.

The process continues until one of the convergence criteria is met. The primary convergence criterion is that the objective function of the best performing chromosome be below a specified small threshold, indicating that the controls are controlling the desired parameter very closely to the desired set point. A secondary convergence criterion is that the best chromosome remains unchanged for three generations, indicating that the optimization is stuck. This criterion is introduced to prevent tying up the RTDS simulator with an optimization that is not producing a desired result. When the best performing chromosome does not change for two iterations, the number of chromosomes created for the next generation is doubled in order to give the optimization process more chances to produce a desirable result.

Hardware-In-Loop

The hardware-in-loop setup used for testing the microgrid protection strategies is built around a RTDS unit from RTDS Technologies and three SEL 351S relays coordinated with a SEL RTAC.

SEL 351S

The SEL 351S relays used in this thesis are the best selling digital relays in the U.S. They are well suited for overcurrent protection applications. They can operate in current, voltage, and pilot protection schemes. The relays also have several protection elements that monitor the system simultaneously. Six setting groups can also be predefined and swapped on the fly based on logic

programmed into the relays settings or by external command signals from an operator or automation controller.

Prior to this thesis the relays were not modified and were still configured to accept the normal CT and VT secondary side inputs. This is an issue because the RTDS is not capable of sourcing current from its analog outputs. Therefore, two options exist to provide a current input to the relays using the analog output signals.

The first option is to use power amplifiers to convert the output signals into current waveforms. The voltage signals would also require amplification as the RTDS analog outputs can only produce ± 10 V. This option is not chosen because of the extra expense of the amplifiers and the added safety precautions they would likely require.

The second, more preferable, option is to input both the voltage and current measurements into the relay directly as a control signal. This approach bypasses the normal current and voltage inputs as well as the internal transformers and circuits that convert the electrical inputs into control signals used by the relay logic. Because the relay still expects these scaling factors to be in place, they must be modeled in RTDS instead.

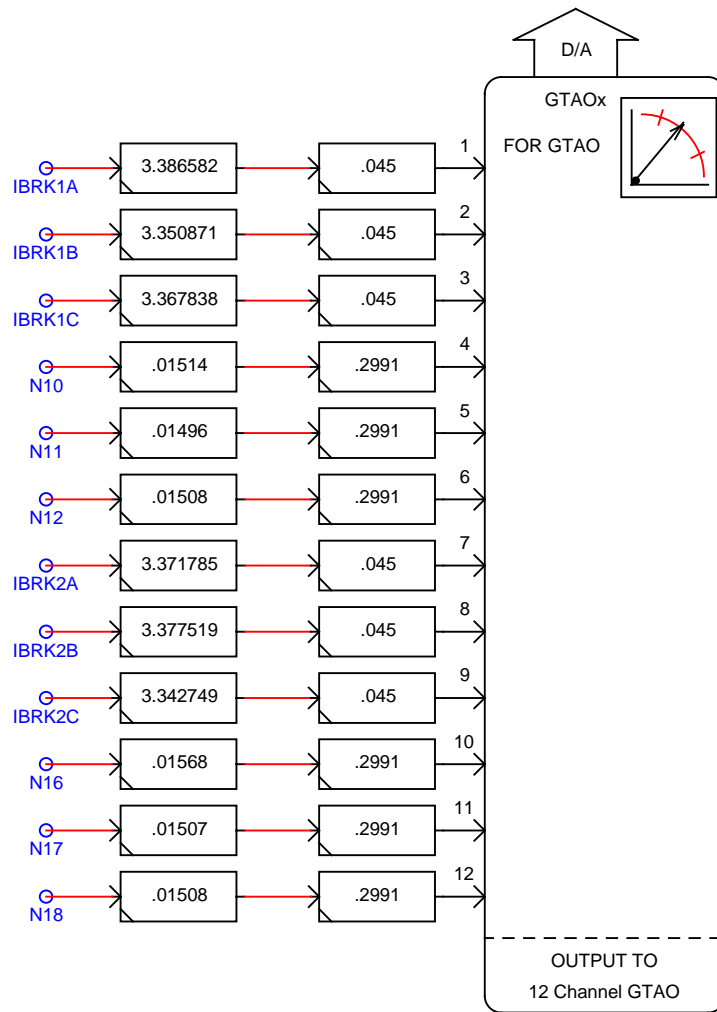


Figure 3.9 RTDS analog output models accounting for analog to digital conversion inside relay.

The ratios of input amps and volts to control voltage that takes place in the normal analog to digital conversion circuit are shown in Table 3.1, obtained from the relay manual. The turns ratios of the internal transformers are found by applying a known voltage from the RTDS into the relay and observing the corresponding reading on the relay's onboard HMI. The pin locations for the inputs, shown in figure 3.10, can be obtained from the relay manual [18]. A wiring

diagram for connecting the current and voltage signals to the ribbon cable connector is shown in the appendix.

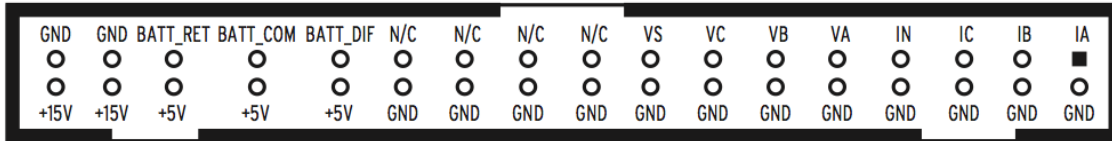


Figure 3.10 SEL 351S input pin out connections.

Table 3.1 Resultant scale factors for 351S input module from relay manual.

<i>Rear Input Channels</i>	<i>Input Channel Nominal Rating</i>	<i>Input Value</i>	<i>Corresponding J2 Output Value</i>	<i>Scale Factor (Input / Output)</i>
I_A, I_B, I_C, I_N	1 A	1 A	45.6 mV	$21.92 \frac{A}{V}$
V_A, V_B, V_C, V_S	300 V	67 V _{LN}	299.1 mV	$223.97 \frac{V}{V}$

The circuit breaker close and trip command circuits must be handled differently than the voltage and current signals. Relays do not output a signal to trip or close circuit breakers. Instead they operate on DC current from the substation auxiliary power system and batteries, which power the circuit breaker control circuit. The relay only controls contacts, which allow the DC current to flow. The RTDS digital inputs require at least 10 mA of current in order to register logic true. Therefore, a 5 V_{DC} power supply is inserted in series with the signal in order to provide the current the circuit requires. These logical inputs are

combined with the circuit breaker logic in RTDS. A wiring diagram for connecting the circuit breaker logic circuits can be found in the appendix.

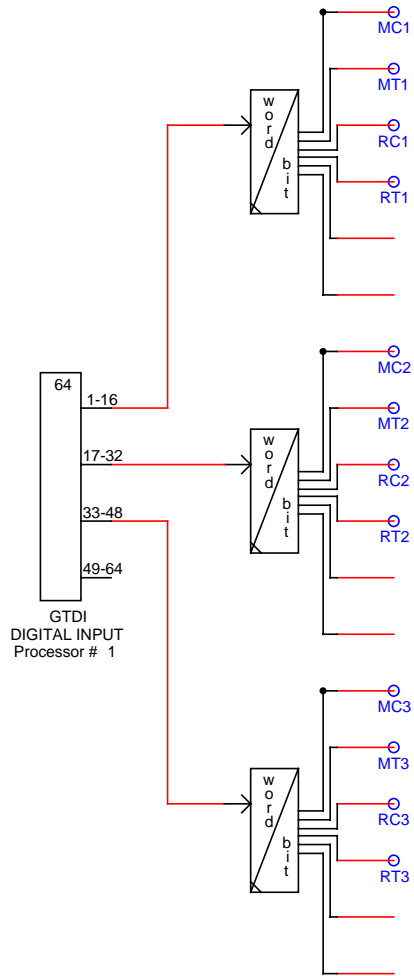


Figure 3.11 Inputs for circuit breaker controls from SEL 351S relays.

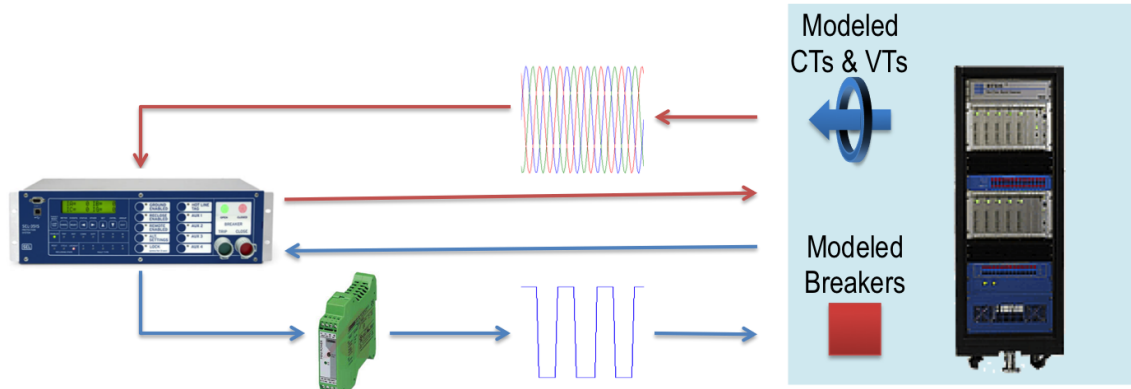


Figure 3.12 Signals between RTDS and 351S relays.

Settings for the relays are stored in text files, which can be modified and loaded onto the relays via either USB, serial, or Ethernet connections. The platform for managing the modification and downloading of these files is AcSELeator Quickset. This software package is freely available from SEL through its SEL Compass download manager.

RTAC and HMI

The SEL RTAC is a common solution for automation in industrial applications and substations. The RTAC can operate on logic input and output circuits like those used on the SEL 351S relays for circuit breaker controls. However, the real power of the RTAC is in the serial communications ports, allowing for effective monitoring of relay statuses and measurements as well as centralized control of relay functions.



Figure 3.13 SEL RTAC 3530.

The RTAC described in this thesis is interfaced with both the RTDS and the three SEL 351S relays. The connections with the RTDS are only used to monitor the status of circuit breakers and the operational state of the inverters. The logic inputs of the RTAC are rated for $24 V_{DC}$, so an additional DC power supply must be used to power these circuits. The signals in the simulation are used to control the individual digital output channels as switches in DC circuits wired into the RTAC inputs. A wiring diagram for this is shown in the appendix.

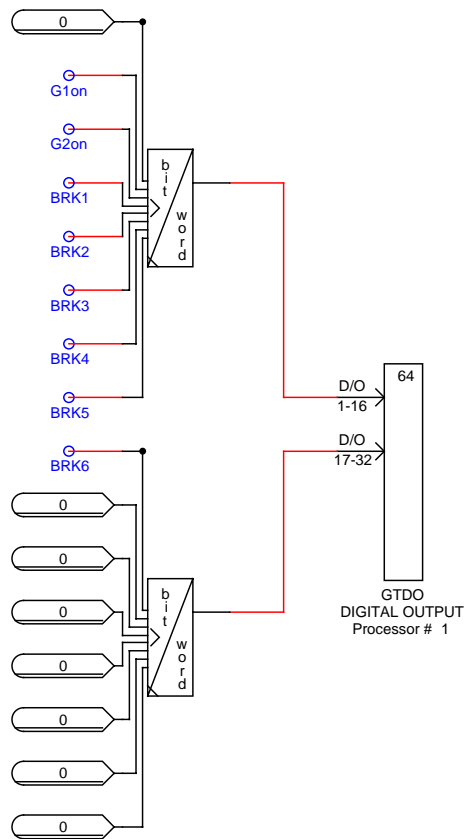


Figure 3.14 Circuit breaker and inverter status output signals to RTAC.

The RTAC is connected to the relays serially using a proprietary SEL communications protocol. For this thesis, a baud rate of 38400 bits per second was chosen because this rate is closer to the expected baud rate in a real world application. Much higher baud rates are available with this hardware, however. It is very important that the auto-detect baud rate option is not chosen when configuring the connections. This option appears at first to be a convenience, but experience has shown that this option will prevent the communications from operating properly.

All of the RTAC settings are stored in an RTAC project file modifiable in the SEL AcSELerator RTAC program. Each relay has to be added in this project file and its communication port, protocol, and baud rate must be specified. Several settings have to be changed for each relay in order for the RTAC to function as intended in this project. The options for monitoring the voltage and current measurements in each relay need to be enabled. It is useful to set up an event server on the RTAC in order to automatically collect event reports from the relays every time they operate.

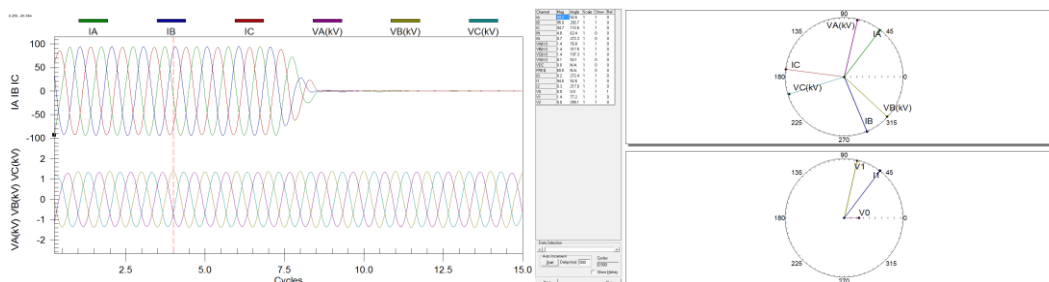


Figure 3.15 Example event collection files.

The relays will not automatically accept trip and close commands sent by the RTAC. In order to allow these signals to be sent to the relays, a transparent access point and transparent access point router must be set up inside the RTAC for each relay to be controlled. The “Fast Operate Enable” setting must also be enabled in each relay’s setting file. This setting allows the relay to receive remote operate commands.

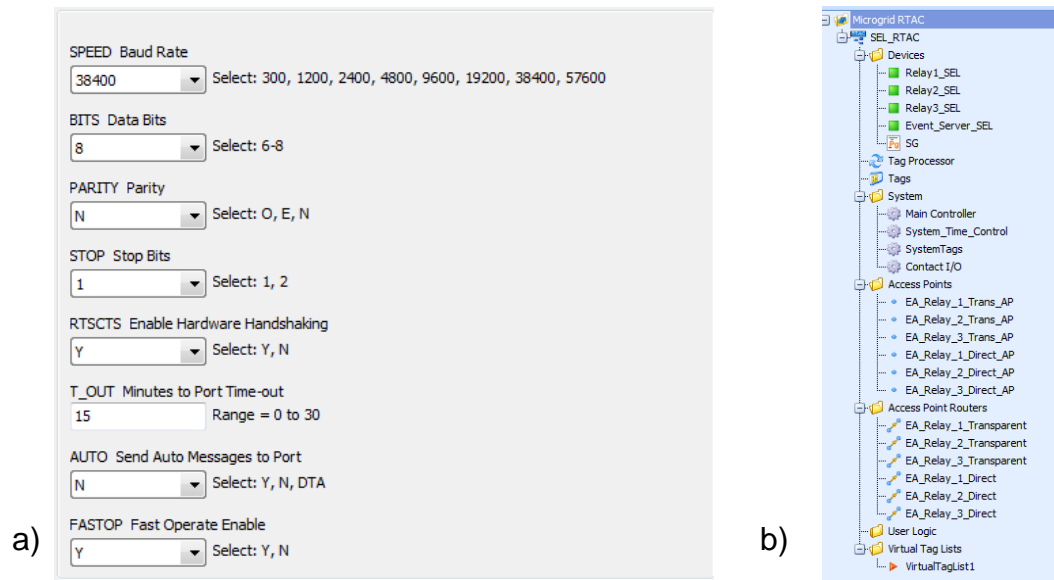


Figure 3.16 a) Relay communication settings. b) RTAC connected devices and access points.

The RTAC tag processor can handle basic tag mapping. However, custom logic programs can also be created. This is a much more powerful option and is used in this thesis to send circuit breaker statuses to relays. Custom logic is also used to initiate setting group changes in the relays based on the status of the microgrid switch. All of the signals for circuit breaker status and setting group changes is handled using relay remote bits.

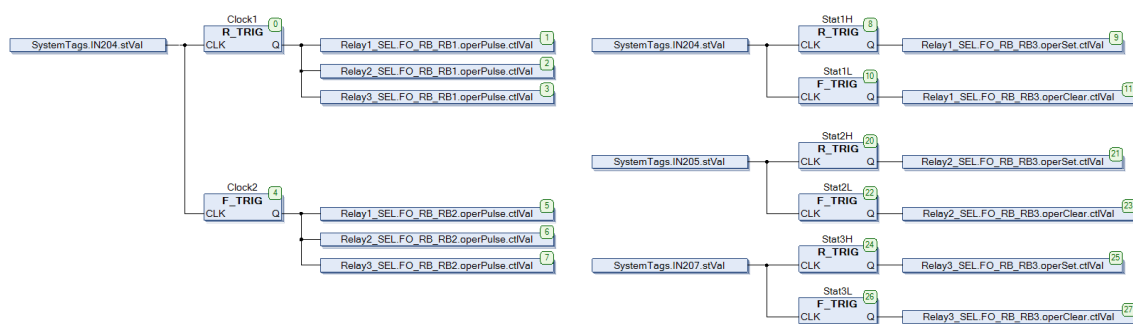


Figure 3.17 Custom logic for breaker statuses and setting group changes using relay remote bits.

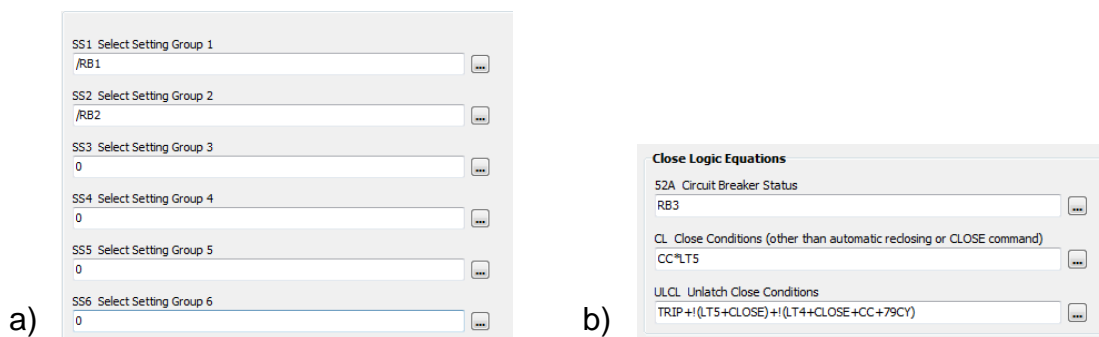


Figure 3.18 a) Remote bits controlling relay setting group changes. b) Remote bit controlling the circuit breaker status signal in the relay.

Creating an HMI to run on the RTAC is relatively simple. The HMI is created using the SEL diagram builder software. Once all of the loaded tags on the RTAC are imported into the diagram builder, associating signals with meters, trends, and breaker controls is straightforward. The breakers that do not have a real relay controlling them are represented with a breaker status block tied to the status of one of the logic inputs connected to the RTDS, while an annunciator tile represents the breakers associated with the SEL 351S relays. The annunciator

tile allows controls and trends associated with that breaker to be displayed on the child diagram instead of cluttering the one line diagram.

When opened in the RTAC web browser, the HMI allows for all of the relevant variables associated with the three relays to be monitored in real time. The HMI also allows breakers to be opened and closed remotely without making direct changes to the simulation. This means that the relays will document the event in an event report stored on the relay. Event reports can be obtained from the RTAC web interface for analysis of the protection's performance.

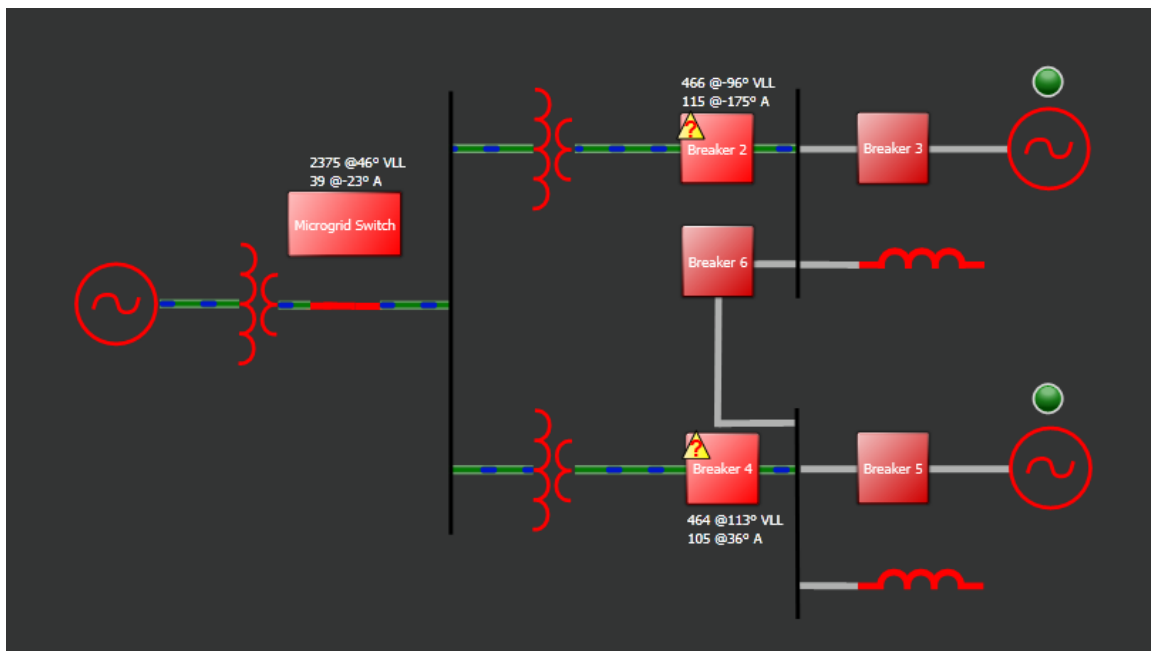


Figure 3.19 RTAC HMI one line diagram.

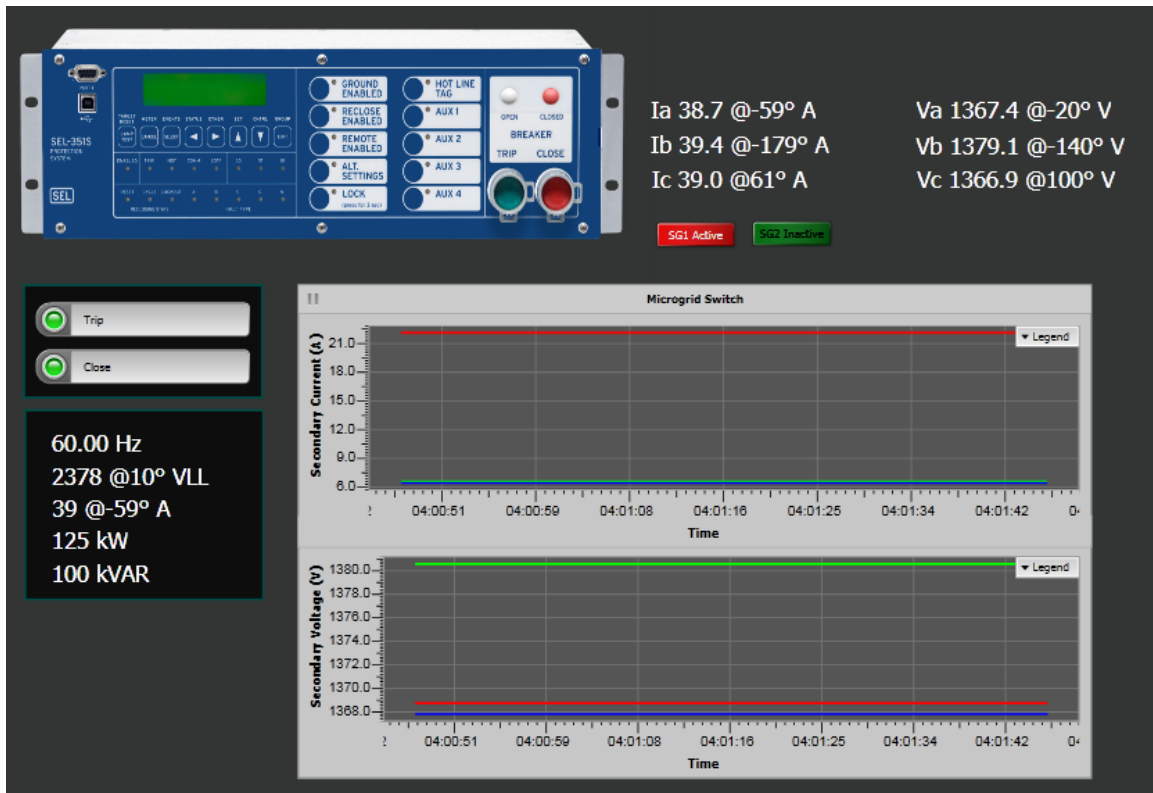


Figure 3.20 RTAC HMI relay child diagram.

Summary

This chapter has detailed the process of modeling the ORNL DECC lab microgrid. The modified genetic algorithm used to tune the DER inverter controls is also described in detail. Connections, settings, and control logic used to configure the relays, RTAC, and their connections to RTDS are also detailed.

CHAPTER 4, RESULTS AND DISCUSSION

Using the model and hardware presented, potential microgrid protection strategies are evaluated. This is done by applying faults on the buses in each of the two buildings that make up the microgrid. In each of these tests, the delay of operation for each relay is measured in order to assess whether or not the appropriate relays operate, and that those relays are operating within an acceptable time range.

Time Overcurrent Protection

The first protection scheme to be tested is a single setting overcurrent scheme using a time overcurrent characteristic and no directional control. This scenario is analogous to converting a portion of a distribution system into a microgrid without giving any consideration to protection modifications. In this case the protection is set for the expected utility fault current. Because, only three physical relays are available at the time of testing, so all other relays are being modeled in RSCAD. Relay settings are shown in table 4.1.

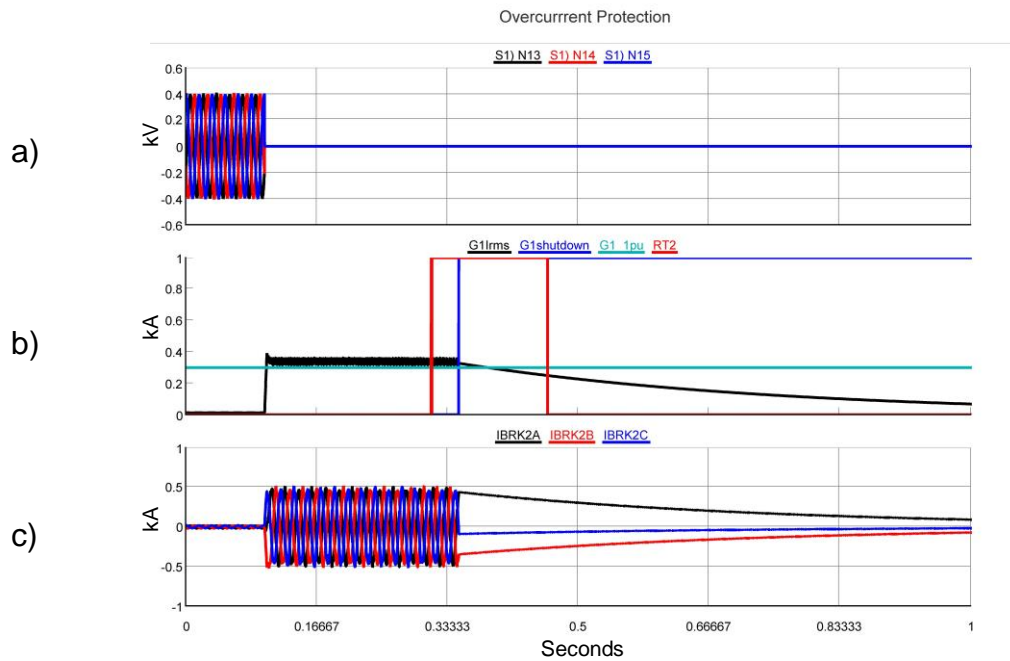
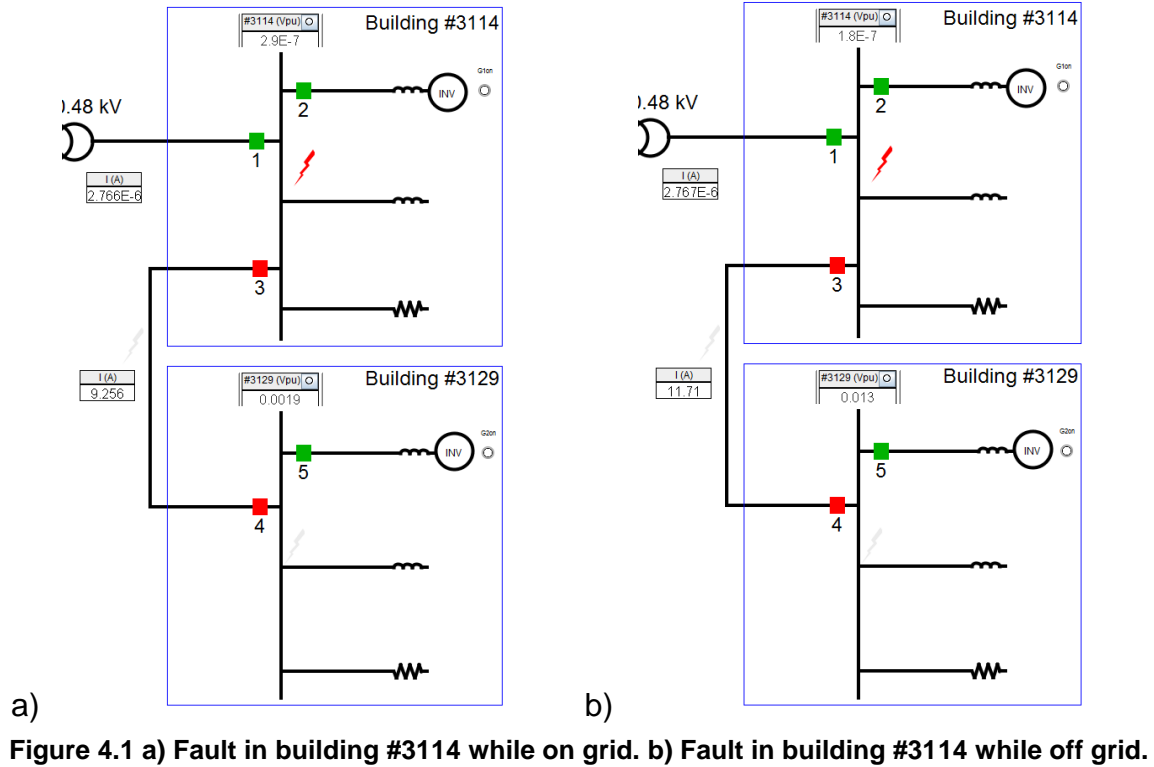
Table 4.1 Overcurrent relay settings.

<i>Relay #</i>	<i>Curve Type</i>	<i>Physical</i>		
		<i>Relay?</i>	<i>I_{pickup}</i>	<i>TD</i>
1	U4	Y	12.0	4.0
2	U5	Y	3.0	0.75
3	U4	Y	12.0	2.52
4	U4	N	12.0	1.25
5	U5	N	3.0	0.75

To test this protection scheme, faults are applied on each of the two buses in the microgrid and the cable between the two buses as well as on a bus outside the microgrid. Three phase faults are applied by inserting an extremely small resistance between the lines and ground, and the response times of the relays measured. The results are shown in the following table and figures.

Table 4.2 Overcurrent protection operating times.

3 Phase Fault		Protection Operation Delay (Cycles)				
Status	Location	Relay #1	Relay #2	Relay #3	Relay #4	Relay #5
On Grid	External	-	14.6	-	-	16.4
	Building 3114	22.1	15.7	-	-	15.7
	Building 3129	-	-	-	15.1	15.3
	Between Buildings	-	-	18.5	-	16.2
Off Grid	External	-	-	-	-	-
	Building 3114	-	14.0	-	-	15.0
	Building 3129	-	14.1	-	-	15.1
	Between Buildings	-	14.2	-	-	15.2



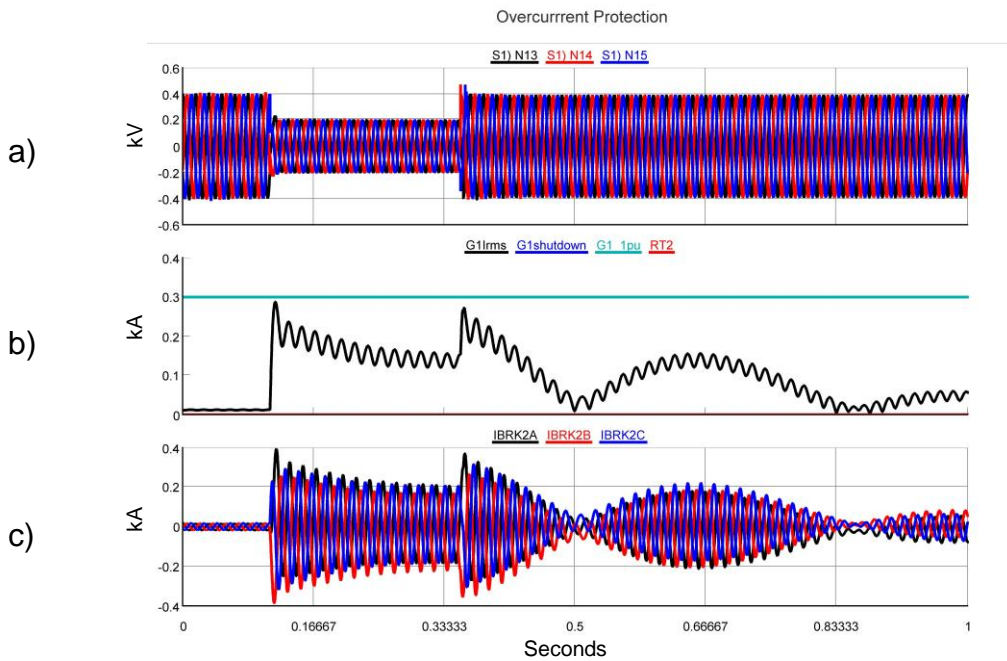
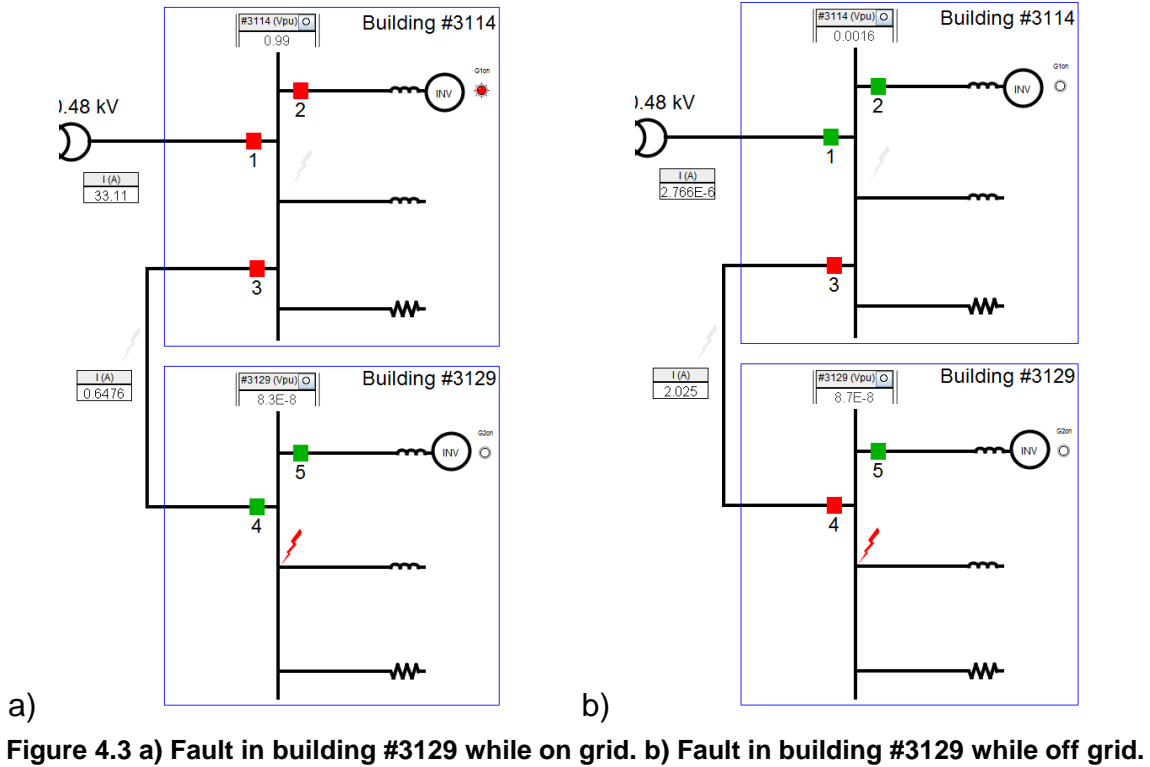


Table 4.2 shows that external faults are not detected by relay 1, resulting in the shutdown of both DERs. This is because relay 1 is set in anticipation of the large fault current provided by the utility but only measures the fault current produced by the DERs. For these inverter-based systems, there's a full order of magnitude difference between the two. Only relays 2 and 5 are set to detect the DER fault currents, so only they operate. When the same fault is applied on the bus in building #3114 relays 2 and 5 operate the same, shown in figure 4.1 a), but now relay 1 observes the utility fault current and operates. Figure 4.1 shows that relays 3 and 4 fail to operate in both the on and off grid cases. This is because they are observing DER fault current in both cases and do not operate because they are set for utility fault current. Were this a normal distribution system, only opening the breaker upstream from the fault would be adequate because no DERs would be present. However, now that DERs are present, it is preferable for relay 3 to operate so that building #3129 can remain in operation.

Figure 4.2 a) shows the phase voltages on the faulted bus, which collapse to zero when the fault is applied as expected. Figure 4.2 b) shows that the inverter output during the fault is held at 1.2 per unit until the trip signal is received from relay 2, causing the inverter to be shut down when the circuit breaker opens. Figure 4.2 c) simply shows the inverter output current flowing through circuit breaker 2.

Table 4.2 shows that a fault applied in building #3129 while on grid is isolated well from the rest of the system. This happens because the fault is occurring at the end of a radial distribution line so the normal distribution

protection methodology works well in this case. However, figure 4.3 b) shows that an off grid fault in building #3129 has the same result as a fault in building #3114 while off grid.

From this test it is observed that this time overcurrent strategy works well to detect fault current provided by the utility, but struggles to detect fault current provided by inverters. Relays protecting each inverter are able to detect their fault current adequately because the fault current provided by them does not change from on grid to off grid operation. However, the current measured by relays on the line between the two buses during faults changes immensely. As a result, a fault in the microgrid while off grid will not be isolated and the inverters will eventually shut down because of the sustained fault current being provided. This scenario is unlikely to damage any part of the system outside of the inverters themselves because the system is designed for utility fault currents.

Also, because this microgrid is radial, a fault occurring on the bus where the microgrid connects to the utility is only cleared on the utility side because the fault current on the microgrid side is inverter fault current and the protection is set for utility fault current. If it is acceptable that a fault inside the microgrid will cause a total loss of the system, then there is no need to modify protection. However, continuing to serve as many loads as possible is the motivation for creating microgrids in the first place, so failing to isolate faults is unacceptable. Therefore, leaving existing protection unmodified is not a viable option.

Variable Setting Overcurrent

Variable setting overcurrent protection is different from the previous time overcurrent scheme only in that it is configured to change protection settings when the microgrid is disconnected from the grid. This allows protection settings to be developed specifically to protect the microgrid and switched in when the utility connection is severed. This is accomplished using two distinct setting groups and an automation controller to initiate the setting change. This configuration represents the minimum additional investment possible that attempts to address the protection challenges associated with microgrids. As in the previous scenario, three relays are physical hardware and the others are modeled in RSCAD.

Table 4.3 Variable setting overcurrent relay settings.

Relay #	Physical Relay?	Setting Group 1			Setting Group 2		
		Curve Type	I_{pickup}	TD	Curve Type	I_{pickup}	TD
1	Y	U4	12.0	4.0	U4	12.0	4.0
2	Y	U5	3.0	0.75	U5	3.0	0.75
3	Y	U4	12.0	2.52	U5	3.0	0.5
4	N	U4	12.0	1.25	U5	3.0	0.5
5	N	U5	3.0	0.75	U5	3.0	0.75

To test this protection scheme, faults are applied on each of the two buses in the microgrid and the cable between the two buses. Three phase faults are applied and the response times of the relays measured. The results are shown in the following table and figures.

Table 4.4 Variable setting overcurrent protection operating times.

3 Phase Fault		Protection Operation Delay (Cycles)				
Status	Location	Relay #1	Relay #2	Relay #3	Relay #4	Relay #5
On Grid	External	-	15.5	-	-	17.4
	Building 3114	21.0	14.9	-	-	15.0
	Building 3129	-	-	-	15.3	15.3
	Between Buildings	-	-	18.7	-	15.1
Off Grid	External	-	-	-	-	-
	Building 3114	-	14.7	11.3	10.4	-
	Building 3129	-	-	10.3	10.0	14.9
	Between Buildings	-	-	10.0	10.5	-

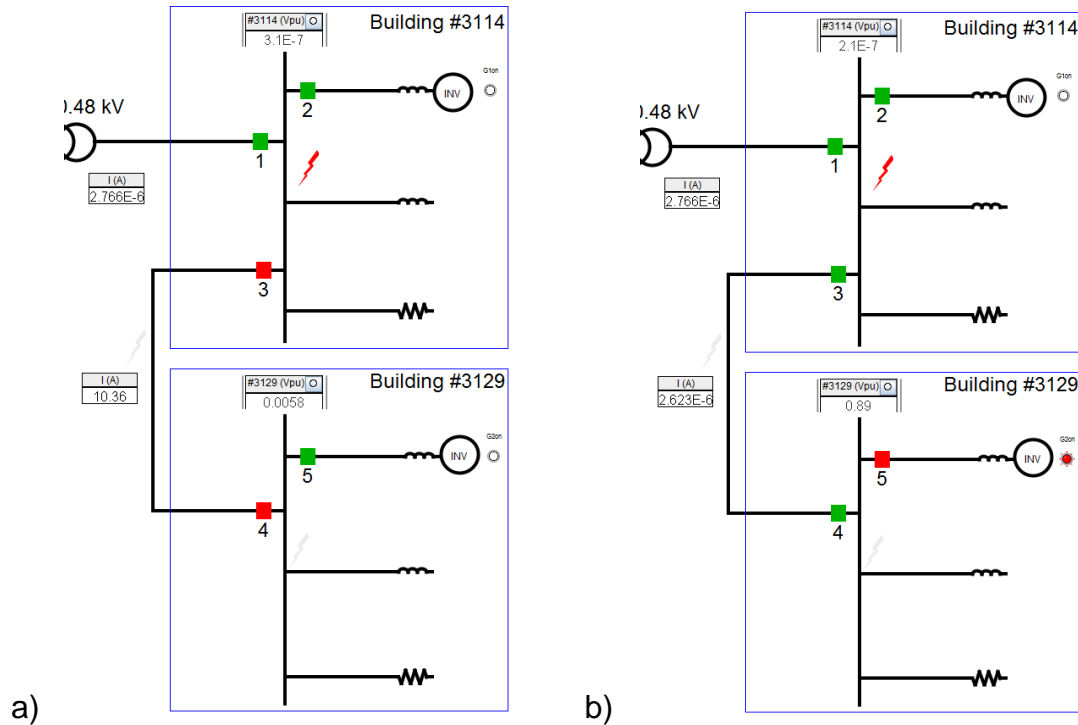


Figure 4.5 a) Fault in building #3114 while on grid. b) Fault in building #3114 while off grid.

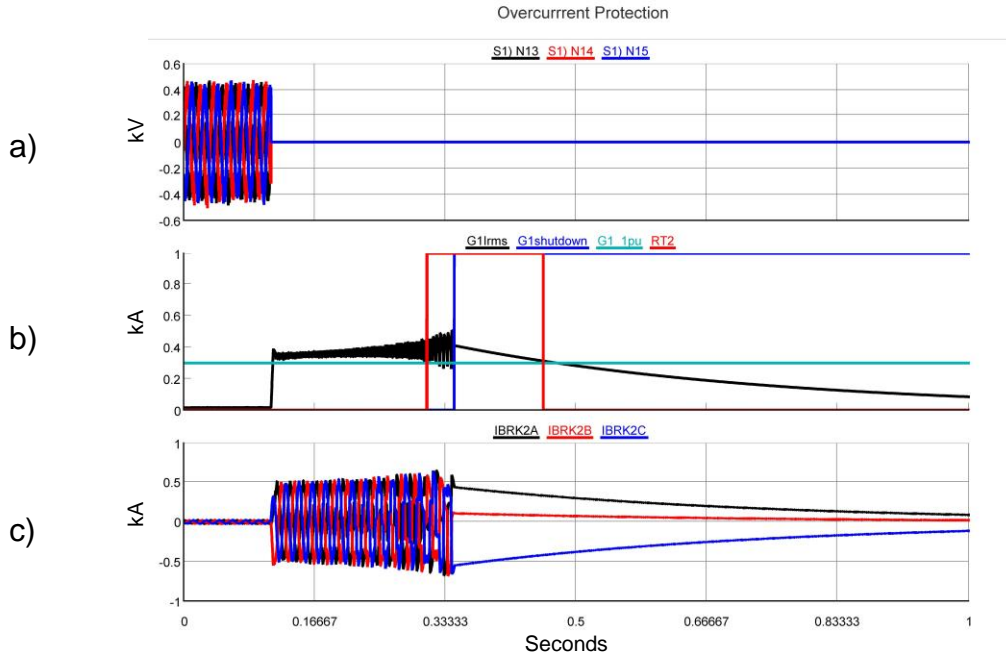


Figure 4.6 a) Building #3114 bus voltages during fault on that bus while off grid. b) Building #3114 inverter rms current output during fault. c) Building #3114 inverter current passing through circuit breaker #2.

From this test it is observed that this time overcurrent strategy continues to detect fault current supplied by the utility. There is no need to change settings on the relays protecting the inverters as their fault current contribution does not change for off grid faults. The difference is that relays protecting lines in the microgrid are now set to operate on fault currents coming from the inverters after the system disconnects from the utility. These modified settings allow faults to be effectively isolated in most cases.

This configuration resolves some, but not all, of the shortcomings associated with leaving protection unmodified. For instance, it is unable to effectively isolate a fault on the bus with the utility connection while the microgrid is connected, shown in figure 4.5 a). This is because when the fault is applied,

the relays are set for utility fault current. By the time the settings are switched, the inverters have already been taken off line. Also, relays between the two buses operate together for off grid faults. This is not a dramatic problem, as the fault is isolated. Yet, it is generally desirable that only one relay on the line operate when the line itself is not faulted. While this configuration performs better than the unaltered configuration, it is still not able to protect for every possible fault contingency.

Variable Setting Overcurrent With Directional Control

Application of directional control on relays protecting the cable between the two buildings in the microgrid promises to allow these relays to discriminate between utility fault current and inverter fault current when faults occur while grid connected. This is observed as an issue for faults occurring on the microgrid cable and the bus connecting the microgrid to the utility. When these faults occur, the grid fault current is easily recognized and the appropriate circuit breaker opens, however, the relays inside the microgrid are set to detect utility fault current moving from one bus to the other. In this situation, the inverter attached to the second bus is feeding the fault, but the relays that should isolate the inverter do not detect the fault current.

By applying directional control, two setting levels can monitor system currents simultaneously. Using the relay at circuit breaker 4 as an example, the first level is polarized forward into the bus and used to supervise a time overcurrent element set for utility fault current. The second level is reverse

polarized toward the cable and used to supervise a time overcurrent element set much lower to detect inverter fault current.

This seems to be an elegant solution, however during implementation several problems arise. One being the lack of a wye connected transformer inside the microgrid. Neutral current from a transformer wye winding is a very good polarizing source for directional control as the neutral current is zero-sequence and flows toward the fault. The absence of this polarizing source forces the use of voltage from a broken delta instrument transformer as a polarizing source.

This introduces the second and third problems, the need to add VTs, and loss of the polarizing source during faults. VTs are being avoided in this thesis for their additional cost and drain on the system. Voltage polarizing will not work in this system because it is compact and has very little impedance between buses. As a result, faults inside the microgrid reduce voltage to near zero across the system. Therefore there is no longer a voltage to polarize the directional control with, as shown in figure 4.7. Thus, the directional control is expected to disappear precisely when it is needed. Attempts to apply directional control despite these serious concerns were unsuccessful. However, it is worth noting that directional control does not work for this very specific microgrid structure. Larger microgrids with larger impedances between buses and transformers providing a polarizing source may prove better suited for directional control.

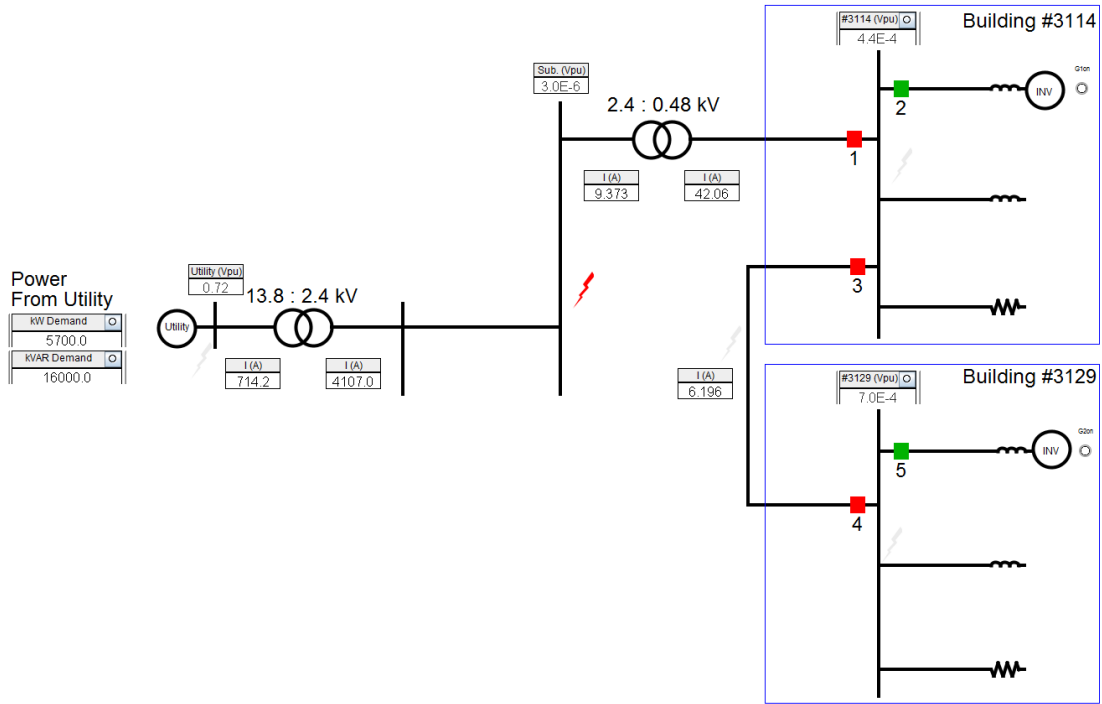


Figure 4.7 All voltage measurements inside microgrid are reduced to zero during faults.

Variable Setting Overcurrent With Bus Differential

This protection scheme is based on the variable setting overcurrent scheme tested previously but uses a differential relay to resolve issues that arise when faults occur on the bus connecting the microgrid to the utility. The time overcurrent settings change based on the status of the microgrid switch, while the differential relay requires no setting change. This is because the differential relay is only concerned with the balance of current entering and leaving the bus.

This configuration makes use of CTs, but additional CTs would likely need to be added to accommodate the differential since the time overcurrent relays are using the existing CTs. Therefore, this scheme has the additional cost of the CTs

and the differential relay itself. Like previous scenarios, three relays are physical hardware and the others are modeled in RSCAD, including the differential relay.

To test this protection scheme, faults are applied on each of the two buses in the microgrid and on the cable between the two buses. Three phase faults are applied, and the response times of the relays measured. The results are shown in the following table and figures.

Table 4.5 Variable setting overcurrent protection with bus differential relay operating times.

3 Phase Fault		Protection Operation Delay (Cycles)				
Status	Location	Relay #1	Relay #2	Relay #3	Relay #4	Relay #5
On Grid	External	-	14.6	-	-	16.0
	Building 3114	3.0	3.0	3.0	-	-
	Building 3129	-	-	-	14.9	15.3
	Between Buildings	-	-	18.2	-	15.1
Off Grid	External	-	-	-	-	-
	Building 3114	-	2.4	2.4	-	-
	Building 3129	-	-	10.5	9.2	15.0
	Between Buildings	-	-	10.1	10.0	-

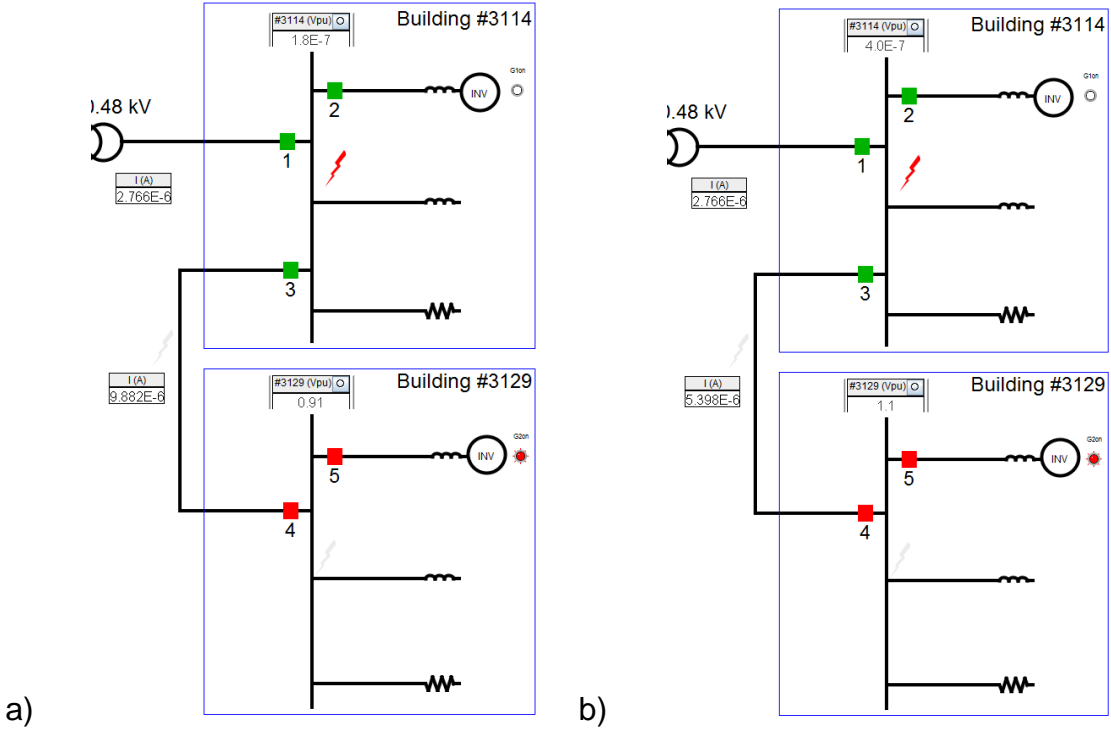


Figure 4.8 a) Fault in building #3114 while on grid. b) Fault in building #3114 while off grid.

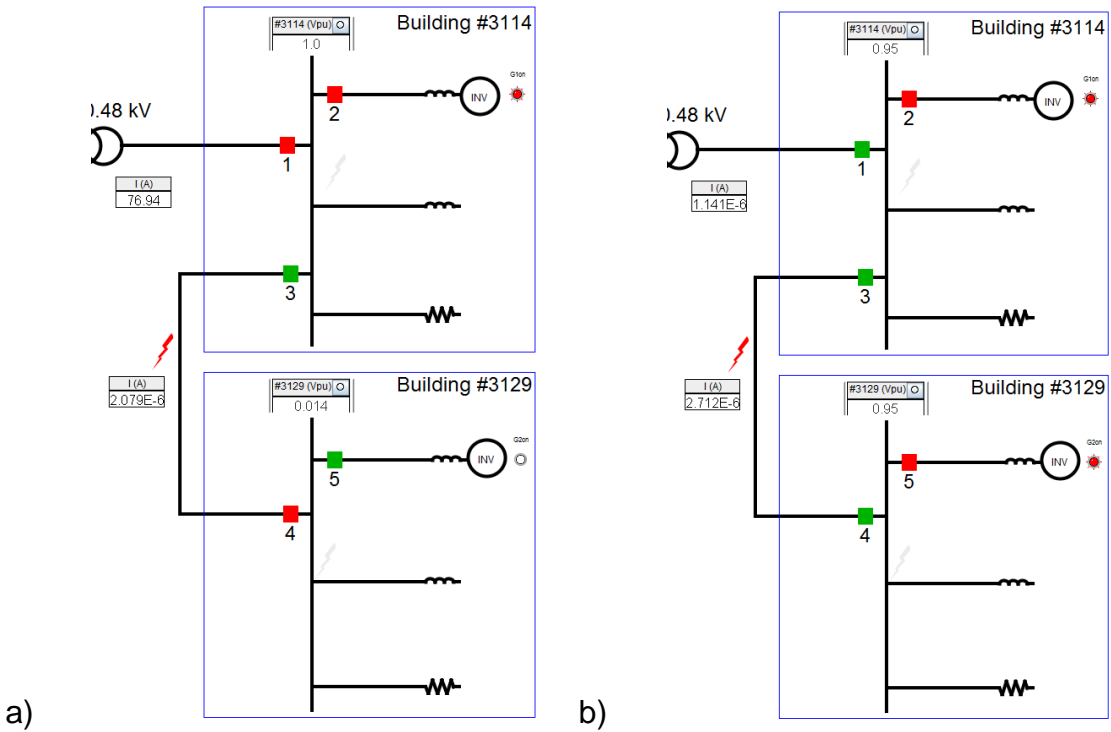


Figure 4.9 a) Fault on the microgrid cable while on grid. b) Fault in the microgrid cable while off grid.

From this test it is observed that this time overcurrent strategy continues to work for protection from on grid fault current. Inverters are still protected, preventing them from continually feeding external faults. The relays protecting lines in the microgrid are set to operate on fault currents coming from the inverters after the system disconnects from the utility. The only failure of this scheme is that a fault on the microgrid cable while grid connected will only be cleared from one end, shown in figure 4.9. This is the same result that prompted the addition of a differential relay to the bus, to successfully isolate bus faults while grid connected. This result suggests that the addition of differential protection on the microgrid cable would allow the microgrid protection to protect against all three-phase microgrid faults.

Differential Overcurrent Protection

The preceding protection strategy shows the benefit of differential protection in microgrids. However, it is desirable to avoid replacing existing protection hardware in order to convert an existing system into a microgrid. Therefore, completely replacing existing overcurrent protection with differential relays is a possible, though less desirable, solution. In order to resolve the desires for effective microgrid protection and minimizing costs, the notion of an overcurrent based differential scheme is being tested. Appropriately choosing CT polarities and wiring multiple CTs together creates a differential protection scheme that makes use of overcurrent relays.

Take a bus differential scheme as an example; all CTs are oriented with their polarities directed into the bus. By then wiring all phase A, B, and C, CT connections into the corresponding secondary current inputs on an overcurrent relay, the relay measures the differential, rather than line, current for that bus. During normal operation, no differential current will be observed by the relay. This is because buses can be assumed to be lossless, and have constant voltage and phase along their span. Losses, voltage mismatches, phase differences, and multi-terminal lines are the major reasons for having specially designed differential relays capable of compensating for these differences. However, the system being tested does not have any of these considerations.

When a fault occurs, a 60 Hz, sinusoidal differential waveform is observed by the overcurrent relay, shown in figures 4.10 and 4.11. The magnitude of the waveform is the difference in instantaneous current entering and exiting the bus. This is because wiring the CTs together has the effect of cancelling the currents passing through the zone of protection, leaving the currents feeding faults inside the zone. The waveforms will correspond to the faulted phases. For instance, a three-phase fault will produce a balanced three-phase differential current, single phase faults produce single phase differential current, and phase to phase faults produce two differential waveforms 180° out of phase with each other. To the relay, these appear no different than normal fault currents.

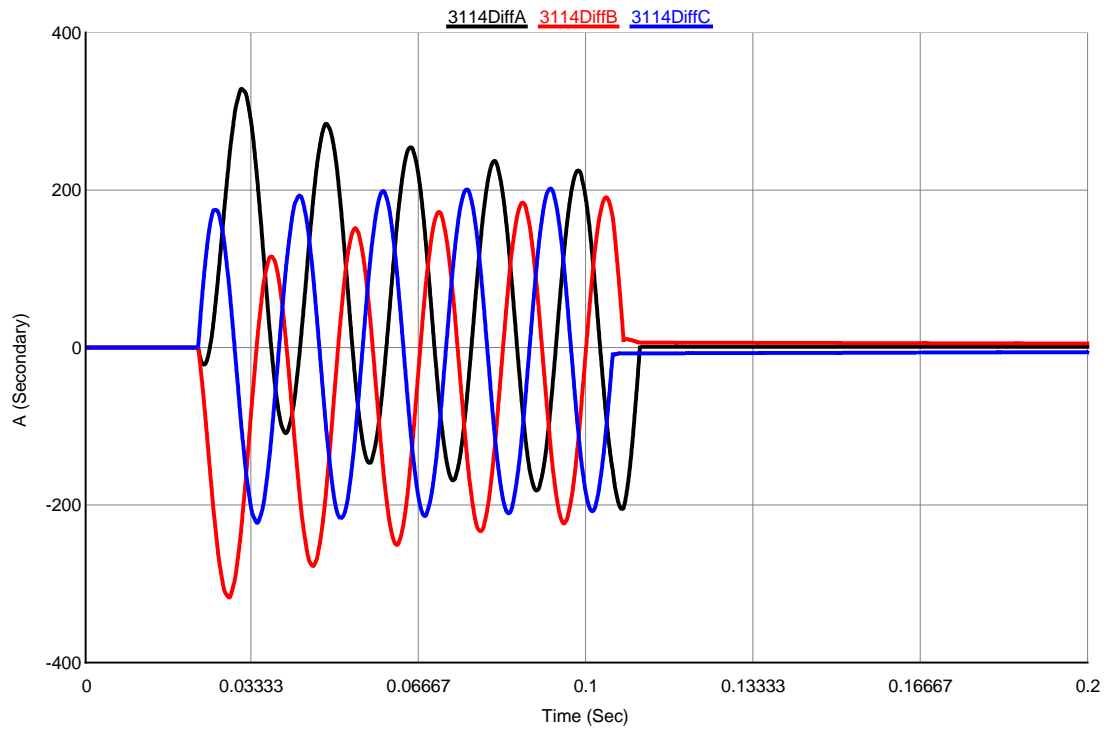


Figure 4.10 Three-phase differential current observed by the relay for a three-phase fault while grid connected.

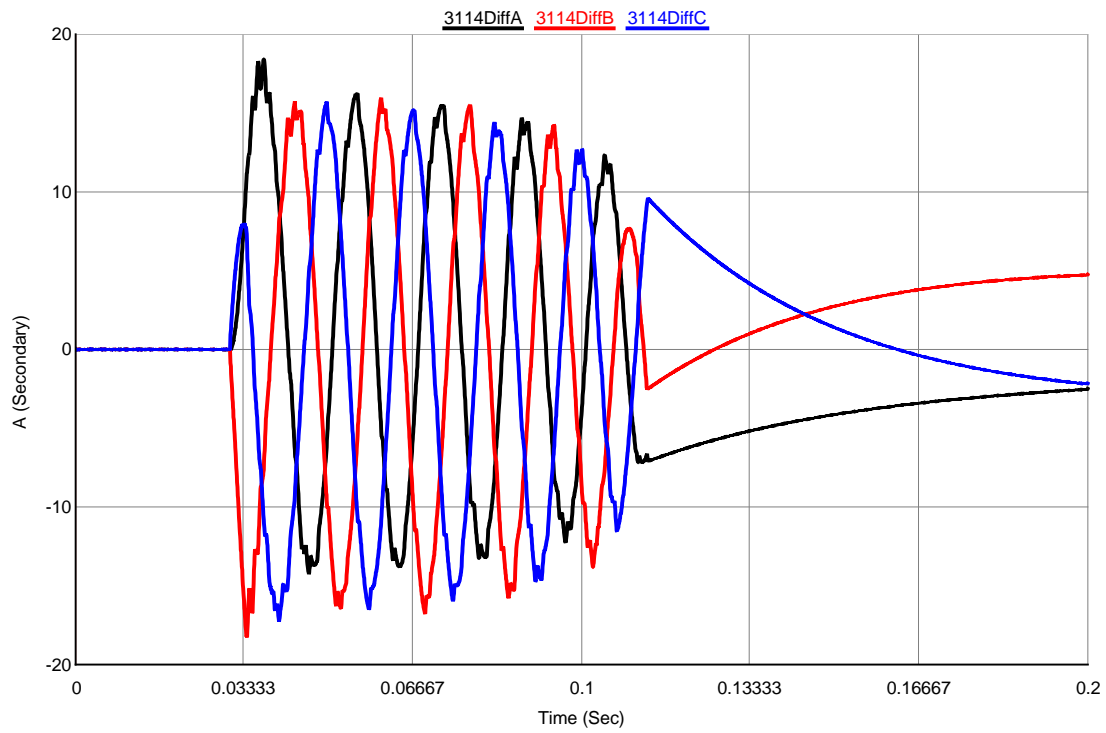


Figure 4.11 Three-phase differential current observed by the relay for a three-phase fault while off grid.

The benefit is that measured differential current is zero under normal operation. This allows a very low current pickup to be selected without fear of tripping on load current, energizing, or islanding. The fact that this protection scheme operates on differential current makes it insensitive to faults outside the protection zone. As a result, there is no need to coordinate with other protection, allowing either the minimum time dial setting, or even an instantaneous characteristic to be selected. This allows internal faults to be cleared extremely quickly.

To test this protection scheme, faults are applied on each of the two buses in the microgrid and on the cable between the two buses. Three phase faults are applied, and the response times of the relays measured. The results are shown in the following tables and figures. All overcurrent characteristics are set to their minimum settings, .25 A pickup current and .5 *second* time dial. The instantaneous overcurrent elements are set to .25 A pickup as well.

Table 4.6 Differential overcurrent protection operating times for three-phase faults using very inverse (U3) curve.

Three-Phase Fault		Protection Operation Delay (Cycles)				
Status	Location	Relay #1	Relay #2	Relay #3	Relay #4	Relay #5
On Grid	External	-	21.3	-	-	21.8
	Building 3114	4.9	4.9	4.9	-	-
	Building 3129	-	-	-	5.8	5.8
	Between Buildings	-	-	5.2	5.2	-
Off Grid	External	-	-	-	-	-
	Building 3114	-	6.2	6.2	-	-
	Building 3129	-	16.5	-	-	19.9
	Between Buildings	-	15.9	-	-	19.1

Table 4.7 Differential overcurrent protection operating times for single-phase faults using very inverse (U3) curve.

Single Phase Fault		Protection Operation Delay (Cycles)				
Status	Location	Relay #1	Relay #2	Relay #3	Relay #4	Relay #5
On Grid	External	-	-	-	-	-
	Building 3114	4.7	4.7	4.7	-	-
	Building 3129	-	-	-	6.2	6.2
	Between Buildings	-	-	6.0	6.0	-
Off Grid	External	-	-	-	-	-
	Building 3114	-	5.9	5.9	-	-
	Building 3129	-	17.0	16.5	16.5	-
	Between Buildings	-	15.8	15.7	15.7	-

Table 4.8 Differential overcurrent protection operating times for three-phase faults using extremely inverse (U4) curve.

Three-Phase Fault		Protection Operation Delay (Cycles)				
Status	Location	Relay #1	Relay #2	Relay #3	Relay #4	Relay #5
On Grid	External	-	20.9	-	-	23.1
	Building 3114	4.2	4.2	4.2	-	-
	Building 3129	-	-	-	3.8	3.8
	Between Buildings	-	-	3.7	3.7	-
Off Grid	External	-	-	-	-	-
	Building 3114	-	3.7	3.7	-	-
	Building 3129	-	21.2	-	-	19.7
	Between Buildings	-	16.1	-	-	19.5

Table 4.9 Differential overcurrent protection operating times for single-phase faults using extremely inverse (U4) curve.

Single Phase Fault		Protection Operation Delay (Cycles)				
Status	Location	Relay #1	Relay #2	Relay #3	Relay #4	Relay #5
On Grid	External	-	-	-	-	-
	Building 3114	3.3	3.3	3.3	-	-
	Building 3129	-	-	-	4.4	4.4
	Between Buildings	-	-	4.4	4.4	-
Off Grid	External	-	-	-	-	-
	Building 3114	-	3.9	3.9	-	-
	Building 3129	-	16.8	-	-	19.7
	Between Buildings	-	15.6	18.9	18.9	-

Table 4.10 Differential overcurrent protection operating times for three-phase faults using short-time (U5) curve.

Three-Phase Fault		Protection Operation Delay (Cycles)				
Status	Location	Relay #1	Relay #2	Relay #3	Relay #4	Relay #5
On Grid	External	-	19.8	-	-	22.7
	Building 3114	3.3	3.3	3.3	-	-
	Building 3129	-	-	-	4.2	4.2
	Between Buildings	-	-	3.9	3.9	-
Off Grid	External	-	-	-	-	-
	Building 3114	-	3.7	3.7	-	-
	Building 3129	-	-	-	6.0	6.0
	Between Buildings	-	-	5.7	5.7	-

Table 4.11 Differential overcurrent protection operating times for single-phase faults using short-time (U5) curve.

Single Phase Fault		Protection Operation Delay (Cycles)				
Status	Location	Relay #1	Relay #2	Relay #3	Relay #4	Relay #5
On Grid	External	-	-	-	-	-
	Building 3114	3.4	3.4	3.4	-	-
	Building 3129	-	-	-	4.5	4.5
	Between Buildings	-	-	3.7	3.7	-
Off Grid	External	-	-	-	-	-
	Building 3114	-	3.4	3.4	-	-
	Building 3129	-	-	-	7.5	7.5
	Between Buildings	-	-	7.1	7.1	-

Table 4.12 Differential overcurrent protection operating times for three-phase faults using instantaneous overcurrent characteristic.

Three-Phase Fault		Protection Operation Delay (Cycles)				
Status	Location	Relay #1	Relay #2	Relay #3	Relay #4	Relay #5
On Grid	External	-	21.2	-	-	22.4
	Building 3114	3.1	3.1	3.1	-	-
	Building 3129	-	-	-	2.8	2.8
	Between Buildings	-	-	3.3	3.3	-
Off Grid	External	-	-	-	-	-
	Building 3114	-	3.2	3.2	-	-
	Building 3129	-	-	-	3.6	3.6
	Between Buildings	-	-	3.7	3.7	-

Table 4.13 Differential overcurrent protection operating times for single-phase faults using instantaneous overcurrent characteristic.

Single-Phase Fault		Protection Operation Delay (Cycles)				
Status	Location	Relay #1	Relay #2	Relay #3	Relay #4	Relay #5
On Grid	External	-	-	-	-	-
	Building 3114	3.3	3.3	3.3	-	-
	Building 3129	-	-	-	3.3	3.3
	Between Buildings	-	-	3.6	3.6	-
Off Grid	External	-	-	-	-	-
	Building 3114	-	3.3	3.3	-	-
	Building 3129	-	-	-	2.8	2.8
	Between Buildings	-	-	3.8	3.8	-

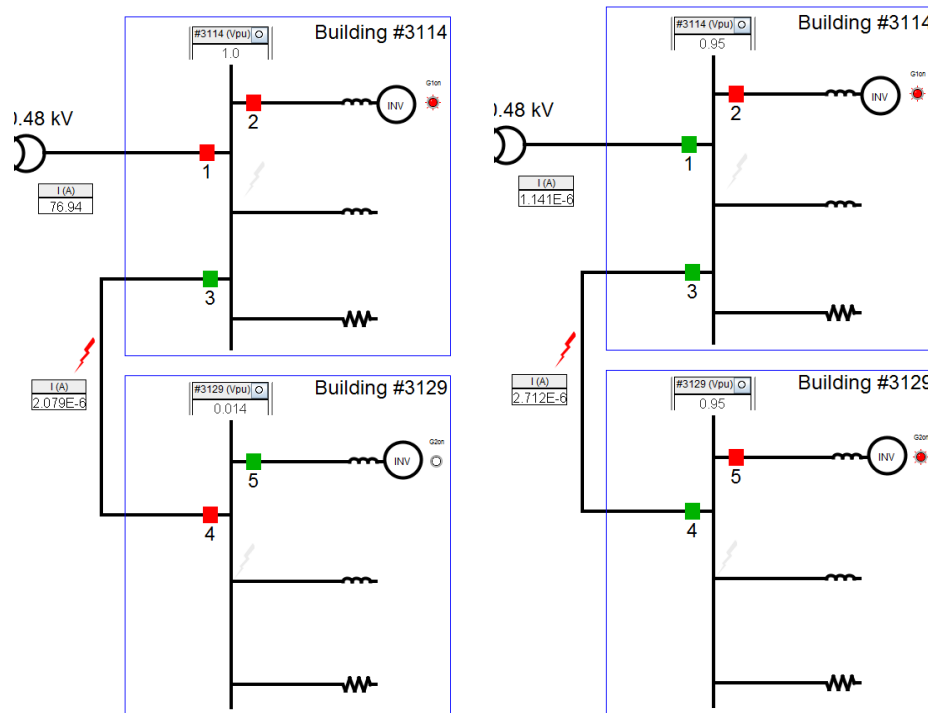


Figure 4.12 a) Fault on microgrid cable while on grid. b) Fault on microgrid cable while off grid.

This test demonstrates that a completely differential protection scheme is desirable for microgrid applications. Three and single-phase faults are successfully cleared for all locations inside the microgrid. The test also demonstrates that using overcurrent relays to monitor differential current works

well for protecting the buses and short lines comprising the ORNL microgrid system. Based on the results it is apparent that either an instantaneous or short time overcurrent characteristic is the preferable choice of operating characteristic. This test does not, however, offer a solution for isolating the microgrid from external faults. Yet, differential protection need only be implemented up to a delta-wye transformer where directional relay can be polarized using the transformer neutral current.

Because this is essentially a differential protection scheme, there is no need for setting group changes, or even digital relays, in order to implement this specific scheme. The result of this is that existing systems can be retrofitted as microgrids and existing overcurrent and instantaneous electromechanical relays can be repurposed for use in differential overcurrent protection. A consideration in evaluating each protection technology has been cost. This scheme has very low cost because it makes use of protection devices likely already in use in systems to be retrofitted as microgrids.

Summary

This chapter demonstrates the inadequacy of leaving protection unchanged when converting a distribution system into a microgrid. It is also shown that variable setting overcurrent protection protects well for islanded faults but is unable to isolate microgrid faults from the inverters while grid connected. Directional supervision is shown not to be a workable solution for this system.

However, it remains a possible solution for systems with larger impedances or those containing wye connected transformer windings with a grounded neutral.

The benefit of differential protection for microgrid applications is apparent from testing. It is also shown that overcurrent relays can be secure, selective, and rapid in clearing microgrid faults.

CHAPTER 5, CONCLUSIONS AND FUTURE WORK

Several protection technologies and strategies have been evaluated for their effectiveness in microgrid protection. The process for constructing a real time, hardware in loop microgrid protection apparatus has also been developed.

Conclusions

The protection challenges introduced in microgrid systems require more complex and innovative solutions than those encountered in a standard distribution system. Microgrids will likely see use in military installations, emergency shelters, hospitals, and other critical loads before gaining wide acceptance in residential, commercial, and industrial systems. The criticality of these loads makes allowing sources to self isolate from faults and black-starting the microgrid impractical and unacceptable.

Therefore, a differential protection scheme is the preferable choice for low voltage microgrids where systems are compact and faults affect the entire microgrid. When funding for overhauling protection systems when converting to a microgrid is a problem, short time overcurrent and instantaneous overcurrent relays are an acceptable option for implementing the differential scheme. However, backup protection is always a requirement. This backup protection on low voltage systems should consist of overcurrent protection able to change settings for on and off grid conditions. This backup will not be as selective as the differential scheme, but it is able to isolate faults well in most cases. It is worth

noting that these conclusions are based on testing conducted on a radially connected, low voltage microgrid. Meaning that other options including voltage and directional protection may still be viable options for different microgrid voltage levels and configurations. It is also worth noting that this testing was conducted on totally inverter-based system. Systems with rotating machines will have larger off grid fault currents, making protection requirements less difficult to satisfy. Also, the inverter control methodology has a significant impact on the behavior of inverters during faults, which, in turn, affect the protection requirements.

The main contributions of this thesis are, results of hardware-in-the-loop protection testing, an exploration of microgrid and protection modeling techniques, and an apparatus for studying protection and hardware integration into the ORNL DECC Lab microgrid. Results of protection testing involving physical relays are hard to come by, and this thesis provides valuable results on protection schemes likely to be considered for low voltage microgrid installations. Furthermore, the testing apparatus developed for this thesis can be reproduced and is easily applicable to additional protection testing for microgrids and traditional power systems. Also, this thesis is a useful resource for design of microgrid simulations, controls, and testing, particularly with low voltage microgrids.

Future Work

Variable setting overcurrent is recommended for use as a backup to the differential scheme. This scheme relies on communication channels to initiate setting group changes. If a differential scheme has failed, it is possible that communication channels may fail as well. Therefore, it is preferable that relays detect the need to change settings autonomously. One method of accomplishing this is based on negative sequence current. Relays typically see large negative sequence current from the utility, but this is diminished when the microgrid disconnects from the utility. Relay settings can be developed to use negative sequence to supervise overcurrent elements. Loss-of-potential logic could be used in a similar way to supervise protection settings.

Another possibility is to use islanding detection schemes in inverters to detect when the microgrid disconnects from the utility. When islanding is detected, inverters can be set to output a specific magnitude of negative sequence current. Again, this current is picked up by the relays and settings are adjusted appropriately.

The testing in this thesis was conducted on a very specific type of microgrid. Now that the hardware is in place and the model constructed, it will be beneficial to conduct similar testing on microgrids at different voltage levels, configurations, and with different mixes of inverter-based and rotating sources.

Summary

This chapter concludes that differential protection is the preferable solution for low voltage microgrid protection. It also concludes that variable setting overcurrent protection is likely the best choice for backing up the differential protection. This scheme relies on communication channels, so it is also stated that future work should include testing methods to remove the dependency upon communication channels. Future work should also include conducting similar testing on different voltage levels and microgrid configurations.

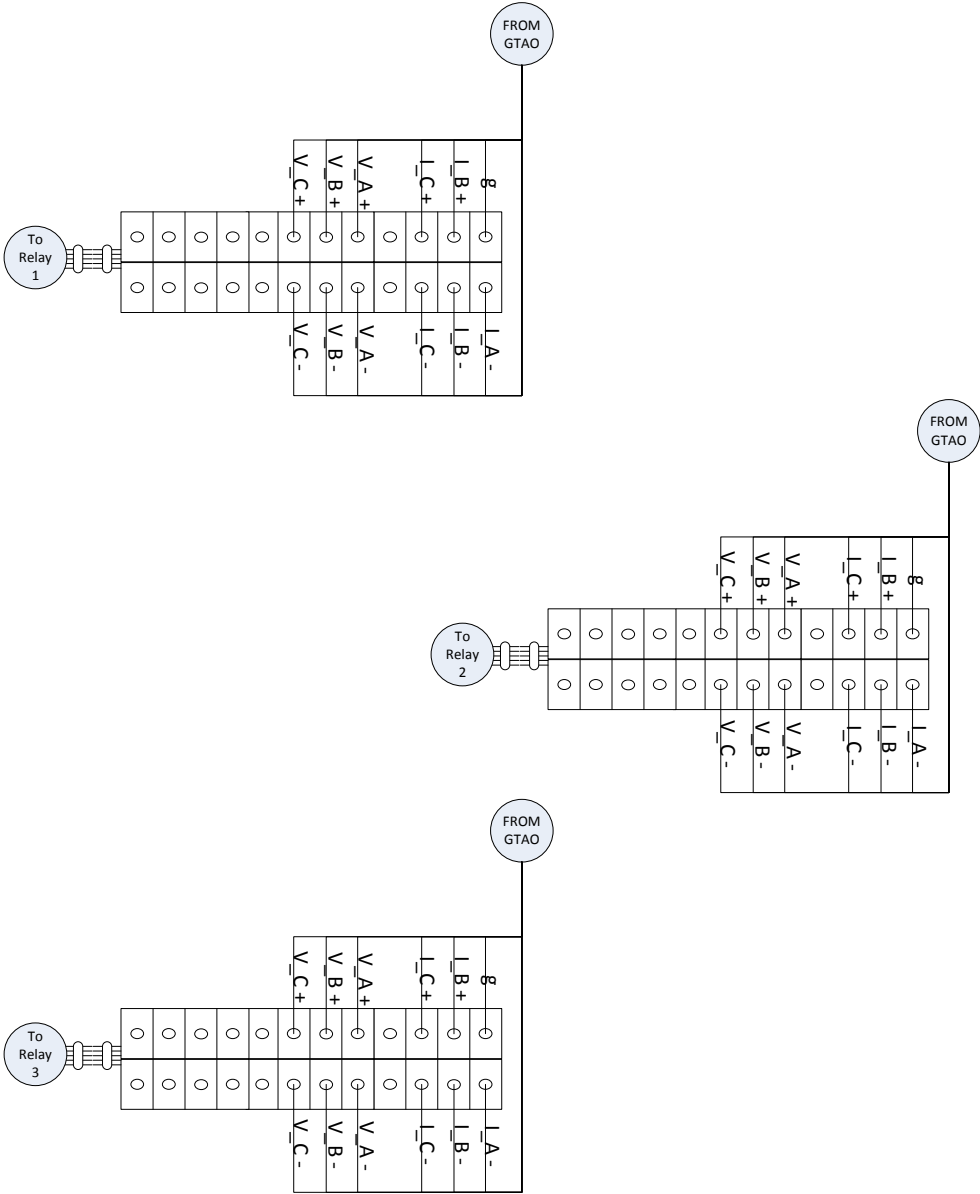
REFERENCES

- [1] Chris Marnay, Nan Zhou, Min Qu, and John Romankiewicz. (2012, June) International Microgrid Assessment: Governance, INcentives, and Experience (IMAGINE). [Online].
<http://der.lbl.gov/sites/der.lbl.gov/files/LBNL-5914E.pdf>
- [2] John H. Kueffner, "Wind Hybrid Power System For Antarctica Inmarsat Link," in *INTELEC '86*, International, 1986, pp. 297-298.
- [3] Tarek Abdallah et al., "Control Dynamics of Adaptive and Scalable Power and Energy Systems for Military Micro Grids," Engineer Research and Development Center, US Army Corps of Engineers, Washington, Final Report ERDC/CERL TR-06-35, 2006.
- [4] J. Lewis Blackburn and Thomas J. Domin, *Protective Relaying Principles and Applications*, 3rd ed., H. Lee Willis, Ed. Boca Raton, FL, USA: CRC Press, 2007.
- [5] SEL. (2008) Power System Protection Fundamentals. [Online].
<http://web.eecs.utk.edu/courses/spring2012/ece522/Protection%20primer.ppt>
- [6] IEEE, "ANSI/IEEE Standard 100," in *IEEE Standard Dictionary of Electrical and Electronics Terms*. Piscataway, NJ, USA: IEEE.
- [7] Edward Wilson Kimbark, *Power System Stability*, Paul M. Anderson, Ed. Piscataway, NJ, USA: IEEE Press, 1995, vol. 2.
- [8] RTDS Technologies. (2010, December) Real Time Digital Simulator Controls Library Manual (RSCAD Version).
- [9] Schweitzer Engineering Laboratories. (2013) Real-Time Automation Controller (RTAC). [Online]. <https://www.selinc.com/SEL-3530/>
- [10] RTDS Technologies. (2010, December) Real Time Digital Simulator] Hardware Manual (RSCAD Version).
- [11] Stephen J. Chapman, "Transmission Lines," in *Electric Machinery and] Power System Fundamentals*, Stephen W. Director, Ed. New York, USA: McGraw-Hill, 2002, p. 470.
- [12] Remus Teodorescu, Marco Liserre, and Pedro Rodriguez, "Grid Converter] Control for WTS," in *Grid Converters for Photovoltaic and Wind Power Systems*. Chichester, United Kingdom: John Wiley & Sons, Ltd, 2011, pp. 205-235.
- [13] F Scapino, "Modelling the Connection of Alternative Energy Sources to the] Three-phase Grid for Circuit Simulation," in *IEEE Industrial Electronics, IECON 2006 - 32nd Annual Conference on*, 2006, pp. 1834-1839.
- [14] Ioanna Xyngi, "An Intelligent Algorithm for Smart Grid Protection] Applications," Delft University of Technology, Athens, Dissertation Nov. 2011. [Online]. <http://repository.tudelft.nl/view/ir/uuid%3A3221d00a-4964-4d42-abb7-f9c45b4006e7/>
- [15] I. Xyngi and M. Popov, "Smart protection in Dutch medium voltage] distributed generation systems," in *IEEE PES Innovative Smart Grid*

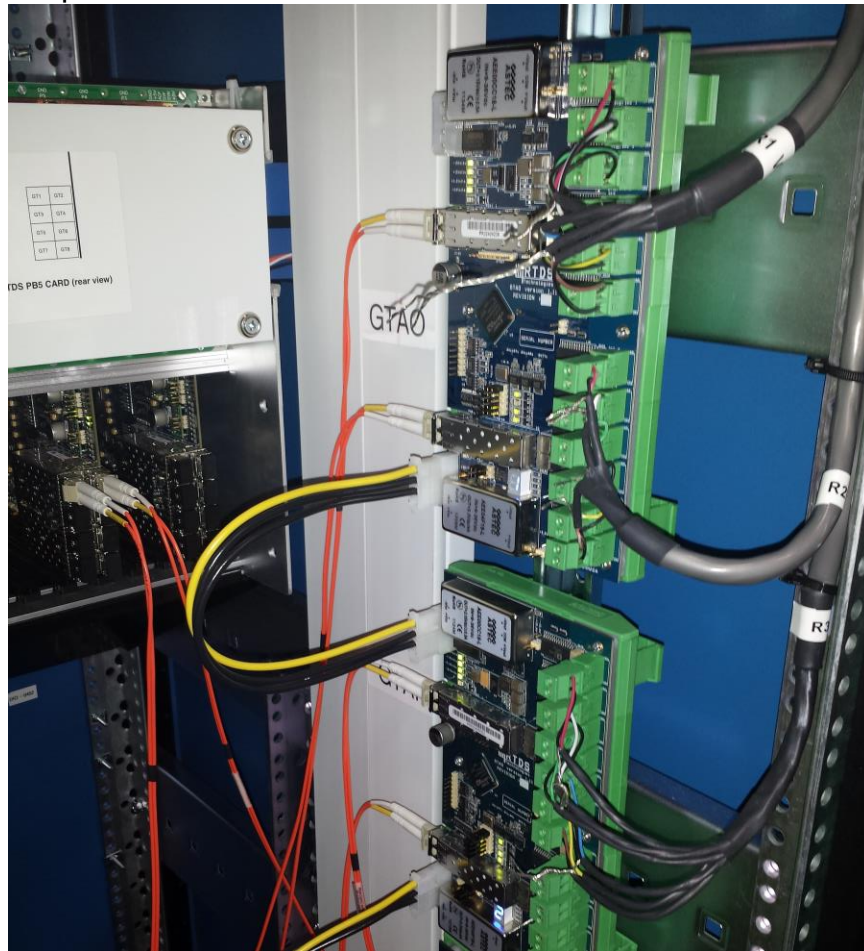
- Technologies Conference Europe*, Gothenburg, 2010.
- [16 Edward Jeroen Coster. (2010, Sep.) Repository TU/e. [Online].
] <http://repository.tue.nl/676122>
- [17 Richard O. Duda, Peter E. Hart, and David G. Stork, *Pattern Classification*,
] Second Edition ed. New York, USA: John Wiley & Sons, Inc., 2001.
- [18 Schweitzer Engineering Laboratories, Inc., "SEL 351S Protection System
] Instruction Manual," Pulman, USA, Instruction Manual 2013.

APPENDIX

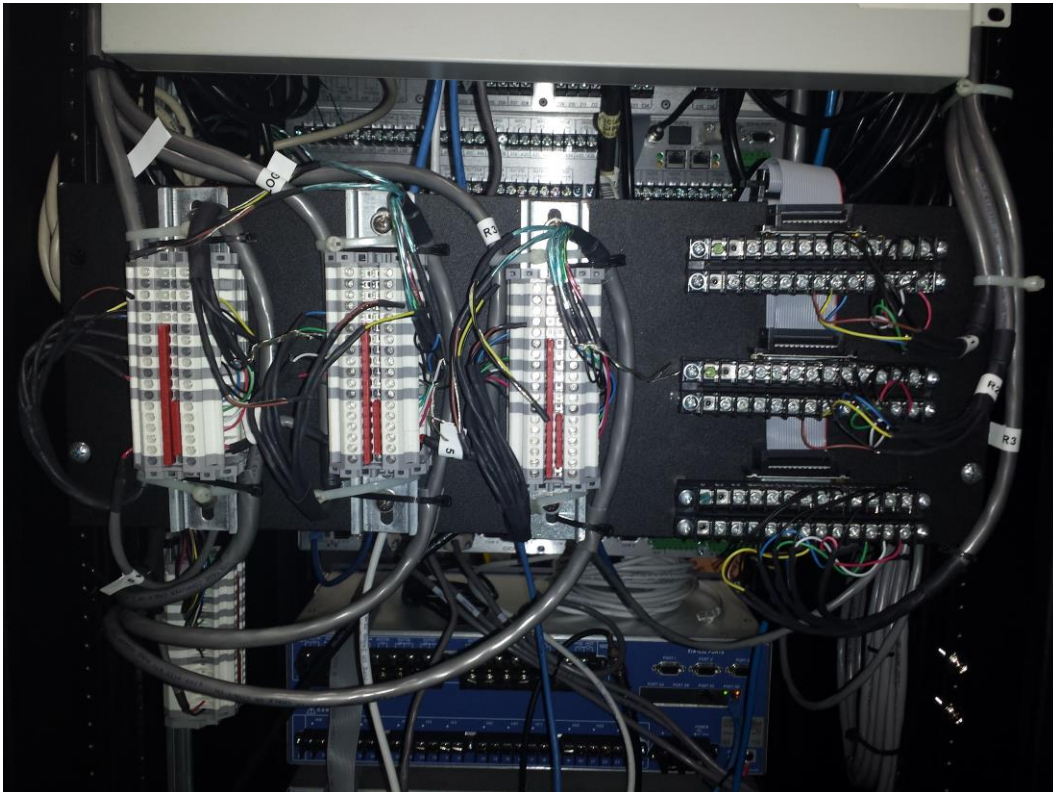
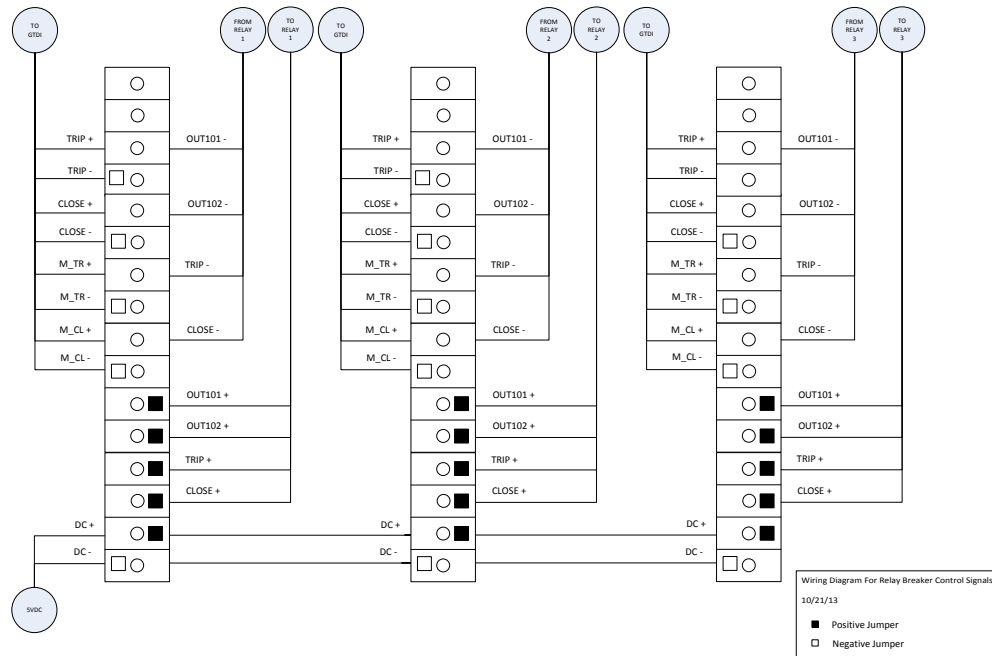
Relay ribbon cable connections:



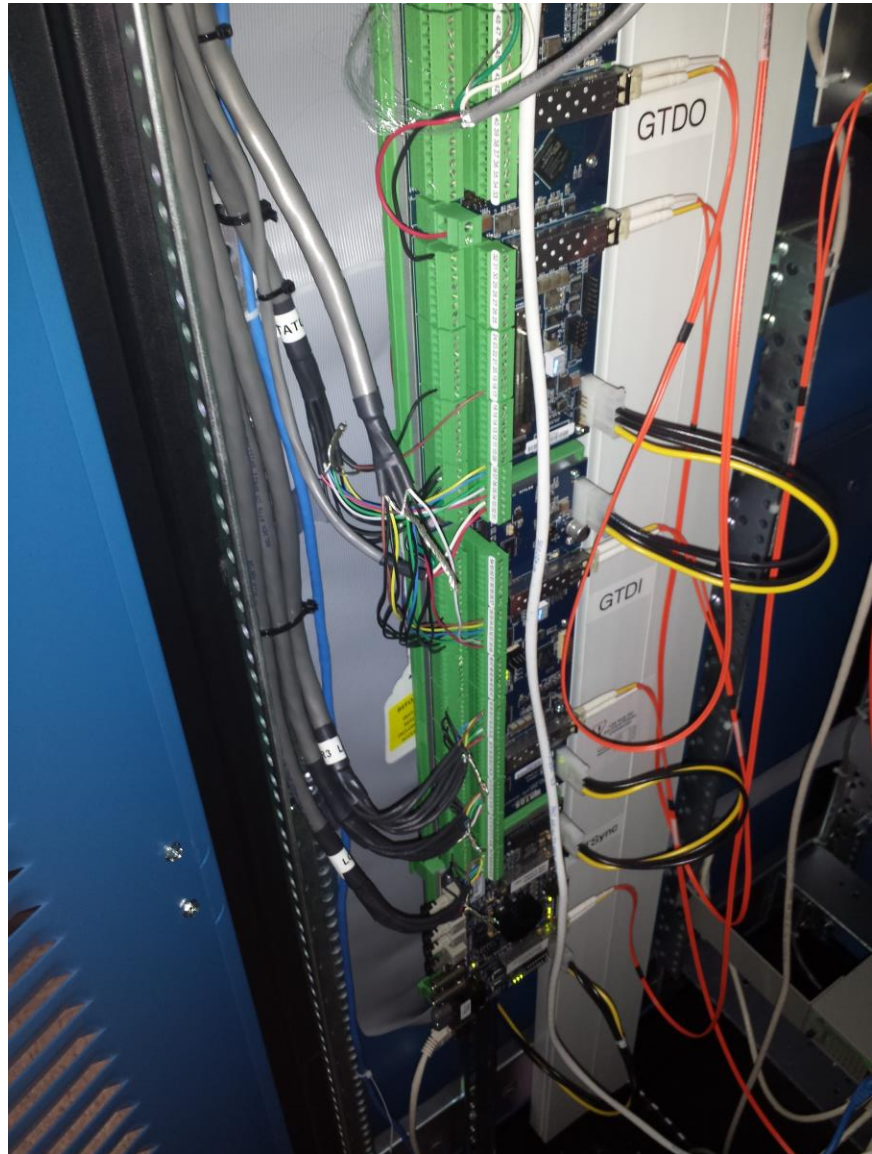
Analog signal outputs from RTDS:



Relay logic connections:



Relay logic signal I/O in RTDS:



Genetic algorithm for control tuning:

```
CHAPTER 1, CLEAR ALL
CHAPTER 2, CLOSE ALL
CHAPTER 3, CLC
CHAPTER 4,
CHAPTER 5, FORMAT LONG G
CHAPTER 6,
CHAPTER 7, %% SET NUMBER OF PARAMETERS, GENERATIONS, AND CHILDREN
PER GENERATION
CHAPTER 8, GLOBAL JTCPOBJ T
CHAPTER 9,
CHAPTER 10, T = CPUTIME;
CHAPTER 11,
CHAPTER 12, GAINS = 4;
CHAPTER 13, CHILD = 100;
CHAPTER 14,
CHAPTER 15, %% IMPLEMENT GENETIC ALGORITHM
CHAPTER 16, JTCPOBJ = JTCP('REQUEST','127.0.0.1',4570);
CHAPTER 17,
CHAPTER 18, I = 0;
CHAPTER 19, FLAG = 0;
CHAPTER 20, B = 1000*ONES(6,1);
CHAPTER 21, NEW_GEN = REPMAT([1E2;1E1;1E0;1E-1;1E-2;1E-3;],1,GAINS);
CHAPTER 22, FITNESS = B;
CHAPTER 23, HOLDOVER = REPMAT([1E6,0,0,0,0,0,0,0],2,1);
CHAPTER 24, WHILE B(1) > .01 && FLAG == 0
CHAPTER 25,     B
CHAPTER 26,     I = I+1;
CHAPTER 27,     CHILDREN = ZEROS(CHILD,GAINS);
CHAPTER 28,     FOR II = 1:CHILD
CHAPTER 29,         FOR III = 1:GAINS % CROSSOVER , PRODUCING CHILDREN FROM
COMBINATIONS OF PARENTS WITH LIKLIHOOD OF BEING USED PROPORTIONAL TO
THE FITNESS FUNCTION
CHAPTER 30,             INDEX = RANDOM('UNIFORM',0,SUM(FITNESS(:,1)));
CHAPTER 31,             IF INDEX <= FITNESS(1,1)
CHAPTER 32,                 CHILDREN(II,III) = NEW_GEN(1,III);
CHAPTER 33,             ELSE IF INDEX <= SUM(FITNESS(1:2,1))
CHAPTER 34,                 CHILDREN(II,III) = NEW_GEN(2,III);
CHAPTER 35,             ELSE IF INDEX <= SUM(FITNESS(1:3,1))
CHAPTER 36,                 CHILDREN(II,III) = NEW_GEN(3,III);
CHAPTER 37,             ELSE IF INDEX <= SUM(FITNESS(1:4,1))
CHAPTER 38,                 CHILDREN(II,III) = NEW_GEN(4,III);
CHAPTER 39,             ELSE IF INDEX <= SUM(FITNESS(1:5,1))
CHAPTER 40,                 CHILDREN(II,III) = NEW_GEN(5,III);
CHAPTER 41,             ELSE %IF INDEX <= SUM(FITNESS(1:6,1))
CHAPTER 42,                 CHILDREN(II,III) = NEW_GEN(6,III);
CHAPTER 43,             END
CHAPTER 44,         END
CHAPTER 45,     END
CHAPTER 46, END
CHAPTER 47, END
CHAPTER 48, END
CHAPTER 49, END
```

```

CHAPTER 51, CHILDREN = CHILDREN.*ABS(RANDOM('NORMAL',1,1,CHILD,GAINS)); %
MUTATION , MULTIPLYING EACH ELEMENT BY A RANDOM NUMBER FROM A CHI-
SQUARED DISTRIBUTION,
CHAPTER 52, % I'M NOT SURE IF THIS IS A GOOD WAY TO DO THE MUTATION
CHAPTER 53,
CHAPTER 54, OBJECTIVE = ZEROS(CHILD,1);
CHAPTER 55, FOR II = 1:CHILD
CHAPTER 56,     FPRINTF('\N%S%D','GENERATION: ',I)
CHAPTER 57,     FPRINTF('\N%S%D\N','PARAMETER SET: ',II)
CHAPTER 58,     FPRINTF('%S\N',DATESTR(CLOCK))
CHAPTER 59,     X = CHILDREN(II,:); % ITERATE THROUGH LIST OF CHILDREN
PARAMETER SETS
CHAPTER 60,     % SEND TO RTDS
CHAPTER 61,     OBJECTIVE(II,:) = GET_OBJ(X,I,II); % REPLACE WITH OBJECTIVE
FUNCTION FROM RTDS
CHAPTER 62, END
CHAPTER 63,
CHAPTER 64, I = OBJECTIVE == 0;
CHAPTER 65, OBJECTIVE(I) = 100000;
CHAPTER 66,
CHAPTER 67, FOR III=1:2
CHAPTER 68,     ROW =
[HALDOVER(III,2),HALDOVER(III,3),HALDOVER(III,4),HALDOVER(III,5)];
CHAPTER 69,     OBJECTIVE = [OBJECTIVE;HALDOVER(III,1)];
CHAPTER 70,     CHILDREN = [CHILDREN;ROW];
CHAPTER 71, END
CHAPTER 72, [B,I] = SORT(OBJECTIVE,'ASCEND'); % SORT PARAMETER SETS
FROM BEST TO WORST BASED ON THE OBJECTIVE FUNCTION
CHAPTER 73, NEW_GEN = CHILDREN(I(1:6),:); % USE TOP 10 SETS TO PRODUCE
NEXT GENERATION
CHAPTER 74, FITNESS = ONES(6,1)./B(1:6);
CHAPTER 75, BEST(I,:) = NEW_GEN(1,:);
CHAPTER 76,
CHAPTER 77, HALDOVER = CAT(2,OBJECTIVE(I(1:2)),NEW_GEN(1:2,:));
CHAPTER 78,
CHAPTER 79, AVG_BEST(I,:) = MEAN(NEW_GEN,1);
CHAPTER 80, ACCURACY(I,1) = B(1)
CHAPTER 81,
CHAPTER 82, CSVWRITE('TUNING_RESULTS.CSV',CAT(2,ACCURACY,BEST));
CHAPTER 83, IF LENGTH(ACCURACY)>2
CHAPTER 84,     IF ACCURACY(I) == ACCURACY(I-2)
CHAPTER 85,         FLAG = 1;
CHAPTER 86,     END
CHAPTER 87, END
CHAPTER 88, END
CHAPTER 89,
CHAPTER 90, JTCP('CLOSE',JTCPOBJ);
CHAPTER 91, DISP('ITERATION FINISHED.');
```

Function for passing gains to simulation:

```
CHAPTER 94, FUNCTION F = GET_OBJ(X,I,J)
CHAPTER 95, %%
CHAPTER 96, % TALK WITH RSCAD WITH 'LISTENONPORT' CAPABILITY
CHAPTER 97, % THIS M FILE SHOULD BE ON THE SAME DIRECTORY AS THE 'JTCP.M'
FILE.
CHAPTER 98, % PART OF THE .M FILE IS BORROWED FROM RSCAD TRAINING FILES
CHAPTER 99, % THIS .M FILE WILL GENERATE A FITNESS FUNCTION FOR GA
OPTIMIZATION
CHAPTER 100, % PIK-2012.03.05 (FOR THE RTDS PART)
CHAPTER 101, % CREATED BY KUMARAGURU PRABAKAR
CHAPTER 102, %%
CHAPTER 103, EXPR2 = 'OBJ\$\$=\$(?<VAR_VALUE1>(-)?\D+(\.D+)?)\$*END';
CHAPTER 104,
CHAPTER 105, GLOBAL JTCPOBJ
CHAPTER 106, DISP(' ');
CHAPTER 107,
CHAPTER 108, MSG2 = SPRINTF('SETSLIDER "DRAFTVARIABLES : G2KPF" = %.8F;',
X(1));
CHAPTER 109, DISP(MSG2);
CHAPTER 110, JTCP('WRITES', JTCPOBJ, MSG2);
CHAPTER 111,
CHAPTER 112, MSG2 = SPRINTF('SETSLIDER "DRAFTVARIABLES : G2KIF" = %.8F;',
X(2));
CHAPTER 113, DISP(MSG2);
CHAPTER 114, JTCP('WRITES', JTCPOBJ, MSG2);
CHAPTER 115,
CHAPTER 116, MSG2 = SPRINTF('SETSLIDER "DRAFTVARIABLES : G2KPV" = %.8F;',
X(3));
CHAPTER 117, DISP(MSG2);
CHAPTER 118, JTCP('WRITES', JTCPOBJ, MSG2);
CHAPTER 119,
CHAPTER 120, MSG2 = SPRINTF('SETSLIDER "DRAFTVARIABLES : G2KIV" = %.8F;',
X(4));
CHAPTER 121, DISP(MSG2);
CHAPTER 122, JTCP('WRITES', JTCPOBJ, MSG2);
CHAPTER 123,
CHAPTER 124, JTCP('WRITES',JTCPOBJ,'START;');
CHAPTER 125,
CHAPTER 126, JTCP('WRITES',JTCPOBJ,'SUSPEND 10;');
CHAPTER 127, JTCP('WRITES',JTCPOBJ,'TEMP_FLOAT = METERCAPTURE("OBJ");');
CHAPTER 128, JTCP('WRITES',JTCPOBJ,'SPRINTF(TEMP_STRING, "OBJ = %F END",
TEMP_FLOAT);');
CHAPTER 129, JTCP('WRITES',JTCPOBJ,'LISTENONPORTHANDSHAKE(TEMP_STRING
);');
CHAPTER 130, JTCP('WRITES',JTCPOBJ,'STOP;');
CHAPTER 131,
CHAPTER 132, PAUSE(1)
CHAPTER 133, %%
CHAPTER 134, RMSG = [];
CHAPTER 135, RMSG2 = 'DUMMY';
```

```

CHAPTER 137, WHILE (ISEMPTY(REGEXP(RMSG2, EXPR2, 'ONCE')) == 1)
CHAPTER 138,   RMSG = [RMSG JTCP('READ',JTCPOBJ)];
CHAPTER 139,   RMSG2 = CHAR(RMSG);
CHAPTER 140,   IF(REGEXP(RMSG2, EXPR2))
CHAPTER 141,     [~, VALUE] = REGEXP(RMSG2, EXPR2, 'TOKENS', 'NAMES');
CHAPTER 142,     FTEMP2 = STR2DOUBLE(VALUE.VAR_VALUE1);
CHAPTER 143,     F=FTEMP2;
CHAPTER 144,     MSG2 = SPRINTF('VALUE RETURNED: %F', FTEMP2);
CHAPTER 145,     DISP(MSG2);
CHAPTER 146,     BREAK;
CHAPTER 147,   ELSE
CHAPTER 148,     CONTINUE;
CHAPTER 149,   END
CHAPTER 150, END

```


Vita

Kevin M. Dowling was born in Knoxville, TN. He received his B.S. degree in electrical engineering from the University of Tennessee, Knoxville in 2012. While pursuing a M.S. degree in electrical engineering from the University of Tennessee, he worked as a graduate research assistant in the CURENT engineering research center. In his time as a GRA he



conducted research with the Power and Energy Systems group at Oak Ridge National Laboratory in Oak Ridge, TN. While there, he was a co-developer of the IGATE-E demand response analysis tool and was responsible for conducting hardware-in-the-loop testing on microgrid protection strategies and hardware. After receiving his M.S. degree, he began working as a utility transmission planning engineer.